Targeting STAT3 in Ovarian Cancers: Reciprocal Activation of NF-kB by STAT3 Inhibition

TABLE OF CONTENTS

ABSTRACT

The transcription factor STAT3 normally modulates cell proliferation with a rapid and transient downstream effect. However, in tumor cells, inappropriately activated STAT3 alters the gene expression profile and renders tumor cells unresponsive to cell death signals. In this study, we examine the biological and biochemical effects of some STAT3 inhibitors on ovarian and cervical cancer cells. Furthermore, we study the reciprocal relationship between STAT3 and NF-κB—another prosurvival transcription factor—in ovarian cancer cells.

Inappropriate activation of STAT3 occurs in many cancers and often results in resistance to conventional chemotherapies. In addition, overactive STAT3 signaling in tumor cells has been correlated with resistance to conventional chemotherapies. Therefore, for cancer patients, targeted inhibition of STAT3 potentially constitutes a powerful therapeutic tool. Initially, when ovarian cancer cells that depend on STAT3 for pathogenesis are treated with STAT3 inhibitors (i.e. nifuroxazide, ST3-01, etc), significantly reduced viability was observed. Surprisingly, results from quantitative RT-PCR analysis and reporter assays have identified an unexpected reciprocal relationship between STAT3 inhibition and NF-κB activation. Furthermore, reducing STAT3 expression by RNAi seemed to result in the upregulation of NF-κB genes including A20 and IL-8, which was consistent with the effects of STAT3 inhibitors. Moreover, the combination of reducing the levels of both STAT3 and the NF-κB subunit p65 was found to abrogate the upregulation of NF-κB target genes seen when STAT3 levels alone were reduced. This suggests that p65 expression is important for the activation of NF-κB by STAT3 inhibition. Subsequently, NF-κB nuclear translocation was examined in whole cell populations as well as in single cells. The results showed that no apparent p65 nuclear translocation was observed upon STAT3 inhibition, suggesting an alternative mechanism of NF-κB activation.

In summary, this work demonstrates that inhibiting STAT3 with novel drugs or chemotherapeutic agents leads to activation of NF-κB, which may provide a prosurvival signal, thus limiting the therapeutic potential of these drugs and promoting resistance to these agents.

GLOSSARY

STATs	Signal transducers and activators of transcription
pSTAT3	tyrosine phosphorylated STAT3
tSTAT3	total STAT3, including the phosphorylated and unphosphorylated STAT3
pSTAT1	phosphoryalted STAT1
p38 MAPK	p38 mitogen-activated protein kinases
INFγ	type II interferon; interferon gamma
TNFα	tumor necrosis factor alpha
IL-6	interleukin 6
IL-8	interleukin 8
BCL3	B-cell lymphoma 3
BCL6	B-cell lymphoma 6
Bcl-xL	B-cell lymphoma-extra large
MCL1	induced myeloid leukemia cell differentiation protein Mcl-1
SOCS3	Suppressor of cytokine signaling 3
VEGF	Vascular endothelial growth factor
A20	also known as TNFAIP3, or tumor necrosis factor, alpha-induced protein 3
CCL5	Chemokine (C-C motif) ligand 5, also know as RANTES (Regulated on Activation, Normal T cell Expressed and Secreted).
BIRC3	Baculoviral IAP repeat-containing protein 3.
NFKBIE	Nuclear factor of kappa light polypeptide gene enhancer in B-cells inhibitor, epsilon

INTRODUCTION

Ovarian carcinoma, as the most lethal gynecological malignancy, constitutes more than one third of all cancers occurring in women (1). It was thought that more than 90% of ovarian cancers arise from the epithelium of the ovary, while recent studies have proposed models postulating that the early transformation of high-grade serous ovarian cancer (HGSOC) originates in the fallopian tube secretary epithelial cells (FTSEC) (2, 3). Because of the high rate of mortality and morbidity associated with ovarian cancer, routine screening and early detection become important in personalizing the therapeutic approach and improving the overall prognosis for patients. A thorough understanding of the pathogenesis of ovarian cancer requires the identification of the oncogenes and tumor suppressors, as well as the molecular mechanisms that connect these potential therapeutic targets. In the past decades, with significant progress made in deciphering important signal transduction cascades, it becomes clear that the STAT pathway plays an important role in the pathogenesis of several cancers, including ovarian cancer (4).

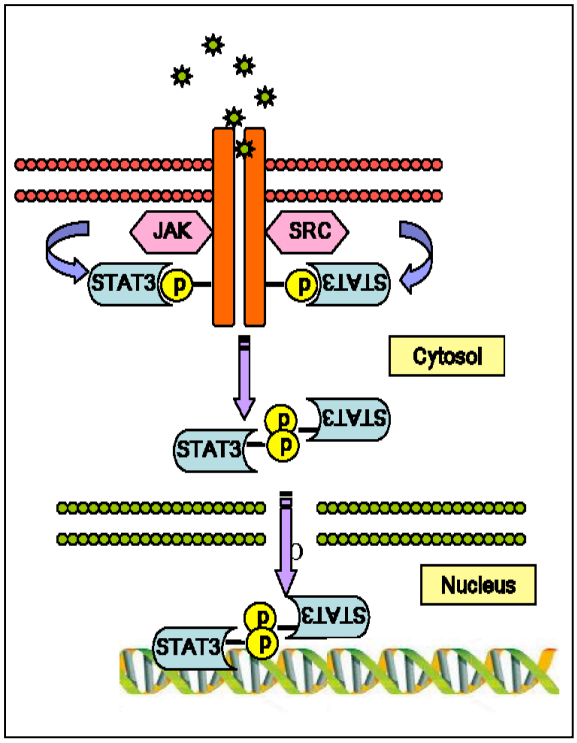

Signal transducers and activators of transcription, or STATs, are a family of transcription factors that were originally described as latent cytoplasmic transcription factor responding to a diverse collection of cytokines and growth factors (5). In the absence of cytokine or growth factors, STAT proteins remain in their inactive state as monomers in the cytoplasm. When an appropriate ligand binds to the respective receptor, the Janus kinase (JAK) associated with the receptor becomes phosphorylated and activated. Consequently, the JAKs phosphorylate STATs on specific residues and the activated STATs then dimerize and translocate into the nucleus to modulate target gene expression. Normally, STAT activation is ligand dependent and the downstream effect is rapid and transient, because specific phosphatases quickly de-phosphorylate and inactivate the STATs. Under this tight regulation, STAT signaling in normal cells is associated with cell survival, proliferation,

development, and differentiation. However, mutations in the STAT3 signaling pathway resulting in constitutively activated STATs are associated frequently with uncontrolled cell growth and malignant transformation. In fact, an increasing number of cell lines derived from primary tumors, as well as a subset of primary human cancers contain constitutively activated STAT proteins, particularly Stat3 (6).

The constitutively activated Stat3 not only provides survival and proliferation signals for cancer cells, but also confers chemotherapeutic resistance. Moreover, constitutive Stat3 activation alters the gene expression profile and disrupts the delicate balance between pro- and anti-apoptotic proteins, thus rendering tumor cells particularly unresponsive to cell death signals (7). Because it is dispensable in normal cells but essential to tumor cells, Stat3 constitutes an excellent molecular target with good therapeutic potential (8). More specifically, in ovarian cancers, aberrantly activated Stat3 promote tumorigenesis via de-regulation of cell cycles and protection from apoptosis. Inhibition of Stat3 therefore comprises substantial value in treatment of ovarian cancers through restriction of cell growth, aggravation of tumor cell death, and ultimately, reversal of malignancy (9, 10). More specifically, for some of the ovarian cancers that develop resistance to other chemotherapeutic agents but depend on STAT3 signaling for proliferation and metastasis, STAT3 inhibition can increase their sensitivity to chemotherapy and render them susceptible for apoptosis. Thus, targeted inhibition of Stat3 is a powerful therapeutic tool, when used in conjunction with current chemotherapies to improve the survival rate and prognosis for ovarian cancer patients (11, 12).

Knowing that constitutively activated STAT3 associates with increased malignancy of ovarian cancer, several chemotherapeutic agents that specifically target the STAT3 pathway have been developed. Nifuroxazide, for example, is a drug that has been approved in East Asia and Europe to treat acute adult diarrhea and is extremely well tolerated. Recently, nifuroxazide has been shown to also specifically inhibit STAT3 activity in multiple myeloma cells **(**13). In addition, another drug CYT can act as an ATP-competitive inhibitor for both Janus kinases JAK1 and JAK2. Because JAK1 is upstream of STAT3 and plays a crucial role for phosphorylation and activation of STAT3, its inhibition can directly result in an effective reduction of STAT3 phosphorylation, thus decrease STAT3 activities. Other STAT3 inhibitors and their mechanisms of actions are also under active research. One of the candidates, ST3-01, a STAT3 inhibitor developed in our lab, reduces STAT3 activity in both hematopoietic cancer cells and solid tumors. Interestingly, previous studies

postulated that ST3-01 and some of its analogues such as ST3-01A and ST3-01B, inhibits STAT3 via routes different from blocking the phosphorylation of STAT3. The mechanism of action for ST3-01 is still unclear, but it is thought to disrupt the interactions between STAT3 and important cofactors, which are crucial for effective STAT3 DNA binding and gene expression.

Having the various STAT3 inhibitors available, we aim to inhibit the STAT3 pathway in ovarian cancer cell lines as well as in primary patient cancer cells. To gain a better understanding of the efficacy of some of the novel STAT3 inhibitors, additional pathways are investigated to understand the molecular mechanisms by which STAT3 inhibitors exert their effects in ovarian cancer cells. One pathway of interest is the NF-κB pathway, which is commonly associated with inflammation, autoimmune diseases, viral infection, and cancer (14). Evidences from previous studies associate the increased malignancy with the elevated intracellular levels of STAT3 and NF-κB activities. Although the NF-κB pathway consists of multiple subunits including RelA/p65, c-Rel, RelB, NF-κB1/p50 and NF-κB2/p52 (15), the predominant form of NF-κB is the p65/RelA-p50 dimer, which like Stat3 remains in the cytoplasm in their inactive state. However, unlike Stat3 that remains in the cytosol in its de-phosphorylated form, the p65-p50 dimer is associated with the inhibitor of NF-κB protein IκBα under basal conditions. Once stimulated by extracellular signals, the upstream kinase IκB kinase (IKK) then phosphorylates IκBα, therefore targeting it for ubiquitination and proteasome degradation. The liberated p65-p50 dimer then translocates into the nucleus, binds to DNA, and regulates endogenous NF-κB target gene expression (16).

NF-κB can also be regulated by a family of upstream activating kinase complexes such as IKKα, IKK, and IKKγ/NEMO. Therefore, the combination of these activating complexes with the family of inhibitors (IκBs) generates numerous possibilities in the downstream molecular functions and the ultimate physiological manifestations (17). Moreover, besides this canonical pathway, two alternative pathways (non-canonical and NF-κB1-p105) have also been suggested to activate NF-κB depending on the microenvironmental differences and cellular conditions.

Interestingly, p65/RelA-p50 dimer generally promotes transcription of endogenous genes that are pro-survival and pro-proliferation. On the other hand, the p52-RelB dimer that is the main player of the non-canonical pathway is more involved in B-lymphocyte differentiation. On the contrary, the

homodimers of p50 or p52 are normally thought to exhibit inhibitory effects (18). Although not emphasized here, further phosphorylation of NF-κB subunit, for instance, p65/RelA, may potentially influence the specificity and accuracy of NF-κB target gene transcription. It is through this complex signaling network that various kinases serving as central regulators to connect cellular response and tumor pathogenesis to a particular cancer microenvironment (19). As cancer cells undertake rigorous metabolic processes, they generate a large array of stress factors leading to cancer progression, one of which being the reactive oxygen species (ROS) generated from oxidative stress (20). More specifically, DNA damage resulting from ROS can promotes inflammation through NF-κB responsive genes including cyclooxygenase-2 (Cox-2) and inducible nitric oxide synthase (iNOS). In general, ROS activates NF-κB through IKK; however, in different types of cells, various protein machinery and complexes are likely to be employed for the activation of NF-κB (21).

In this study, we set out to examine the effects of a range of STAT3 inhibitors in ovarian cancer cells. Particularly, while we aimed to investigate closely the mechanism of actions of these STAT3 inhibitors, we also studied the corresponding statues of alternative pathways when STAT3 is inhibited. We determined that even though STAT3 inhibitors decrease viability of ovarian cancer cells, they did so via different mechanisms. Furthermore, in the process of blocking STAT3 activity in ovarian cancer cells, both STAT3 inhibitors and STAT3 RNAi, which reduced the STAT3 mRNA levels, were associated with the consistent upregulation of additional target genes. More specifically, we observed a constant IL-8 upregulation, indicating that either IL-8 is negatively regulated by STAT3 under normal conditions or that additional pathways are activated in response to STAT3 inhibition. Consistent with IL-8, a panel of NF-κB target genes seemed to be induced to various extents when STAT3 is pharmacologically inhibited or knocked-down. Therefore, we proposed that the NF-κB pathway, as discussed earlier, relates to STAT3 reciprocally, such that when STAT3 is inhibited, the cancer cells activate NF-κB either as a stress response or as a compensatory strategy. Because this activated NF-κB pathway can compromise the effectiveness of chemotherapy and render ovarian cancer cells unresponsive to STAT3 inhibitors, we analyzed the mechanisms via which NF-κB is induced. We found that a reduction of p65/RelA levels in ovarian cancer cells significantly inhibited the NF-κB target gene expression induced by STAT3 inhibitors or STAT3 RNAi. To better understand the role of p65, we attempted to relate p65 nuclear translocation to STAT3 inhibition. However, a substantial nuclear translocation of p65 was not observed at a single

cell level or in a population when STAT3 is inhibited. This suggests that alternative mechanisms are involved in this reciprocal relationship between STAT3 and NF-κB pathways. Plausible models linking the two pathways are explained in this study, include the activation of the non-canonical NF-κB pathway, induction of additional stress-responsive pathways, and the involvement of p50 homodimers, which represses the NF-κB target gene expression by blocking p65/RelA DNA binding in the nucleus.

METHODS AND MATERIALS

Cell Culture and Reagents

OVCAR8 cells and SKOV3 cells were obtained from Dr. Ronnie Drapkin's lab at Dana-Farber Cancer Institute and grown in RPMI media containing 10% fetal bovine serum (FBS). The HeLa p65EGFP cell line was obtained from Dr. Susanne Gaudet (Dana-Farber Cancer Institute, Boston) and was grown in DMEM media containing 10% FBS. FT33-Tag-Myc cells were given by Dr. Ronnie Drapkin's lab and were grown in DMEM/F12 media with 10% FBS. A498, RCC786 and RCC 769 cell lines were provided by Dr. James Mier's lab and were grown in RPMI+10% FBS. The reporter cell line NF-κB-Luc cells were originally generated in our lab (13) and were grown in DMEM media with 10% FBS. Primary patient cells were isolated from ovarian tumor tissue provided by Brigham and Women's Hospital (Boston) post surgery. Isolation of epithelial cells from primary tumor tissue began with disintegration of tumor by scalpel dissection followed by cell strainer selection. Single cells passing a sterile cell strainer were then grown selectively on either collagen-coated dishes or regular tissue culture flasks in DMEM/F12 media with 10% FBS. Over a period of a week, the non-attaching hematopoietic cells as well as remaining epithelial cells were continuously removed and transferred into new culturing dishes and flasks to allow selection. The dishes and flasks containing attached epithelial cells were given multiple washes to remove any hematopoietic cells before the cells were used for experiments. The cytokines used for stimulation were 10ng/mL IL-6 (Peprotech), 10ng/mL TNFα (Peprotech), 10ng/mL IFNγ, 10 ng/mL OSM (R&D Systems), and 10 ng/mL LIF (Chemicon).

Viability Assays

Cells (OVCAR8 and SKOV3, 10^3/well; primary ovarian tumors $3x10^3$/well) were plated in opaque 96-well dishes in duplicates and allowed 24 hours to attach. Compounds (nifuroxazide, ST3-01, and CYT) or vehicle was added to the cells such that the final volume per well was kept to 100μL. Depending on the length of treatment, after the incubation time (1 day, 2 days, or 3 days), cell viability was assessed via the CellTiter-Glo Luminescent Cell Viability Assay (Promega, 50 μL/well) and quantitated on the Luminoskan luminometer.

Immunoblotting

Cells were harvested and lysed in lysis buffer (50 mM Tris, pH 8.0, 250 mM NaCl, and 0.5% NP40) supplemented with sodium vanadate and Complete Protease Inhibitors (Roche, Indianapolis, IN). Lysates were isolated after centrifugation and protein concentration was measured using the Bradford Reagent (Bio-Rad, Hercules, CA). After 2× sample buffer (0.125 M Tris, pH 6.8, 4% SDS, 20% glycerol + 4% β-mercaptoethanol) was added to the lysates, each sample was boiled for at least 5 minutes at 100°C. For immunoblotting of STATs, p65, and p50, samples were loaded on an 8% poly-acrylamide gel. Proteins were resolved on the gel before they were transferred to nitrocellulose membrane, which was then blocked in 5% milk in TBST for at least 1 hour. Blots were quickly rinsed and incubated with the specific primary antibody (1:10000 dilution) overnight at 4°C. The following day, the membrane was first washed in TBST for 15 minutes, followed by 1 hour incubation with HRP (horseradish peroxidase)–labeled secondary antibody. Additional washes (3x with 5% TBST, 20 minutes per wash) were implemented and the blots were developed using ECL Western Blotting Reagent (Pierce, Rockford, IL). For multiple immunoblottings on the same membrane, antibodies directed towards phosphorylated STATs were prioritized and blots were stripped with stripping buffer (SDS, Tris) at 65°C for 30 minutes, washed with TBST, and re-blocked with 5% milk, before re-probing with antibodies against total protein levels. Antibodies used include: phospho-specific STAT3 (9131), PARP (9542) from Cell Signaling; tubulin (T-5168; Sigma); STAT3 (sc-482) from Santa Cruz Biotechnology.

Nuclear-Cytoplasmic Fractionation

Nuclear and cytoplasmic fractions were isolated using the Nuclear Extract Kit (Active Motif North America, Carlsbad, CA). Briefly, cells were obtained and transferred in ice cold 10% PBS + phosphatase inhibitor. After 5 minutes centrifugation at 4°C, the pellet was resuspended in pre-chilled 1x hypotonic buffer for exactly 15 minutes on ice. Detergent was added to each sample before the samples were vortexed for 10 seconds and centrifuged for 30 seconds at 14,000 x *g*, 4°C. After the cytoplasmic fraction was transferred to a separate tube, the pellet was mixed with Complete Lysis Buffer AM1 (with DTT and Protease Inhibitor Cocktail) via votexing for 30 seconds. The samples were then snap frozen in dry ice and thawed on ice, before they were vortexed again for 30 seconds and centrifuged for 10 minutes at 14,000 x *g*, 4°C. The protein concentration was quantified with Bradford Reagent (Bio-Rad, Hercules, CA). Analysis of the nuclear and cytoplasmic fractions followed the same procedure for immunoblots, as previously described.

Short Interfering RNA

OVCAR8 cells were transfected with 10 uM/L of STAT3 siRNA (Dharmacon, Inc, Thermo Scientific, MA), NF-κB p65 siRNA (Cell Signaling, Beverly, MA), or Control siRNA (Dharmacon, Inc, Thermo Scientific, MA) using Lipofectamine RNAi Max (Invitrogen, Inc. Carlsbad, CA) following the protocol from the manufacturer. Cells were harvested for mRNA analysis or immunoblotting 2 days or 3 days after transfection.

Viral Infections and Reagents

293Tcells were transfected with VSV-G, MLV, and STAT3–expressing vectors following the Lipofectamine 2000 (Invitrogen, Inc. Carlsbad, CA) protocol provided by the manufacturer. Supernatant was collected 24 hours, 48 hours, and 72 hours after transfection. After the supernatant was filtered with a needle top filter, it was then added to pre-plated FT33-Tag-Myc or FT33-Tag-Ras cells at a 1:1 ratio with media (+ 8 μg/mL polybrene). After incubated for 24 hours, media was removed and the FT33 cells were split and two pools were generated by infecting cells at distinct times. To ensure stable integration, cells were selected with G418 (Invitrogen, Inc. Carlsbad, CA) was added after replacement of media. For plncx2 and plncx2-STAT3 vectors, FT33 cells were selected in 2000μg/mL Geneticin for more than two weeks.

Dual Luciferase Reporter Assay

Low efficiency bacteria (H5α) was transformed with empty vector (plncx2) or luciferase reporter vectors (M67-Luc and NF-κB-Luc) and allowed to grow overnight in the dark at 37°C with ampicilin selection. After harvesting bacteria, the vectors were purified following the manufacturer's protocol with the Qiagen Midi Prep Kit (Qiagen, Hilden, Germany). The purified vectors in TE buffer was salt precipitated with 5M NaCl, sterilized with 70% EtOH, and resuspended in sterile Ultrapure water. The cells were plated (24 well plates, duplicates) and allowed 24 hours to attach before they were transfected with the purified vectors at 1mg/well, using Lipofectamine RNAi (Invitrogen, Inc. Carlsbad, CA). Six hours post transfection the media was removed and fresh media was added to each well. The following day, Dual Luciferase Reporter Assay was performed with the Promega Kit (Fitchburg, WI) and analyzed with the Luminoskan luminometer.

Gene expression analysis

Cells after appropriate treatments were harvested in pre-chilled 1x PBS and RNA was isolated using the RNeasy kit (QIAGEN, Valencia, CA). After the concentration of RNA was quantified via NanoDrop 2000 spectrophotometer (Thermo Scientific, Waltham, MA), Taqman reverse transcription kit (Applied Biosystems, Foster City, CA) was used to generate cDNA. Quantitative real-time polymerase chain reaction (qPCR) was performed using SYBR green master mix (Applied Biosystems). Each sample was plated in triplicates and a 7500 real time PCR system (Applied Biosystems) was employed for qPCR. The data analysis compared different genes in average fold change ± SE of the 3 replicates.

Scivax 3D cell culture

Plating Cell lines (FT33-Tag-Myc + STAT3C and FT33-Tag-Ras + STAT3C). Each plate was first equilibrated with DMEM/F12 50/50+ 10% FBS. After spinning down the medium, 1X10^4 cells per well were plated. Photomicrographs were taken at 72 hours post plating.

OVCAR8 RNAi. Cells were reverse transfected with 10nM siRNA to control or STAT3 using RNAi Max lipofectamine reagent following the manufacturer's protocol (Invitrogen). Medium was not exchanged during the course of the experiment. Photomicrographs were taken at 72 hours post transfection/plating.

OVCAR8 Drug treatments. OVCAR8 cells were similarly plated in Scivax 3D culture plates as described previously in RPMI + 10% FBS. Seventy-two hours after plating cells, drugs were added to make a final concentration of 1X. Images were taken 72 hours after drug treatment.

Compounds

Nifuroxazide (Chembridge), pimozide (Sigma-Aldrich), pyrimethamine (Sigma-Aldrich), paclitaxel (Nova Plus), doxorubicin (Nova Plus) celastrol (EMD Biosciences), Jak inhibitor (EMD Biosciences), CYT (kindly provided by David Barbie, DFCI), and ST3-01 analogues (Enamine) were all dissolved in DMSO at a concentration of 150 mM. The DMSO was diluted to a final concentration of 0.1% in all of our experiments.

RESULTS

STAT3 is associated with increased proliferation and spheroid formation of epithelial derived serous ovarian tumors

Since both type I and type II ovarian tumors have been thought to originate from the ovarian surface epithelium (OSE), recent studies postulates compelling models depicting the fallopian tube secretary epithelial cells (FTSEC) as the cells-of-origin for high grade serous ovarian cancers (HGSOC) (22). To test whether constitutively activated STAT3 contributes to the genomic instability and pathogenesis of ovarian cancer, we collaborated with Dr. Drapkin, whose lab piloted the transformation of primary fallopian tube cells from pathology into tumorigenic serous ovarian carcinoma by immortalization and transduction of oncogenes such as *c-Myc* and *H-Ras*. We obtained these transformed fallopian tube cell lines, the FT33-Tag-Myc and FT33-Tag-Ras cells, from Dr. Drapkin's lab. After stable transfection of STAT3C, the constitutively activated STAT3, we select with Geneticin to ensure that STAT3C was stably expressed in two individually selected pools (FIGURE 1A, FIGURE 1B). Compared to the FT33-Tag-Myc cells transformed with empty vector, we observed that without cytokine or drug treatments, the STAT3C transformed FT33-Tag-Myc cells proliferated more rapidly (FIGURE 1C). This result was consistent for two individually selected pools (FIGURE 1D), thus suggesting that constitutively activated STAT3 provides a growth advantage for enhanced malignancy to the transformed fallopian tube cells. On the contrary, the *H-Ras* transformed fallopian tube cells, FT33-Tag-Ras, grew more slowly after stable STAT3C transfection compared to those transfected with the empty vector (FIGURE 1C, FIGURE 1D). This suggests that H-Ras, the mutation of which are not seen in HGSOC (23), negatively associates with STAT3 activity. In other words, H-Ras activity may be reciprocally inhibited when STAT3 is activated and vice versa.

Having shown that STAT3C provides advantage in proliferation for FT33-Tag-Myc cells but not for FT33-Tag-Ras cells, we next wanted to evaluate the role of STAT3 in assembly and structure formation of transformed fallopian tube cells. STAT3C transfected FT33-Tag-Myc and FT33-Tag-Ras cells were plated in Scivax plates, which was designed for optimal for 3D spheroid formation. We observed that STAT3C transformed FT33-Tag-Myc cells formed spheroids (FIGURE 1E-1, 1E-2, 1E-3), whereas FT33-Tag-Ras cells did not (FIGURE 1F-1, 1F-2). This suggests that STAT3C is important for the cell-cell adhesion and therefore the overall structure of the ovarian cancer.

Moreover, consistent with the previous observation in viability, this data indicates that STAT3 and H-Ras may be negatively associated or mutually exclusive in cancer, as the activation of one pathway seems to inhibit the other. More importantly, the ability of spheroid formation may be closely associated to not only the survival and proliferation of the ovarian cancer cells, but also to the sensitivity of these cancer cells to chemotherapeutic agents *in vivo*. Therefore, this further supports the central role of STAT3 in cancer pathogenesis by both enhancing the proliferation potential and promoting the spheroid potential.

STAT3 inhibitors reduce the viability of ovarian cancer cells that have constitutively activated STAT3.

Since STAT3 is activated in most ovarian tumors, we wanted to evaluate the efficacy of these STAT3 inhibitors on ovarian cancer viability. We performed viability assays in OVCAR8 cells, which are ovarian cancer cells known to have constitutively activated STAT3. Initially, we treated OVCAR8 cells with nifuroxazide, while DMSO was used as a negative control. After 2 days or 3 days, we assessed the viability of the OVCAR8 cells via ATP-bioluminescence. At a dose of 5uM, the viability of OVCAR8 cells was reduced by 72% after 48 hours treatment, while a reduction of over 95% is observed after 72-hour treatment (FIGURE 2A). This result is consistent with the hypothesis that these ovarian cancer cells are dependent on continuous STAT3 signals for survival and proliferation and that nifuroxazide, a STAT3 inhibitor, efficiently decreases STAT3 signals, thus blocking the growth of these OVCAR8 cells.

Similarly, when nifuroxazide at 5uM was added to SKOV3 cells, which are also ovarian cancer cells contain constitutively activated STAT3, a 40% reduction was observed after 48 hours compared to that of vehicle control (FIGURE 2B). The overall efficacy is less robust in SKOV3 cells compared to OVCAR8 cells, possibly due to variability between different ovarian cancer cell lines. Nevertheless, the observed reductions in viability of both SKOV3 and OVCAR8 cells demonstrates that nifuroxazide as a STAT3 inhibitor affects the survival and growth of ovarian cancer cells that depend on STAT3 activity.

Moreover, to show that this effect is clinically relevant, we were able to isolate cells from primary ovarian tumors and grew them selectively in tissue culture. Viability assays revealed a 43% reduction

for cells obtained from Patient #2 and a 21% reduction for cells obtained from Patient #3 with nifuroxazide treatment at 5uM for 48 hours (FIGURE 2C, FIGURE 2D). This result further supports the important of STAT3 signaling in ovarian cancer cells. At the same time it also suggests that ovarian cancer is a collection of cells of heterogeneity that respond to STAT3 inhibitors in distinct ways. The disparity in sensitivity to nifuroxazide across these different ovarian cancer cells can be explained by different subsets of mutations, overlie of which includes mutations in the JAK/STAT3 pathway.

Given that nifuroxazide is effective in reduction of viability of ovarian cancer cells that depends on STAT3 activation, we next wanted to know if other STAT3 inhibitors have similar effects. We treated OVCAR8 cells with ST3-01 and CYT, which are two additional inhibitors of STAT3 discussed earlier. Decreases in cell viability were observed with both drugs. More specifically, a reduction of at least 40% at 5uM after 48 hours treatment was observed (FIGURE 2E, FIGURE 2F), implying that STAT3 activity is critical for the survival of these ovarian cancer cells. However, ST3-01 treatment did not result in significant reduction of viability in primary ovarian cancer cells from patients (FIGURE 2G). This difference again can be explained by the phenotypic and genotypic heterogeneity of ovarian cancers (24).

Not all STAT3 inhibitors block the STAT3 function via inhibition of STAT3 phosphorylation.

Given that these inhibitors are effective in reducing the viability of STAT3 dependent ovarian cancer cells, we then aimed to investigate the mechanisms of these STAT3 inhibitors. Since it was known that some STAT3 inhibitors such as nifuroxazide prevent the phosphorylation of STAT3, we performed western blot analysis with phospho-STAT3 antibody to detect changes in STAT3 phosphorylation post 24-hour treatment of different STAT3 inhibitors. Janus kinase inhibitor (JAK-I), which directly inhibits the phosphorylation of the Janus kinase (JAK) upstream of STAT3, was used as a positive control. Comparing to JAK-I, nifuroxazide seemed to block STAT3 phosphorylation in OVCAR8 cells directly, which is similar to how it acts in multiple myeloma cells (FIGURE 3A). Similarly, CYT blocked STAT3 phosphorylation via inhibition of JAK, as expected (FIGURE 3B**).** By contract, ST3-01 treatment did not affect the phosphorylation of STAT3, suggesting that other mechanisms may be involved.

We decided to also test additional panel of drugs in SKOV3 cells and in HeLa cells, including ST3-01A and ST3-01B, which are analogues of ST3-01 also developed in our lab. The panel also includes: atovaquone (AQ), which is currently used as prophylaxis for cancer patients and have been shown to inhibit STAT3 phosphorylation in many hematologic cancer cell, pimozide, which is a psychotropic drug shown to have STAT5 inhibitory effect (25), and pyrimethamine, which is an antimalarial compound that has been identified as a STAT3 inhibitor in polycystic kidney diseases (26). According to the analysis of phospho-STAT3 levels, only CYT seemed to block STAT3 phosphorylation in SKOV3 cells (FIGURE 3C), whereas in HeLa cell a reduction in phosphorylation of STAT3 was observed with all drugs except for pyrimethamine (FIGURE 3D). One possible explanation is that the effects of pimozide, pyrimethamine, and atovaquone are more transient in SKOV3 cells, whereas the effect of CYT is more prolonged and sustained. Alternatively, different cells lines with different subsets of mutated signaling molecules could respond to STAT3 inhibitors differently. For example, in SKOV3 cells, additional or unconventional pathways can be activated or inhibited by these inhibitors via direct or indirect routes and that can lead to rescue of STAT3 phosphorylation. Moreover, the decrease in STAT3 phosphorylation in HeLa cells with ST3-01A and ST3-01B can be secondary or even tertiary effects from the interplay of multiple pathways.

STAT3 inhibitors disrupt cell-cell adhesion and formation of spheroids in ovarian cancers.

Knowing that STAT3 activation contributes to the spheroid formation of *c-Myc* transformed fallopian tube cells, we wanted to further test the effect of STAT3 inhibitors on spheroid formation of ovarian cancer cells that depends on constitutively activated STAT3. OVCAR8 cells were plated on Scivax plates and incubated for 72 hours to allow spheroid formation. Vehicle and STAT3 inhibitor ST3-01were then added to wells containing OVCAR8 spheroids. After 72 hours treatment, the shape and structure of the spheroids were re-assessed under the microscope. Compared to the cells treated with vehicle (FIGURE 4A), the spheroid structure formed prior to ST3-01 treatment seemed to be disrupted (FIGURE 4B), suggesting that STAT3 activity is important for spheroid formation of ovarian cancer cells.

Similarly, OVCAR8 cells were plated and reversely transfected with STAT3 RNAi to reduce the intracellular levels of STAT3. The spheroids formed with control siRNA appeared to be well organized (FIGURE 4C-1, 4C-2), whereas the spheroid structure seemed to be disrupted with STAT3 RNAi. Even though there remained some visible 3D spheroid-like structures with STAT3 RNAi, but the spheroids were irregular (FIGURE 4D-1), as they appeared to be loosely arranged and unorganized (FIGURE 4D-2). This may be due to a reduction of cell-cell adhesion when STAT3 is inhibited, suggesting the crucial role of STAT3 in not only individual cells but in the overall tumor formation and structure. Furthermore, all of these observations indicate that both STAT3 inhibitors such as ST3-01 and STAT3 RNAi may disrupt the gross configuration, organization, and arrangement of the ovarian cancer spheroids, therefore affecting the proliferation, expansion, and metastasis of ovarian cancer cells.

STAT3 inhibition via STAT3 RNAi leads to upregulation of IL-8.

Given that STAT3 inhibitors are potent in killing ovarian cancer cells, we proposed that ovarian cancer cells with constitutively activated STAT3 relied extensively on STAT3 signals for their survival and proliferation. To further confirm the importance of STAT3 in ovarian cancer cells, STAT3 RNAi was used to significantly reduce the intracellular levels of STAT3 in OVCAR8 cells. After 2 days or 3 days following transfection of STAT3 RNAi, cell viability was subsequently evaluated. Surprisingly, with significant reduction in both phosphorylated STAT3 (pSTAT3) and total STAT3 (tSTAT3) protein levels (FIGURE 5A-1), no significant reduction in cell viability was observed (FIGURE 5A-2). Given that STAT3 plays such an essential role in ovarian cancer cells, we performed Real-Time PCR (qPCR) to assess the levels of known endogenous STAT3 target genes. Unexpectedly, many of the STAT3 target genes are upregulated when STAT3 levels are reduced in cells 24 hours post transfection (FIGURE 5B-1, 5B-2, 5B-3). This result suggests that alternative pro-survival pathways may be activated when STAT3 levels are reduced.

To determine whether this gene upregulation effect is globally present in the ovarian cancer cells due to some off-target effects of STAT3 RNAi, we then analyzed a panel of endogenous STAT3 target genes in OVCAR8 cells transfected with SiSTAT3. Out of the panel of nine genes, four genes (SOCS1, SOCS3, survivin and VEGF) were downregulated, whereas two genes (Bcl-2 and KLF4) are upregulated to different extents (FIGURE 5C). This demonstrates that a reduction of

intracellular STAT3 levels does not lead to global upregulation of all genes, since suppressor of cytokine signaling 3 (SOCS3), which is a well-characterized STAT3 target gene, is downregulated with STAT3 RNAi as expected. In addition, we observed that A20, a known NF-κB target gene, as well as IL-8, were up regulated, suggesting that the mechanism of STAT3 inhibition is complex and may involve alternative pathways.

Furthermore, the fact that IL-8 in particular was upregulated by about 8-fold appeared to indicate a potential significance of this upregulated gene. To address this interesting point, we repeated the STAT3 RNAi experiment and performed qPCR to examine the levels of IL-8 in OVCAR8 cells 24 hours, 48 hours, and 72 hours post transfection. In all three time points, IL-8 was upregulated and the upregulation appeared to gradually augment with the length of the STAT3 knock-down (FIGURE 5D). Since levels of IL-8 have been suggested in ovarian cancer cells to associate with increased malignancy and metastasis (15), investigating this considerably enhanced IL-8 gene may provide valuable insights to how STAT3 inhibition can affect these cells. Additionally, previous findings have shown that enhance STAT3 activities associate with higher IL-8 levels in fibroblasts, indicating that STAT3 is an activator for IL-8 gene expression (27). However, STAT3 can also act as a negative regulator for IL-8 in glioblastoma, making the role of STAT3 for IL-8 expression less clear (28). Overall, the specific role of STAT3 is likely to be cell-specific and gene-specific, as STAT3 behaves differently in distinctive types of cells to regulate various target genes. Alternatively, besides the more direct relationship between STAT3 and IL-8, it is possible that one or more additional signaling pathways are altered when STAT3 is inhibited, resulting in the increased IL-8 expression.

STAT3 inhibitors such as ST3-01 can also lead to upregulation of IL-8.

Given that IL-8 is upregulated when STAT3 levels are reduced through STAT3 RNAi, we wanted to decrease STAT3 activity in OVCAR8 cells via a different method using STAT3 inhibitors. The novel STAT3 inhibitor, ST3-01, and JAK inhibitor (JAK-I) were added to naïve OVCAR8 cells for a time course analysis of STAT3 target gene expression profile. The purpose was to see if a STAT3 inhibitor or an inhibitor of the step upstream of STAT3 can recapitulate the effect of STAT3 RNAi. Six hours post treatment, IL-8 levels already started to increase compared to the control gene (GAPDH) (FIGURE 6A), while the other STAT3 target genes remained mostly unchanged. After

12 hours, we observed upregulations of IL-8 and a panel of STAT3 target genes including BCL3, BCL6, Bcl-xL, and MCL1(FIGURE 6B). The pattern was similar to STAT3 RNAi qPCR data, but the magnitude of upregulation was much smaller. However, after 24 hours treatment, the panel of STAT3 target genes gradually began to decline, whereas IL-8 levels remained upregulated by 1.8-fold (FIGURE 6C). Finally, 48 hours post ST3-01 treatment, two of the STAT3 target genes: BCL3 and BCL6, became upregulated again for 1.73-fold and 3.32-fold, respectively. Similarly, IL-8 upregulation continued with 3.94-fold (FIGURE 6D). Considering the trend of IL-8 upregulation, ST3-01 seemed to replicate the effect of STAT3 RNAi, although the amplitude was less prominent. This further suggests that STAT3 may be regulating IL-8 expression either directly as a suppressor of the IL-8 gene, or indirectly via activation or inhibition of alternative pathways. One potential candidate is the NF-κB pathway, which is known to regulate IL-8 gene expression as it also plays a key role in inflammation, survival, and growth of cells (29).

IL-8 upregulation is specific to STAT3 inhibition.

It has been shown that small interference RNA can lead to double stranded RNA (dsRNA) formation in the cytoplasm, which can potentially trigger the anti-viral response that can lead to global upregulation of genes (30). More specifically, when the dsRNA is recognized by cells as virus mistakenly, aberrant IFN-γ, or type II interferon, will be released, leading to rapid and robust cytokine release (31). To address this potential problem, we stimulated OVCAR8 cells with IFN-γ for 1 hour or 3 hours, and then analyzed gene expression levels. Analysis of phosphorylated STAT1 (pSTAT1) levels indicated an induction of pSTAT1 in OVCAR8 cells stimulated with IFN-γ, which was consistent with the fact that IFN-γ is known to activate STAT1 **(FIGURE 7A**). Moreover, SOCS1, which is a known STAT1 target gene, was upregulated by 2.4-fold 1-hour post IFN-γ stimulation and 3.9-fold 3 hours post IFN-γ stimulation, as expected. In addition, qPCR data illustrated that while some of the STAT3 target genes were upregulated (BCL3 and BCL-xL), IL-8 was downregulated with IFN-γ stimulation, indicating that IFN-γ release in response to the dsRNA does not result in IL-8 upregulation. This suggests that IL-8 is not upregulated by non-specific dsRNA effects (FIGURE 7B).

To ensure that the IL-8 gene upregulation is specific to STAT3 RNAi and is not a generalized phenomenon, OVCAR8 cells were transfected with STAT3 RNAi, a small interference RNA for a

phosphatase N6 (SiPTP), and a small interference RNA for Jak kinase 2 (SiJAK). qPCR analysis revealed that IL8 was upregulated by 9.0-fold and 6.6-fold with SiSTAT3 and SiJAK, respectively, whereas SiPTP had no effect on IL-8 levels (FIGURE 7C). Furthermore, another well-characterized NF-κB gene, A20 (also, TNFaIP), is upregulated by 1.2-fold with SiSTAT3 and 1.9-fold with SiJAK, but no upregulation is observed for SiPTP. This further demonstrates that IL-8 upregulation is related to reduction of STAT3 levels.

Having shown that the STAT3 RNAi effects on IL-8 upregulation were specific, we next evaluated whether the correlation between STAT3 and IL-8 is specific if STAT3 is inhibited by commonly used chemotherapeutic agents. Naïve OVCAR8 cells were treated with two chemotherapeutic agents and the resulting gene expression profiles were compared: Doxorubicin, which is a widely used drug, kills rapidly dividing cancer cells by intercalating nonspecifically in DNA (32). Paclitaxel, an anti-mitotic drug for chemotherapy, has been shown to reduce STAT3 activity via destabilizing the interaction between STAT3 and microtubule. After 24 hours, qPCR result confirmed that doxorubicin, a relatively non-specific agent, failed to cause an upregulation of IL-8, whereas paclitaxel, which reduced STAT3 target genes at a concentration of 0.1uM, lead to a 219-fold upregulation of IL-8 (FIGURE 7D). Interestingly, the extent of IL-8 induction was dose-dependent for paclitaxel, as a larger increase in IL-8 levels associated with higher dose of paclitaxel. This further suggests that this reciprocal relationship between the mRNA level of IL-8 and the activity of STAT3 is important and specific.

IL-8 upregulation caused by STAT3 inhibition may be a marker for NF-κB pathway activation.

Since IL-8 upregulation is correlated with STAT3 inhibition in OVCAR8 cells, we hypothesize that either STAT3 negatively regulates IL-8 gene or alternative pathways were activated. Previously, we found that not only IL-8, but also some of the STAT3 target genes such as BCL3, BCL6, and Bcl-xL were upregulated when STAT3 was inhibited via STAT3 RNAi. This suggests that the activation of another pathway is likely to cause the unexpected upregulation of many genes. Since IL-8 and these other target genes are well-known target genes for the NF-κB pathway, which is characterized as pro-inflammatory and pro-survival, we propose that NF-κB pathway may lead to IL-8 upregulation.

To confirm that IL-8 is an NF-κB target gene in OVCAR8 cells, we stimulated OVCAR8 cells with tumor necrosis factor alpha (TNFα), which is a cytokine that activates the NF-κB pathway (33). Significant upregulations of some of the NF-κB target genes including BIRC3, p105, and RelA are identified through qPCR (34). More specifically, 3 hours post TNFα stimulation, the NF-κB target genes p105 and RelA were upregulated by 10-fold and 7.6-fold, respectively, while BIRC3 upregulation has reached a 2500-fold, strongly supporting the activation of NF-κB pathway (FIGURE 8A-1). Further evidence is the well-known NF-κB target gene A20, which was induced by 47-fold 30mins post TNFα stimulation. This activation of NF-κB then resulted in an upregulation of IL-8, which peaked over 4000-fold, strongly indicating that IL-8 is an NF-κB target gene in OVCAR8 cells TNFα (FIGURE 8A-2).

To validate further that upregulation of IL-8 is a result of NF-κB activation, we activated NF-κB via an alternative way. Instead of stimulating with TNFα, we seek by overexpressing NF-κB subunits in OVCAR8 cells. To identify the subunit that most effectively activates NF-κB when overexpressed, we overexpressed a panel of NF-κB subunit vectors in NF-κB-Luc cells, which is a cell line that has NF-κB promoter linked to a luciferase gene. More specifically, when NF-κB is activated, the luciferase stably expressed in the NF-κB-Luc cells and the extent of NF-κB activation directly correlates to the intensity of the luciferase signal, making NF-κB-Luc cells a good system to study NF-κB activity (13). The panel of NF-κB subunits vectors consisted of p50, RelA/p65, and RelB, which are three different NF-κB subunits. Comparison of the luciferase activity 24 hours post transfection in the NF-κB-Luc cells revealed that RelA expression was most effective in activating NF-κB pathway, with a signal 8.2-fold above the empty vector, and almost 4-fold above the positive control (TNFα stimulation) (FIGURE 8B). In addition, P50 and RelB overexpressions appeared to also cause NF-κB activation, producing luciferase signals comparable to that produced by TNFα stimulation. This result was consistent with the upregulation of NF-κB target genes (BIRC3 and NFkBIE) and the levels of I-κB protein, which is thought to correlate with the level of NF-κB activity (FIGURE 8C).

Having identified RelA as the most effective NF-κB activating subunit, we transfected and overexpressed RelA subunit in OVCAR8 cells, while p50 and empty vectors were transfected as controls. Twenty-four hours post transfection, we analyzed two of the NF-κB genes A20 and IκB. It was clearly shown by qPCR data that overexpression of RelA led to upregulation of A20, since A20 was upregulated by 3.6-fold (FIGURE 8D). Moreover, I-κB was upregulated by 2.5-fold, further indicating the activation of the NF-κB pathway. In addition, we also analyzed a panel of STAT3 target genes and observed a general trend of upregulation. More explicitly, the upregulation of BCL3, BCL6, and MCL1 could be explained by the fact that while they are STAT3 target genes, they may also be regulated by the NF-κB pathway (see discussion). Furthermore, qPCR data for gene expression 48 hours post transfection showed upregulation of IL-8 and A20 (FIGURE 8E). In both cases, corresponding to the activation of NF-κB pathway, IL-8 is induced by 23-fold and over 30-fold 24 and 48 hours post transfection, respectively. These overexpression studies further demonstrate that IL-8 is a NF-κB target gene in ovarian cancer cells.

NF-κB activation is related to STAT3 inhibition in both OVCAR8 cells and in primary ovarian cancer cells.

To further prove that the NF-κB pathway reciprocally activates in response to STAT3 inhibition, we first inhibited the STAT3 pathway via STAT3 RNAi and then used the dual luciferase reporter assay to directly study the NF-κB and STAT3 promoter activity globally. OVCAR8 cells were co-transfected with wildtype *Renilla* control reporter vector that provides constitutive expression of *Renilla* luciferase, and the vector of a promoter of interest fused to a luciferase reporter. In our case, the promoter vectors of interest were the NF-κB-Luc and M67-luc, corresponding to the NF-κB and STAT3 promoters, respectively. After normalizing the luciferase signals of the promoter vectors to that of the *Renilla* vector, the STAT3 dependent reporter activity was reduced by 81% with STAT3 RNAi, indicating that the STAT3 transcriptional activity has been reduced. Reciprocally, the NF-κB dependent reporter activity was induced by 1.6-fold, suggesting an increase in NF-κB activity (FIGURE 9A).

Similarly, we analyzed promoter activity via dual luciferase assay in OVCAR8 cells that were treated with STAT3 inhibitors. We observed that for both 24 hours and 30 hours of treatment, the STAT3 dependent luciferase reporter activities were reduced by about 10-20%, implying to a decreased STAT3 promoter activity. Conversely, the NF-κB luciferase reporter activity was induced by 20% with JAK-I treatment (FIGURE 9B), further suggested that NF-κB activation is due to STAT3 inhibition.

Having shown that NF-κB may be activated when STAT3 is inhibited in OVCAR8 cells, we next examined this reciprocal relationship in cells obtained from ovarian cancer patients. We first observed that cells from Patient #2 contained constitutively phosphorylated STAT3 that was effectively inhibited by 1 hour JAK-I treatment (FIGURE 9C-1). Next, we treated these cancer cells from Patient #2 with two doses of ST3-01. After 24 hours treatment, qPCR detected a clear and consistent upregulation of NF-κB genes including BIRC3, CCL5, NFkBIE, p105, RelA, and A20, suggesting that STAT3 inhibition in primary ovarian patient cells also leads to activation of the NF-κB pathway (FIGURE 9C-2).

Subsequently, we wanted to inhibit STAT3 via RNAi in ovarian cancer cells obtained from patients. When cells from Patient #3 were transfected with STAT3 RNAi for 72 hours, the constitutively activated STAT3 protein levels were significantly reduced (FIGURE 9D-1), as were STAT3 mRNA levels as quantified via qPCR analysis. Correspondingly, STAT3 target genes such as BCL3 and SOCS3 showed significantly reduced expression levels, as expected. On the contrary, NF-κB target genes such as BIRC3, MAP3K, and CCL5 were upregulated. Particularly, CCL5 encodes a chemokine protein that plays an active role in leukocyte recruitment to inflammatory sites. Previously identified as a NF-κB target gene, CCL5 was activated by 10.9-fold (FIGURE 9D-2). All of the above findings provided strong evidence that the NF-κB pathway may be reciprocally related to STAT3 pathway.

A reciprocal relationship between NF-κB activity and STAT3 activity exists in ovarian cancer cells.

Having shown that NF-κB activation was likely related to STAT3 inhibition, we stimulated OVCAR8 cells with IL-6 to increase STAT3 activity and examine the NF-κB response. Based on the qPCR analysis, most of the STAT3 target genes are upregulated (BCL3: 1.85x, BCL6: 1.23x, Bcl-xL: 2.43x) 3 hours post stimulation, whereas IL-8 was downregulated by 64% (**FIGURE 10A**). This again supports the previous observation that STAT3 activation leads to reduction of NF-κB signaling. To ensure that this phenomenon is not specific only to IL-6 stimulation, we tested a set of NF-κB target genes in response to stimulations of a panel of cytokines including IL-6, Leukemia inhibitory factor (LIF), which is a IL-6 class protein that is thought to activate STAT3, and Oncostatin M (OSM), which is a pleotropic cytokine that belongs to the IL-6 family. All three cytokines have been shown to activate the JAK/STAT pathway, particularly STAT3 (35). The result demonstrated that in general, the STAT3 activating cytokines OSM and LIF either generated minimal change or led to downregulation of NF-κB target genes, suggesting that a reciprocal relationship between the NF-κB and STAT3 pathways may exist. More specifically, for example, NFkB2 gene is downregulated by 71% and 64% with OSM and LIF treatment, respectively (FIGURE 10B). However, IL-6 stimulation, which led to a downregulation of IL-8, resulted in upregulation of some of the NF-κB target genes. This unexpected result can be explained by the fact that IL-6 is regulated by NF-κB subunit p65 and can alter the NF-κB activity under certain conditions (36).

To investigate whether this reciprocal relationship applies to STAT3 when NF-κB is altered in cancer cells, we activated the NF-κB pathway in OVCAR8 cells by overexpressing NF-κB subunits including p50, RelA/p65, and RelB. The luciferase signal of the promoter was carefully normalized to the *Renilla* signal and the ratio was used for comparison. As we anticipated, RelA was more effective in activating NF-κB, as the NF-κB luciferase reporter activity was induced by 246-fold above the empty vector. Reciprocally, STAT3 promoter activity was reduced by 70% with RelA overexpression, indicating that STAT3 may be inhibited when NF-κB is activated (FIGURE 10C). In this case, since RelA led to a very significant upregulation of NF-κB promoter activity, it was possible that most of the transcriptional machinery proteins such as RNA polymerase II and associated transcription factors were recruited to the NF-κB promoter sites, leaving the STAT3 promoter sites relatively unoccupied and thus inactive. This can also explain why the

overexpressions of p50 and RelB appears to not activate NF-κB promoter activity significantly, but they seem to correlate to a diminished M67 luciferase reporter signal, or a reduction in STAT3 promoter activity.

The reciprocal relationship between NF-κB and STAT3 is also observed in Renal Cell Carcinoma with constitutively activated STAT3.

To demonstrate that this reciprocal relationship between NF-κB and STAT3 pathways is not limited to ovarian cancer cells, we selected three renal cell carcinoma (RCC) cell lines and treat them with JAK-I for 3 hours. Analysis of phosphorylated STAT3 demonstrated that RCC769 cells have no constitutively activated STAT3, whereas RCC786 cells and A498 cells contain various amount of pSTAT3, which was successfully inhibited by JAK-I (FIGURE 11A). Next, levels of STAT3 target genes and IL-8 were analyzed. In cells with activated STAT3, RCC786 cells appeared to be no significant changes in STAT3 and NF-κB target gene expression, possibly due to the fact that this was an early time point (FIGURE 11B-1). However, the pattern of gene expression in A498 cells was very similar to that of OVCAR8 cells, with BCL3, BCL6, Bcl-xL and MCL1 all reduced and IL-8 upregulated by 3.3-fold (FIGURE 11B-2). A20 was slightly downregulated in this case, but it can be a late NF-κB target gene and has not yet been upregulated. Overall, this conveys that the NF-κB pathway is activated when STAT3 is inhibited not only in ovarian cancer cells but also in kidney cancer cells.

Next, we perform STAT3 RNAi in all three RCC cell lines. Seventy-two hours post transfection, STAT3 protein levels were significantly reduced in all three cell lines (FIGURE 11C). We noticed that the reciprocal relationship was shared between ovarian cancer cell lines and RCC cell lines. However, only in cells with constitutively activated STAT3 did we detect the NF-κB activation responding to STAT3 inhibition. For example, in RCC769 cells that don't depend on activated STAT3, IL-8 upregulation was not observed when STAT3 pathway was inhibited (FIGURE 11D-1). On the contrary, IL-8 was upregulated by 1.66-fold in RCC786 cells, which had the most activated STAT3 at baseline (FIGURE 11D-2). Similarly to the RCC786 cells, STAT3 target genes were reduced with STAT3 RNAi, while IL-8 was upregulated by 2.57-fold (FIGURE 11D-3) in A498

cells that had moderate levels of pSTAT3. All of these data indicates that this reciprocal relationship probably only applies to cancer cells that depend on constitutively activated STAT3.

NF-κB subunit p65 translocates into the nucleus upon NF-κB activation.

To investigate the mechanism of NF-κB activation upon STAT3 inhibition, we focused on one very important NF-κB subunit p65, since in previous findings the overexpression of p65 more effectively activated NF-κB pathway compared to that of the other NFκB subunits. In the canonical pathway, when NF-κB is activated, p65 translocates into the nucleus and regulates gene expression. To detect any potential p65 nuclear translocation when NF-κB is activated in ovarian cancer cells, we performed nuclear-cytoplasmic fractionation, which separated the nuclear compartment from the cytoplasmic fraction. OVCAR8 cells were first stimulated with IL-6, TNFα, and a combination of both cytokines for 30mins, 60mins, and 90mins, and the separated nuclear and cytoplasmic fractions were then analyzed by western blot. The result was evident in that pSTAT3 translocated into the nucleus with IL-6 stimulation and both p65 and p50 translocated into the nucleus upon TNFα stimulation (FIGURE 12A). IL-6 stimulation also led to an overall increase in the levels of pSTAT3, both in the nucleus and in the cytoplasm. However, in this case activated STAT3 led to no apparent decrease in nuclear translocation of p65 or the overall levels of p65, nor did activated NF-κB affect pSTAT3 nuclear translocation. Similarly, in SKOV3 cells, a nuclear-cytoplasmic fractionation reveals that STAT3 is phosphorylated as it translocates into the nucleus. Correspondingly, the nuclear translocation of P65 and p50 are also obvious when SKOV3 cells are stimulated with TNFα (FIGURE 12B).

NF-κB subunit P65 is crucial for the NF-κB activity and NF-κB target gene expression.

Knowing that p65 nuclear translocation follows immediately after NF-κB activation, we reduced the levels of p65 subunits in OVCAR8 cells to examine if p65 was important for NF-κB activity. We used a small interference RNA specific for p65 and co-transfect it with STAT3 RNAi, which was known previously to induce NF-κB gene expression. Compared to the Control RNAi, we detected an over-99%-reduction of STAT3 protein levels with STAT3 RNAi and an over-90%-reduction of

p65 protein levels with p65 RNAi (FIGURE 13A). We next performed the dual luciferase assay to analyze the STAT3 and NF-κB activities. Three days post transfection, a reduction of p65 levels in OVCAR8 cells results in a 72%-reduction of NF-κB luciferase reporter signal (FIGURE 13B), whereas it was moderately induced by STAT3 RNAi alone, consistent with previous findings. Moreover, the dual STAT3 and p65 RNAi weakened the NF-κB dependent reporter luciferase signal compared to that of STAT3 RNAi alone. This suggests that a reduction of p65 levels abrogates the NF-κB activation correlated to STAT3 inhibition.

We noted that p65 RNAi appeared to result in a consequential decrease in the M67 luciferase reporter signal. Since IL-6 can be a potential p65 target gene, a decline in p65 protein levels may result in reduced IL-6 gene expression. Because as an important cytokine, the secretion of IL-6 facilitates the activation of gp130 receptor and phosphorylation of JAK/STAT3, a diminished IL-6 level probably directly relates to an abatement of the level of pSTAT3 and thus the decreased STAT3 promoter activity.

To understand how important p65 subunit is for NF-κB activation when STAT3 is inhibited, we implemented qPCR following the co-transfection of p65 RNAi and STAT3 RNAi to inspect the target gene levels. After 72 hours of knock-down, we examined the NF-κB target genes in response to a combination treatment of STAT3 RNAi and p65 RNAi. qPCR analysis showed a very consistent pattern across the panel of NF-κB target genes. Particularly, STAT3 RNAi leads to upregulation of NF-κB target genes, whereas p65 RNAi leads to moderate to significant reduction of the NF-κB target genes. Interestingly, the combination of STAT3 RNAi and p65 RNAi reduced or almost abolished the effect of NF-κB target gene upregulation corresponding to STAT3 RNAi alone. This suggests that the increased NF-κB activity corresponding to STAT3 inhibition is diminished by a reduction of p65. For example, IL-8 was upregulated by 14-fold with STAT3 RNAi, whereas p65 RNAi completely eliminated IL-8 gene expression, denoting the importance of p65 in IL-8 expression. With the combination of STAT3 and p65 RNAi, the mRNA levels of IL-8 remained very low: about less than 2% compared to that of STAT3 RNAi alone (FIGURE 13C-1). This demonstrated that p65 RNAi prevented the upregulation of IL-8 in response to STAT3

inhibition via STAT3 RNAi. Therefore p65 probably plays a central role in this reciprocal relationship between STAT3 and NF-κB pathways.

Next, we notice that the STAT3 target genes have a very generalized pattern, in which there is a greater reduction of STAT3 target genes with p65 RNAi alone compared to that of STAT3 RNAi alone or the dual RNAi. For example, MCL1 mRNA level remain unchanged with STAT3 RNAi, but has shown a 50%-reduction with p65 RNAi alone and a 40% reduction with the dual STAT3/p65 RNAi (FIGURE 13C-2). The reason behind this can be explained from two perspectives: 1. Many of these so-called STAT3 target genes, namely BCL3, BCL6, Bcl-xL, and MCL1 can potentially be co-regulated by NF-κB. Therefore knocking down p65 leads to a downregulation of these genes, but the extent of downregulation varies because they are regulated by p65 to different degrees. More specifically, the balance between STAT3 and NF-κB regulation differs because even though a specific gene responds to both STAT3 and NF-κB , the relative expression levels when STAT3 and NF-κB are activated differ for different genes. 2. p65 is a transcriptional regulator of IL-6 gene, which directly relates to the levels of activated STAT3. Therefore, p65 RNAi abates the STAT3 activity, leading to a reduction of STAT3 target genes. SOCS3, the negative regulator of STAT3, is thought to be a more "pure" STAT3 target gene, therefore it shows a 40% reduction in response to STAT3 RNAi and a 5% reduction in response to the dual RNAi.

To ensure that this effect is not due to a particular sequence of STAT3 RNAi, we conducted the same experiment using a different STAT3 siRNA. This STAT3 RNAi was shown to also effective reduce STAT3 protein levels (FIGURE 13D). Dual luciferase assay produced a very similar pattern, showing an augmented NF-κB luciferase reporter activity by 2.45-fold with STAT3 RNAi and a 7-fold reduction in response to p65 RNAi. Moreover, when the cells were treated with a combination of STAT3 RNAi and p65 RNAi, a decreased level of NF-κB luciferase reporter activity with was observed, suggesting that p65 RNAi abrogates the increase in NF-κB activity corresponding to decreased STAT3 activity (FIGURE 13E).

Similar pattern was also observed for the gene expression analysis for both STAT3 target genes **(FIGURE 13F-1**) and NF-κB target genes **(**FIGURE 13F-2) when using this STAT3 SiRNA

(STAT3 RNAi #2). Specifically, all of the NF-κB target genes showed expected upregulations with STAT3 RNAi alone and their levels decreased with different magnitudes with p65 RNAi alone. More importantly, with a combination of STAT3 RNAi and p65 RNAi, the expression levels of NF-κB target genes were considerably lower compared to STAT3 RNAi alone. More specifically, the levels of NF-κB target genes with the combination RNAi treatment always fall in between the levels of STAT3 RNAi alone and p65 RNAi alone. Since a reduction in NF-κB subunit p65 demolished the effects of STAT3 inhibition, this further supports the theory that NF-κB and STAT3 pathways maybe reciprocally related. Furthermore, p65 seems to be a critical link for NF-κB activation when STAT3 is inhibited.

No significant p65 nuclear translocation is observed when STAT3 is inhibited.

Knowing that p65 is important for NF-κB function and may be the key to the crosstalk between NF-κB and STAT3, we next wanted to inspect p65 nuclear translocation when STAT3 was inhibited as a more direct way to ascertain that p65 subunit activity was linked to STAT3 inhibition.

In all of our earlier experiments, we have examined the effect of STAT3 inhibition in a population of cancer cells. To ensure that the translocation of p65 occurs as a generalized phenomenon and does not happen for only a subset of cells in the population, we collaborated with Dr. Gaudet lab in tagging p65 protein with GFP and stably transfecting the fusion vector into naïve HeLa cells. This florescent p65 can be visualized directly under microscope, but it remains inactive without TNFα stimulation. This specific HeLa p65EGFP cell line allows us to observe and quantify the translocation of p65 a single cell level upon TNFα stimulation. Evident from the microscopic image, p65 remained in the cytoplasm for all naïve HeLa p65EGFP cells (FIGURE 14A-1**)**. As soon as TNFα was added to the HeLa cells, the fluorescent signal streamed into the nucleus, indicating nuclear translocation of p65 (FIGURE 14A-2). Furthermore, we noticed that for HeLa p65EGFP cells, the effect of TNFα stimulation was not transient but lasted for a few hours (FIGURE 14A-3). Even two hours post TNFα stimulation, p65 nuclear translocation still occurred to all cells, denoting the activation of the NF-κB pathway.

Studying at a single cell level provided us the advantage of visualizing physical p65 nuclear translocation and enabled us to conclude whether p65 nuclear translocation happened in majority of cells. Therefore, single cell microscopy allowed us to gain a better understanding of how many cells in a population responded to particular stimuli (TNFα or STAT3 inhibition) by activating the NF-κB pathway. Since we have tested p65 nuclear translocation in HeLa p65EGFP with TNFα stimulation, the next question we wanted to answer was whether there would be p65 nuclear translocation when cells were treated with STAT3 inhibitors. We treated HeLa p65EGFP cells with ST3-01 and the nuclear translocation of p65 was carefully monitored up to 22 hours post treatment. However, compared to the TNFα stimulated HeLa cells, which were used as positive controls, there seemed to be no apparent nuclear translocation of p65 with ST3-01 treatment (FIGURE 14B).

We next studied the p65 nuclear translocation in a population by treating OVCAR8 cells with a panel of various STAT3 inhibitors including JAK-I, nifuroxazide, ST3-01, pimozide, and pyrimethamine. Lastly, we also treat OVCAR8 cells celastrol, a natural compound isolated from root extracts of *Tripterygium Wilfordi* that is thought to have anti-inflammatory action by inhibiting the NF-κB pathway (37). The panel of drugs was selected because we wanted to test whether p65 nuclear translocation is specific for a STAT3 inhibitor. In other words, the magnitudes of p65 nuclear translocation in response to these different STAT3 inhibitors with various mechanisms of action were compared via nuclear-cytoplasmic fractionation. We treated cells initially for 6 hours and then separated their nuclear and cytoplasmic fractions to capture any early nuclear translocations of p65. An analysis of the p65 antibody showed that there was some p65 nuclear translocation with ST3-01, nifuroxazide, and pyrimethamine treatment compared to that of DMSO treatment. However, there was also an increase in band intensity for celastrol treated cells, which contradicted our prediction (FIGURE 14C).

Since our previous drug treatments and STAT3 RNAi experiments were done over a period of at least 24 hours to observe a change in NF-κB activity, we then treated OVCAR8 cells with the same panel of drugs for 24 hours and performed nuclear-cytoplasmic fractionation. A slight increase in the amount of p65 following JAK-I and ST3-01 treatment was observed. However, comparing to the intensity of nuclear p65 band when OVCAR8 cells were stimulated with TNFα in previous experiments, the nuclear translocation was minimal (FIGURE 14D). This suggests that p65 nuclear

translocation may not be responsible for the NF-κB activation in response to STAT3 inhibition, even though in the canonical pathway p65 rapidly translocates into the nucleus following NF-κB activation (i.e. due to TNFα stimulation). In addition, we repeated this experiment in SKOV3 cells for 16 hours of drug treatment, and the results showed a similar pattern. More specifically, there appeared to be a slight increase in the amount of p65 translocated into the nucleus following JAK-I, ST3-01, pimozide, pyrimethamine, and celastrol (FIGURE 14E). However, the level of nuclear p65 was not remarkable, indicating again that p65 may not be the major contributor for the NF-κB activation due to STAT3 inhibition. Other subunits of NF-κB as well as some of the STAT3 target genes that are co-regulated by NF-κB can be considered for future experiments.

To further confirm that there is no significant p65 translocation into the nucleus when STAT3 is inhibited, we employed STAT3 RNAi and p65 RNAi to inhibit STAT3 and NF-κB activities separately and in combination in OVCAR8 cells. Cells were harvested 72 hours post transfection and the nuclear and cytoplasmic fractions were separated and analyzed. Analysis of STAT3 antibody and p65 antibody demonstrated knock-down of STAT3 and NF-κB, but no significant p65 nuclear translocation was observed following STAT3 RNAi (FIGURE 14F). This suggests that alternative mechanisms besides p65 nuclear translocation probably link NF-κB activation and STAT3 inhibition in these cells.

DISCUSSION

As one of the members in the family of signal transducers and activators of transcription (STATs), STAT3 signaling is normally tightly regulated by various negative feedback mechanisms, which results in transient downstream effects. However, mutations in the STAT3 pathway that lead to either constitutively activated STAT3 or ablate the negative feedback mechanisms result in prolonged STAT3 signaling, which is known to be associated with many malignancies including ovarian cancer (38, 39). Since constitutive STAT3 signaling is crucial for the survival and proliferation of cancer cells while being dispensable in normal cells, targeting STAT3 with STAT3 inhibitors comprise a promising therapeutic approach for cancer patients (40).

Although STAT3 inhibitors such as nifuroxazide and ST3-01 reduce the viability of different ovarian cancer cell lines and primary ovarian cancer cells, the magnitude of reduction varies greatly among different inhibitors and with different cell types. The can be partly explained by the fact that ovarian cancer is a collection of many molecular anomalies and mutations. In other words, ovarian cancer exhibits tumor heterogeneity like many other cancers do (41). The other reason that potentially contributes to the discrepancy between the effectiveness of different inhibitors is their distinct mechanisms of action. Nifuroxazide decreases the phosphorylation of STAT3 in multiple myeloma cells via inhibition of the Jak family kinases Jak2 and Tyk2 (42). Therefore, for nifuroxazide, similar mechanism is most likely involved in the inhibition of tyrosine phosphorylation of STAT3 in ovarian cancer cell lines (OVCAR8 and SKOV3) and primary tumor cells. Another STAT3 inhibitor ST3-01 appears to not affect the phosphorylation of STAT3 while it is capable inhibiting the endogenous STAT3 activity. The mechanism is unclear, but it probably entails blocking the recruitment of co-factors and co-activators of STAT3 or activating one or multiple alternative signaling pathways.

Knowing that constitutively activated STAT3 seems to be crucial for the pathogenesis of ovarian cancer, it was surprising to find that a reduction of STAT3 levels via RNAi does not lead to significant decrease in cell viability. Moreover, the unexpected upregulation of IL-8, when STAT3 is inhibited by either STAT3 inhibitors or STAT3 RNAi, raises the possibility that IL-8 may play a role in ovarian tumor survival. Previously, IL-8 has been identified as a key mediator in the epithelial-mesenchymal transition (EMT) that leads to increased malignancy and metastasis of ovarian tumors

(43). Therefore, the upregulation of IL-8 can be explained by several models. First, it is like that IL-8 induction is a direct effect of STAT3 inhibition because STAT3 may be a negative regulator of the IL-8 gene. Although STAT3 is an "activator" of transcription, it has been shown to negatively regulate genes such as IL-8 in glioblastoma in earlier literatures (44). While it is reasonable to consider this more direct relationship, the fact that many additional genes are also upregulated with STAT3 inhibition, including some "signature STAT3 target genes", seems to suggest a mechanism whose effects are more extensive. Knowing that IL-8 is one of the signature genes of NFκB pathway, IL-8 upregulation may be the marker of activation of the NF-κB pathway, since McFarland et al. also postulates that STAT3 inhibitor JSI-124 can activate NF-κB pathway in glioblastoma (15).

The NF-κB pathway refers to an assembly of signal responsive subunits that consist of RelA/p65, c-Rel, RelB, NF-κB1/p50 and NF-κB2/p52 (45). Although it is uncommon to find mutations in the NF-κB subunits themselves, most solid and hematopoietic tumors contain aberrantly activated NF-κB maintained either by extracellular stimuli in the tumor microenvironment or via the mutations that activate upstream signaling molecules (28, 46). In normal cells, NF-κB subunits remain in the inactive state bound to an inhibitory protein called I-κB in the cytoplasm (47). In the canonical pathway of NF-κB activation, the engagement of pro-inflammatory cytokines or antigens to various receptors such as cytokine receptors or pattern recognition receptors, respectively, initiates the activation and phosphorylation of the I-κB kinase (IKK) complex. Subsequently, IKK complex phosphorylates IκBα, which is then targeted for proteasome degradation to allow p65 nuclear translocation and gene expression (48, 49). Typically in tumor cells, it has been shown that NF-κB is most commonly activated by TNFα (50). Nonetheless, NF-κB activation can also be achieved alternatively by other kinases such as p38 MAPK that ultimately phosphorylates IκBα and dissociates p65 from I-κB (51).

In our study, IL-8 appears to be a characteristic NF-κB target gene, since IL-8 upregulation is associated with both the overexpression of p65 and with TNFα stimulation, both of which result in either increased protein levels of phosphorylated I-κB or increased expression levels of signature NF-κB target genes, indicating the activation of NF-κB pathway. This association between NF-κB and IL-8 is also not unexpected, since IL-8 upregulation has been linked to NF-κB activation in many other types of tumors. For instance, Wang et al. showed that the TNFα stimulation can lead to activation of p38 MPAK, which then associates with the sequential NF- κB activation and IL-8

upregulation (52). Based on this evidence, it is very likely that IL-8 induction in OVCAR8 cells serves as an indicator of NF-κB activation in response to STAT3 inhibition.

In addition to IL-8, we observe that other NF-κB target genes including A20, BIRC3, CCL-5, and RelA are upregulated. This also provides evidence for NF-κB activation, because their induction correlates to TNFα stimulation and NF-κB subunits overexpression. More specifically, A20, which is a zinc finger protein that participates in negative feedback by blocking TNFα Receptor-Associated Factor-2 (TRAF2)-mediated NF-κB activation (53, 54), is induced when NF-κB is activated in inflammation. Furthermore, some of the STAT3 "signature" target genes have also been previously described as NF-κB target genes in different systems. The mitochondrial membrane molecule Bcl-xL, for example, belongs to the Bcl-2 family and functions as an anti-apoptotic molecule by preventing the release of cytochrome c from the mitochondria, which would lead to caspase activation. As a key protein that is pro-survival, it is a direct target of STAT3 (55, 56), although at early time points its expression appears to not increase in an engineered cell line with inducible STAT3C (57). Because one of the principal hallmarks of cancer cells is their ability to impede intrinsically-programmed or exogenously induced cell death (58), Bcl-xL has recently been identified as an NF-κB target gene in cancer cells. This is not unexpected, since the NF-κB pathway is a pro-survival pathway in cancer cells and Bcl-xL itself acts to prevent apoptosis.

Another good example is BCL3, the protein product of which relates closely to I-κB family and is conventionally thought to act as a cofactor for the NF-κB homodimer in gene expression (59, 60). The induction of BCL3 has also been proposed to require cooperation between the STAT3 and the NF-κB pathways in mouse lung cells (61). Taken together, the upregulation of some of the so-called STAT3 target genes in response to STAT3 inhibition is not too unforeseen. Since these endogenous genes are almost certainly co-regulated by both STAT3 and NF-κB pathways, the effects from an inhibition of the former are compensated by the corresponding and reciprocal activation of the later. Unlike the NF-κB pathway with its clear signature target genes such as A20, we have yet to find a more exclusive set of STAT3 target gene. Although BCL6 and MCL1 are commonly regulated by STAT3 in cells such as fibroblasts and myeloma cells (62), in OVCAR8, it seems that the suppressor of STAT3, or SOCS3, acts mostly like a STAT3 target gene. On the contrary, in other certain cell types such as macrophages, SOCS3 can also respond to NF-κB activation with type I IFN signaling (63, 64). Therefore, in this study, although we analyzed the expression of the STAT3 target genes to

mainly inspect STAT3 activity in ovarian cancer cells, upregulation of these STAT3 target genes may also indicate activation of the NF- κB pathway.

We observe that NF-κB activation is followed by a rapid p65 nuclear translocation at single cell level and within a population of ovarian cancer cells. As an important transcription factor, p65/RELA nuclear translocation plays a central role for the downstream effects of NF-κB activation, namely target gene expression. When this translocation is blocked by pharmaceutical agents, such as selective cyclooxygenase-2 (COX-2) inhibitors, the NF-κB mediated gene expression is severely suppressed (65). This indicates that translocation of p65 is an essential part of the process of NF-κB activation. From our study, shortly after TNFα stimulation, which activates NF-κB, significant p65 nuclear translocation can be observed by western blot with separated nuclear and cytoplasmic fractions. We notice that within the first 30 mins post TNFα stimulation, p65 nuclear translocation is clearly visualized in individual cells as well as in a population consistently. Once p65 translocates into the nucleus, co-regulatory proteins are required for the regulation of gene expression. Just like many other transcription factors, these coactivators and corepressors are recruited to the binding site of p65 to assist in modification of chromatin structure, transactivation control, or direct DNA binding (66). All of these steps are required for successful gene expression following the activation of NF-κB. In our study, we also observed that p65 RNAi prevented the NF-κB target gene upregulation when STAT3 was inhibited (**FIGURE 12**), implying the importance of p65.

However, in our experiments, no significant p65 nuclear translocation is observed when STAT3 is inhibited via STAT3 inhibitors or STAT3 RNAi. It is possible that p65 nuclear translocation occurs at a time point outside of our selected time frame. For example, A20 appears to be encoded by an immediate early response gene, whose expression is rapidly induced by cytokine stimulations (67). Therefore, it may require even earlier p65 nuclear translocation and DNA binding for the accurate and appropriate expression of A20. If this time point occurs before 6 hours drug treatment, then we may potentially have missed this time point and instead captured an equilibrium time point, for which p65 nuclear influx balances efflux in the population of cancer cells. Since NF-κB nuclear dimer only associates with DNA transiently, the promoter-bound dimers may quickly and dynamically equilibrate with free cytoplasmic dimers (68).

Likewise, at a single cell level, continuous surveillance detects no GFP tagged p65 translocation from immediately up to 22 hours post ST3-01 treatment. This seems to contradict the argument of "immediate early" or "late" gene expressions, since all of the earlier time points are taken account of and 22 hours should be long enough for ST3-01 to exert its STAT3 inhibitory effect. However, this observation is made in HeLa cells, not OVCAR8 cells. Since the GFP tagged p65 system was initially developed in HeLa cells, which are know for their population heterogeneity causing inconsistent results in different labs (69), this heterogeneity may result in this particular HeLa cell line to behave differently from another HeLa cell line, rendering the result less conclusive. The stably transfected and overexpressed p65-GFP presumably exhibits no transcriptional activity, but at a population level, the p65-GFP seems to induce pSTAT1 in the p65EGFP HeLa compared to that of the wildtype (Supplementary Figure 1). This effect rapidly diminishes when p65 RNAi is employed to reduce the levels of intracellular GFP tagged and wildtype p65, indicating that p65-GFP vector overexpression in HeLa cells indeed changes the innate properties of the cell (Supplementary Figure 2). Finally, the reciprocal relationship between STAT3 inhibition and NF-κB activation is not very clear in HeLa cells compared to the trend seen in OVCAR8 cells. For example, a reduction in STAT3 levels with STAT3 RNAi does not lead to consistently and steadily upregulated NF-κB target genes (Supplementary Figure 3), suggesting that this reciprocal relationship perhaps only exist in a subset of cancer cells including ovarian cancer cells and renal cell carcinoma.

Even though we may need more time points to detect p65 nuclear translocation, as discussed before, a perhaps more plausible argument for this phenomenon is the non-canonical activation of NF-κB while STAT3 is inhibited. In addition to the well-characterized canonical pathway, alternative mechanisms have been discovered to mediate individual or a subset of NF-κB subunits more specifically (70). On the contrary to the canonical activation of NF-κB, which follows the degradation of I-κBα, the non-canonical pathway does not rely on the phosphorylation of I-κB, but instead depends on the inducible processing of p100 protein to activate the RelB/p52 complex. Evidence based on many genetic studies reveal important roles of the non-canonical pathway in lymphoid organogenesis, B-cell maturation, bone metabolism, and dendritic cell activation. More importantly, once deregulated, the non-canonical pathway has been postulated to associate with lymphoid malignancies (71).

Almost exclusively occurring in lymphoid organs for B-cell and T-cell development, the non-canonical pathway is activated by a small number of ligands such as lymphotoxin B and B cell activating factor (BAFF). NF-κB-inducing kinase (NIK), instead of the I-κB kinase complex (IKK), is activated and subsequentially phosphorylates the IKKα complex. p100—the precursor of p52—is phosphorylated, resulting in the processing and truncation to free the p52/RelB heterodimer (72, 73). In our case, when STAT3 is inhibited in ovarian cancer cells, it is possible that either the alternation in one or more STAT3 target genes or at some downstream crosstalk points the non-canonical NF-κB pathway is activated, leading to the nuclear translocation of p52/RelB instead of the p65 subunit. While some of the target genes are believed to be more restricted to the regulations of the non-canonical NF-κB pathway, many target genes are thought to be shared between the canonical and the non-canonical pathways (75). This can explain why the signature set of NF-κB target genes is activated in response to STAT3 inhibition despite the absence of p65 nuclear translocation.

Alternatively, the NF-κB activation as a consequence of STAT3 inhibition may be the result of a change in the intracellular levels of the Bcl-3 protein, which is characterized as a nuclear member of the inhibitor of NF-κB family and has been shown to exclusively interact with the transcriptionally inactive homodimers of p50 and p52 (76). More specifically, Bcl-3 increases the binding of the p52 homodimer to the NF-κB sites in the presence of excessive nonconsensus DNA when the ratio of Bcl-3:p52 is low. At a higher ratio, phosphorylated Bcl-3 exerts little inhibitory effects for p52 DNA binding, whereas the non-phosphorylated Bcl-3 forms a higher order inhibitory complex with p52 homodimers (77). The selectively activated p52 homodimers are thought to be restricted to human breast cancers. Furthermore, it has been reported that the p52 homodimer complexes with Bcl-3 to upregulate cyclin D1 expression, which may contribute to cancer pathogenesis (78, 79).

More importantly, Bcl-3 interacts to increase the levels of p50, thus promoting the formation and nuclear translocation of p50 homodimers. For example, in human embryonic kidney (HEK) 293T cells, overexpressed Bcl-3 inhibits p50 ubiquitination and consequentially increases the intracellular levels p50 homodimer in a dose-dependent manner. Ultimately, DNA binding of the p50 homodimer increases when Bcl-3 is overexpressed, but the binding affinity remains unaltered (80). Cytokines such as IL-9 and IL-4 can also induce BCL3 gene expression in mouse T lymphocytes and mast cells, which is thought to inhibit the TNF-induced NF-κB dependent transcription and

result in an alternative and delayed I-κBα-dependent NF-κB DNA binding (81). This seems to suggest that Bcl-3 plays a negative role in regulating NF-κB gene expression by stabilizing p50 homodimers, which is consistent with the fact that BCL3 encodes an I-κB protein mentioned earlier (82). However, divergent evidence also points to the activating role of Bcl-3 in the progression of NF-κB target gene expression, resulting in an unclear role of Bcl-3 (83). Ultimately, as a STAT3 target gene in ovarian cancers, the function of Bcl-3 probably varies dramatically in different cancer cells and in different tumor microenvironments.

Finally, knowing that NF-κB pathway is induced when cells are stressed, it is logical to further consider other stress related pathways. One candidate is the p38 MAPK, which appears to be downstream of IL-8 signaling. Conversely, the induction of p38 MAPK via IL-1β in cystic fibrosis cells correlates with an overproduction of IL-8 (84). In the past, p38 MAPK has been shown to stabilize mRNA, which is also thought to be the mechanism for the p38-MAPK-dependent-increases of the intracellular levels of IL-8 (85). Reports have also identified that IL-1β regulates IL-8 expression in vascular endothelial cells via p38 MAPK. The rapid induction of IL-8 following IL-1β is actually mediated by the transcription factors AP-1 and NF-κB, but p38 MAPK modulates the critical DNA binding of AP-1 (86). Moreover, a few kinases have been hypothesized to phosphorylate RelA/p65, one candidate of which is the p38 MAPK. However, the mechanism and the function of p65 phosphorylation and the detailed interactions currently remain unclear. Several models have postulated enhanced recruitment of various transcriptional co-activators and blockages of co-repressors at the promoter site (86). Consistent with our data, it is likely that STAT3 inhibition alone can lead to IL-8 upregulation, either directly by de-suppression or indirectly by activating or inhibiting other pathways regulating IL-8 expression. This upregulation of IL-8 can then activate p38 MAPK via binding to its receptor CXCL1/CXCL2 via paracrine or autocrine pathway. An activated p38 MAPK can then lead to NF-κB pathway activation subsequently.

Taken all together, three different models can account for the reciprocal activation of NF-κB in response to STAT3 inhibition. 1. When STAT3 is inhibited, one or more of its target genes, as well as some of the additional intracellular changes, can lead to activation of the non-canonical NF-κB pathway resulting in the alternative p52/RelB nuclear translocation instead of the more conventional

p65 subunit (SUPPLEMENTARY FIGURE 1). 2. Inhibition of STAT3 leads to a downregulation of BCL3 (FIGURE 6 A-D, FIGURE 9), which precludes the interaction between Bcl-3 and p50 homodimer. Although BCL3 is very likely to be co-regulated by both NF-κB and STAT3, it has been shown to initially decrease in response to STAT3 inhibition, causing destabilization of p50 homodimers, reduction of p50 homodimers levels, and ultimately, decreased DNA binding. Knowing that p50 homodimers can potentially exhibit inhibitory effects on NF-κB gene expression by competing with the conventional p65 subunit or by activating transcription of alternative set of NF-κB genes, we postulate that decreased engagements of p50 homodimers to DNA perhaps lead to the observed upregulated NF-κB target genes via the now dominating canonical p65 pathway. Eventually, the levels of BCL3 return to normal and then become augmented as the activated NF-κB pathway balances the inhibited STAT3 pathway, ultimately exceeding the inhibition (SUPPLEMENTARY FIGURE 2). 3. Knowing that STAT3 acts as a negative regulator of IL-8 in glioblastoma and that IL-8 is upregulated early on, IL-8 can potentially be released in response to STAT3 inhibition when cells are treated with STAT3 inhibitors (6hours post treatment). Once released into the media, the IL-8 can bind to CXCL1/CXCL2 receptors, causing downstream activation of one or multiple pathways including the p38 MAPK as one of the typical stress-response pathways. The consequential NF-κB activation following the p38 MAPK activation then sustains the amplified levels of IL-8, as well as the other NF-κB target genes (SUPPLEMENTARY FIGURE 3).

In conclusion, we postulate several models to explain the reciprocal activation of NF-κB responding to STAT3 inhibition in ovarian cancer cells. However, considering the complexity and numerous cross-talks between signaling pathways in cells, it is likely that the observed phenomenon is the result of a combination of mechanisms. We think that by understanding the relationship between STAT3 and NF-κB pathways in cancer cells, personalized therapy can be achieved for more targeted treatment for cancer patients. More specifically, an inhibition of NF-κB pathway can sensitize ovarian cancer cells to STAT3 inhibitors, rendering them more responsive to apoptosis and to chemotherapy. Ultimately, we hope that this study can raise the awareness that when a targeted pathway is effectively inhibited, alternative pro-survival and pro-growth pathways can be reciprocally activated and that renders the treatment less effective. Therefore, although it is a challenge to design dual inhibitors in ovarian cancer, perhaps an approach to aim at multiple correlated pathways is more efficient for competent eradication of the cancer cells.

SUMMARY

In summary, constitutively activated STAT3 due to aberrant mutations in the STAT3 pathway provides prosurvival signals to cancer cells. Particularly, because activated STAT3 in ovarian cancer cells promotes resistance to chemotherapeutic agents, targeted inhibition of STAT3 constitutes a powerful therapeutic tool to improve the survival rate for ovarian cancer patients. Inhibition of the STAT3 pathway either by STAT3 inhibitors or via STAT3 siRNA leads to unexpected upregulation of IL-8 gene, as well as additional genes that are regulated by the NF-κB pathway. Because this phenomenon appears to be very specifically associated with STAT3 inhibition, we hypothesize that the activation of NF-κB is reciprocally related to STAT3 inhibition in ovarian cancer cells. One of the NF-κB subunits, p65, translocates into the nucleus and plays an important role in the regulation of NF-κB target gene expression. A reduction in the intracellular p65 levels via p65 siRNA abrogates of the activation of the NF-κB pathway by STAT3 inhibition, suggesting that p65 is crucial in the reciprocal activation of NF-κB. However, no significant p65 nuclear translocation is observed at single cell level or in a population, when STAT3 is inhibited. This suggests that one or more additional pathways may be altered with STAT3 inhibition in ovarian cancer cells. Finally, since the NF-κB pathway has been shown to also associate with increased malignancy and metastasis of ovarian cancers, targeting the NF-κB pathway and the STAT3 pathway together may be beneficial for ovarian cancer patients for better prognosis.

FIGURE 1

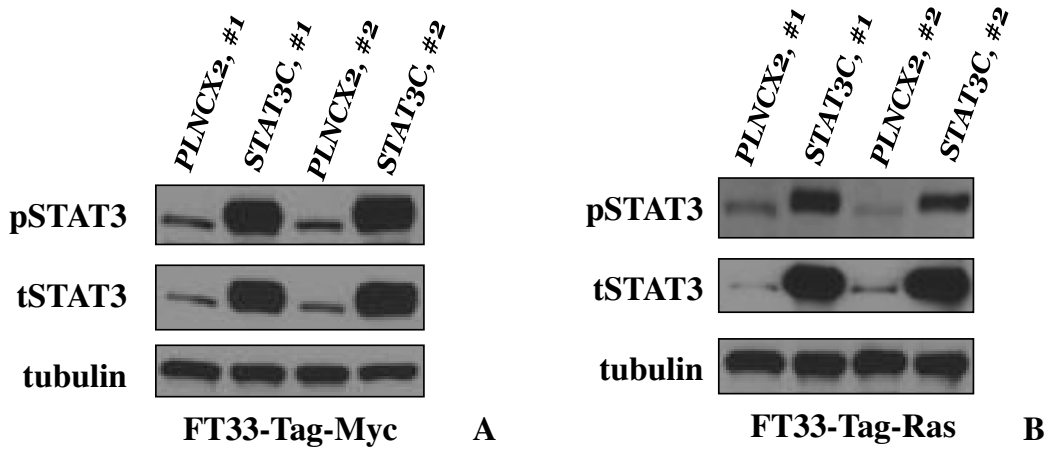

FIGURE 1A: After STAT3C transfection, the FT33-Tag-Myc cells were selected with Geneticin for at least two weeks. Two individual pools (#1, #2) were selected to test for STAT3 expression. Enhanced levels of both phospho-STAT3 and total-STAT3 with STAT3C indicated the transfection is effective.

FIGURE 1B: Similarly, we observe increased levels of phospho-STAT3 and total-STAT3 in FT33-Tag-Ras cells transfected with STAT3C in two individual pools.

FIGURE 1

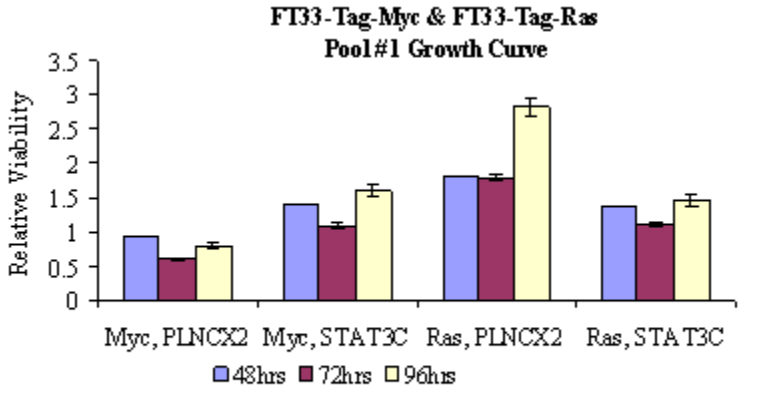

C

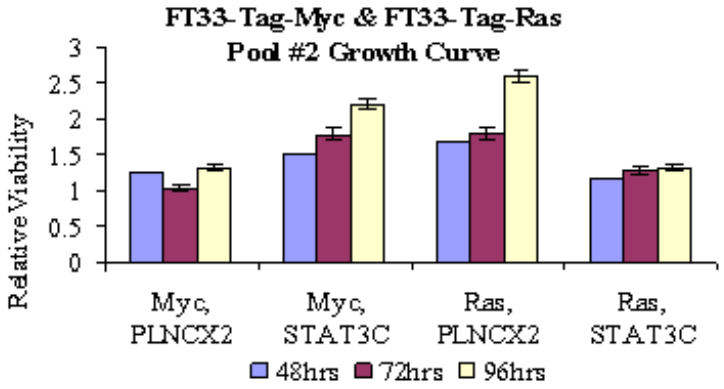

D

FIGURE 1C: FT33-Tag-Myc cells transfected with empty vector or STAT3C were plated in DMEM/F12 50/50 + 10%FBS for 72 hours. The two individual pools were consistent in that STAT3C transformed FT33-Tag-Myc cells grew faster compared to the cells transfected with empty vector. This suggests that the activation of the c-Myc pathway and the activation of the STAT3 pathway may be synergistic to promote cell proliferation.

FIGURE 1D: Similarly, the viability of FT33-Tag-Ras cells transfected with empty vector or STAT3C were compared. On the contrary, the cells with activated STAT3 and H-Ras seemed to grow more slowly compared to that of the control. This suggests that STAT3 and H-Ras may play opposing roles in these cells.

FIGURE 1

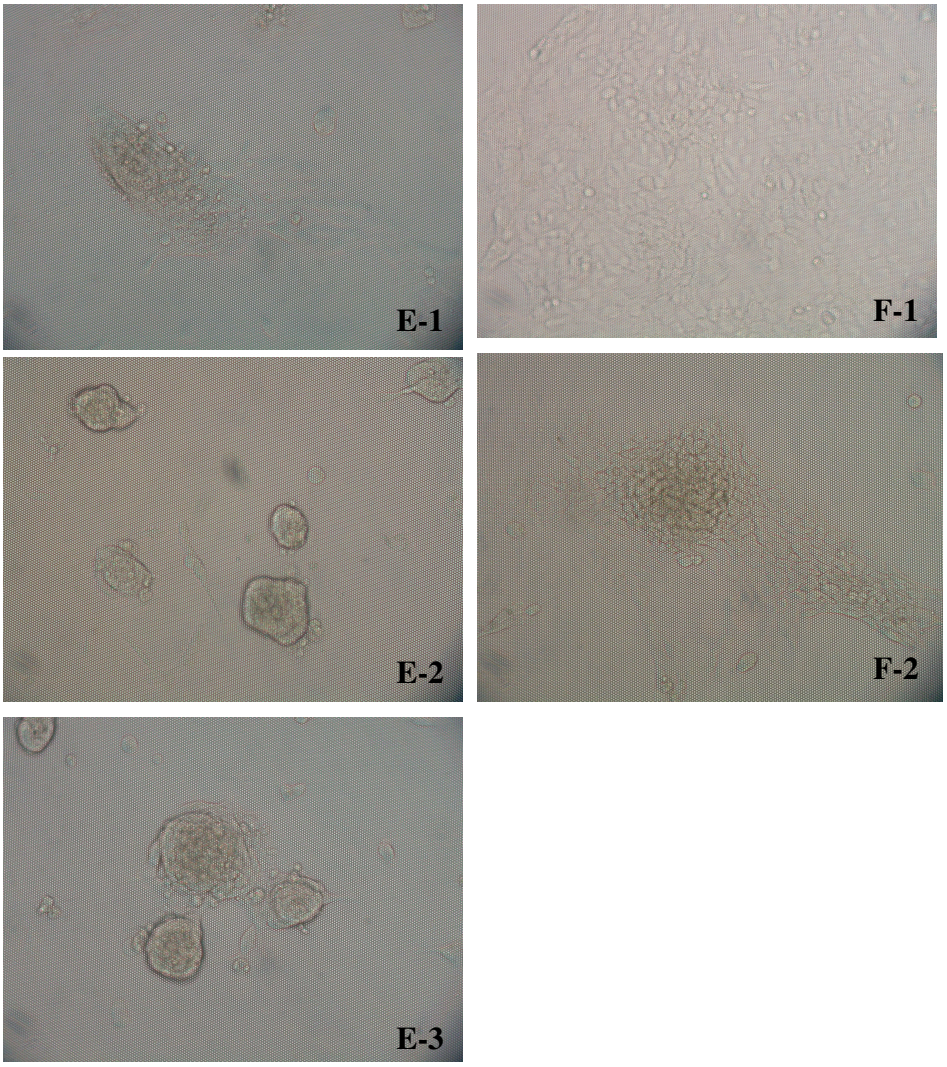

FIGURE 1E

E-1: FT33-Tag-Myc cells transfected with empty vector did not form spheroids

E-2 and **E-3**: FT33-Tag-Myc cells transfected with STAT3C form spheroids, suggesting that activated STAT3 plays an important role in the overall structure of a population of ovarian cancer cells.

FIGURE 1F

F-1: FT33-Tag-Ras cells transfected with empty vector did not form spheroids.

F-2: FT33-Tag-Ras cells transfected with STAT3C did not form spheroids, although they appeared to cluster together.

FIGURE 2

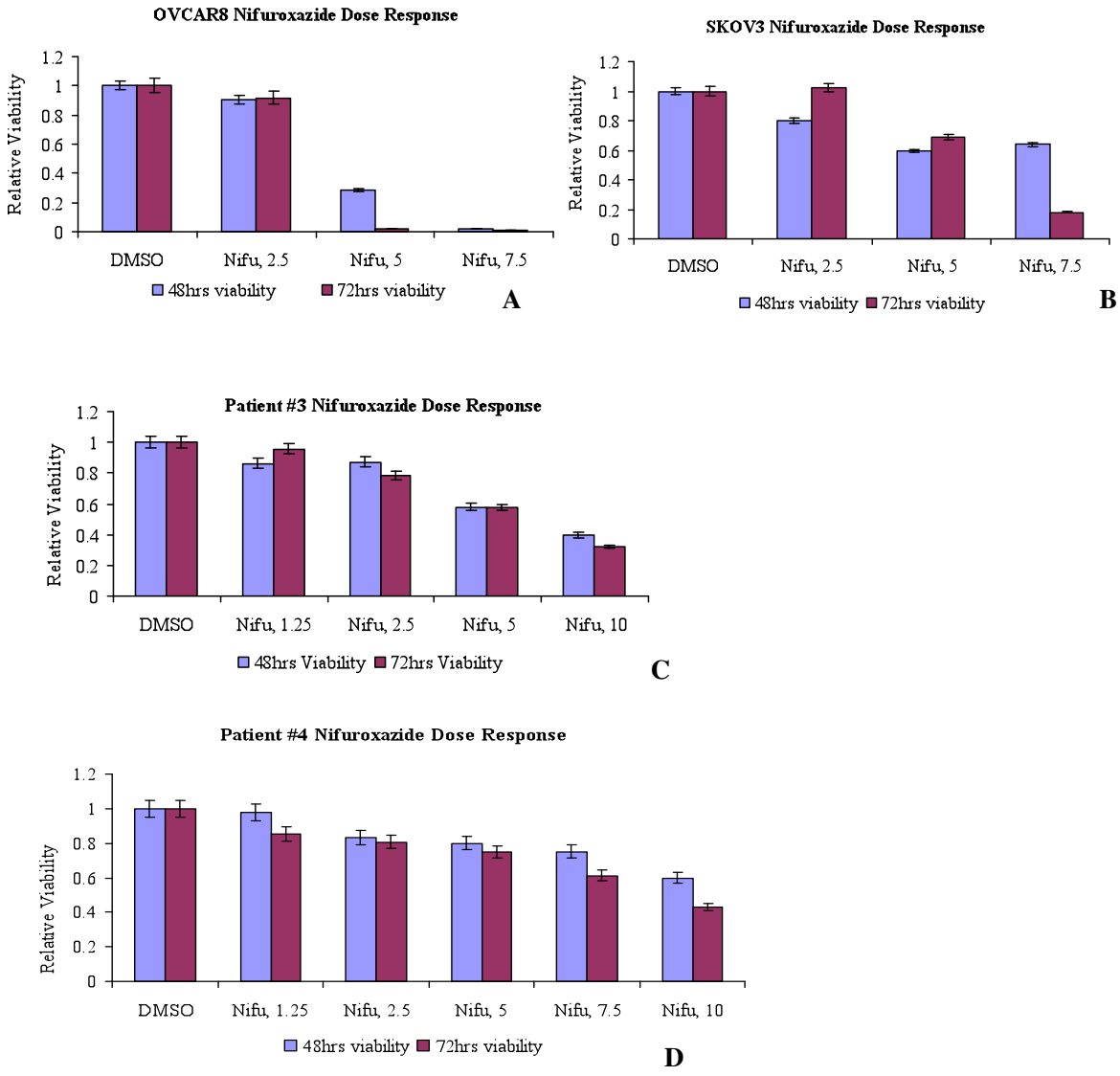

FIGURE 2A: OVCAR8 cells were treated with nifuroxazide for a dose response. Viability decreased rapidly after 2 or 3 days, suggesting that these ovarian cancer cells depend on constitutively activated STAT3 for survival.

FIGURE 2B: SKOV3 cells treated with nifuroxazide showed a smaller decrease in viability after 2 or 3 days of drug treatment. This difference may be due to heterogeneity among ovarian cancer cell lines.

FIGURE 2C and FIGURE 2F: Ovarian cancer cells from Patient #3 and Patient #4 were treated with nifuroxazide. Reductions in viability were observed, but the magnitudes of reduction varied. This reflects that ovarian cancer is a collection of heterogeneous cancer cells with distinct mutations that respond to pharmacological agents differently.

FIGURE 2

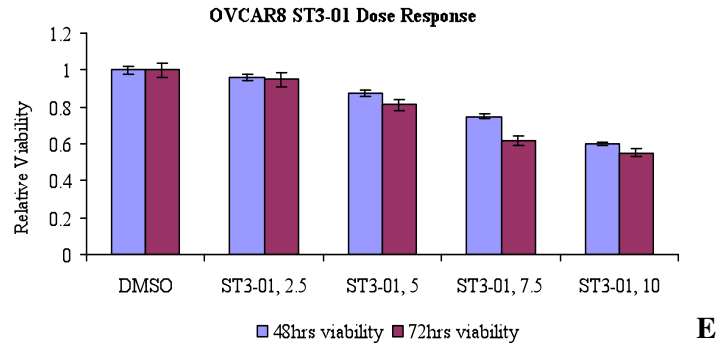

E

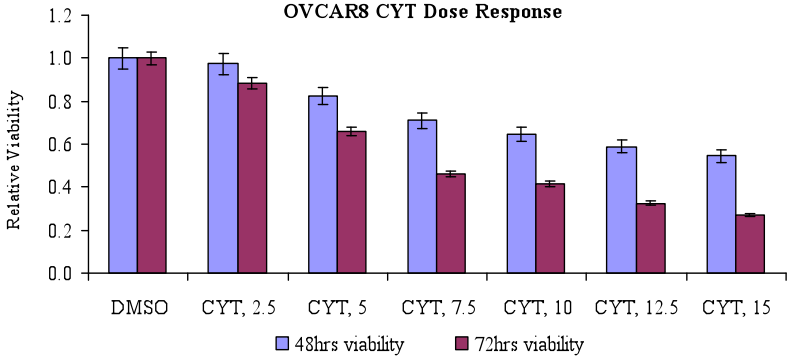

F

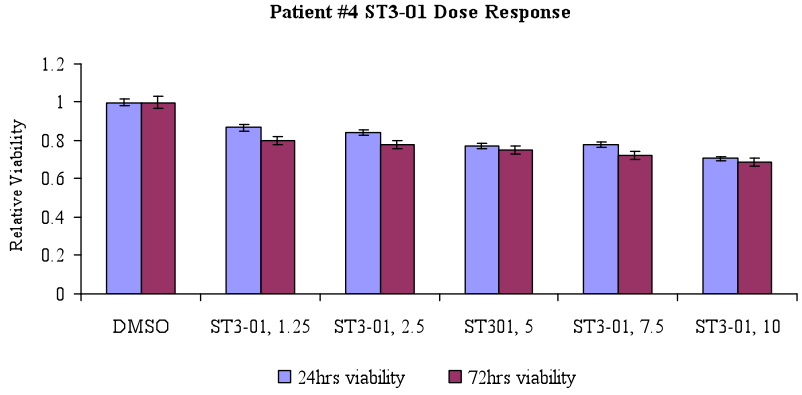

G

FIGURE 2E: OVCAR8 cells were treated with ST3-01 for 2 or 3 days. Reductions in viability were observed, suggesting that inhibition of STAT3 activity affects the growth and survival of OVCAR8 cells.

FIGURE 2F: Viability of OVCAR8 cells decreased with increased dose of CYT treatment.

FIGURE 2G: cancer cells obtained from Patient #4 were treated similarly with ST3-01. Slight reduction was observed.

FIGURE 3

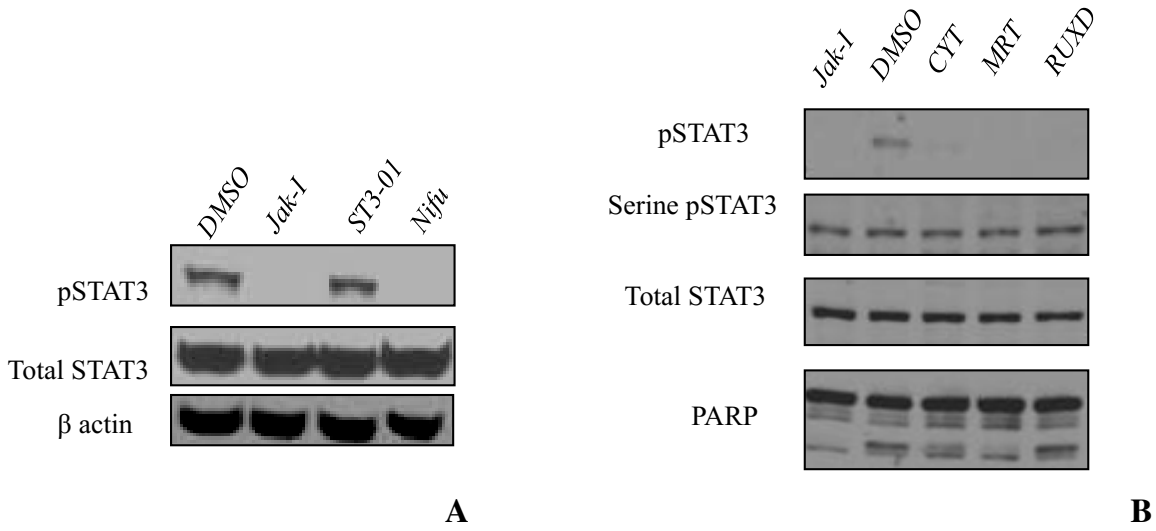

FIGURE 3A: OVCAR8 cells were treated with Janus kinase inhibitor (JAK-I), ST3-01, and nifuroxazide (Nifu) for 24 hours before cells were harvested and proteins were analyzed by electrophoresis and immunoblotting. JAK-I and nifuroxazide appeared to block the phosphorylation of STAT3 directly, whereas ST3-01 did not. This suggests that although these STAT3 inhibitors block STAT3 activity, they do so via different mechanisms of action.

FIGURE 3B: OVCAR8 cells were treated with CYT (JAK and NF-κB inhibitor), MRT (NF-κB inhibitor), and RUXD (JAK inhibitor) for 24 hours. All three inhibitors seemed to inhibit STAT3 tyrosine phosphorylation but not serine phosphorylation.

FIGURE 3

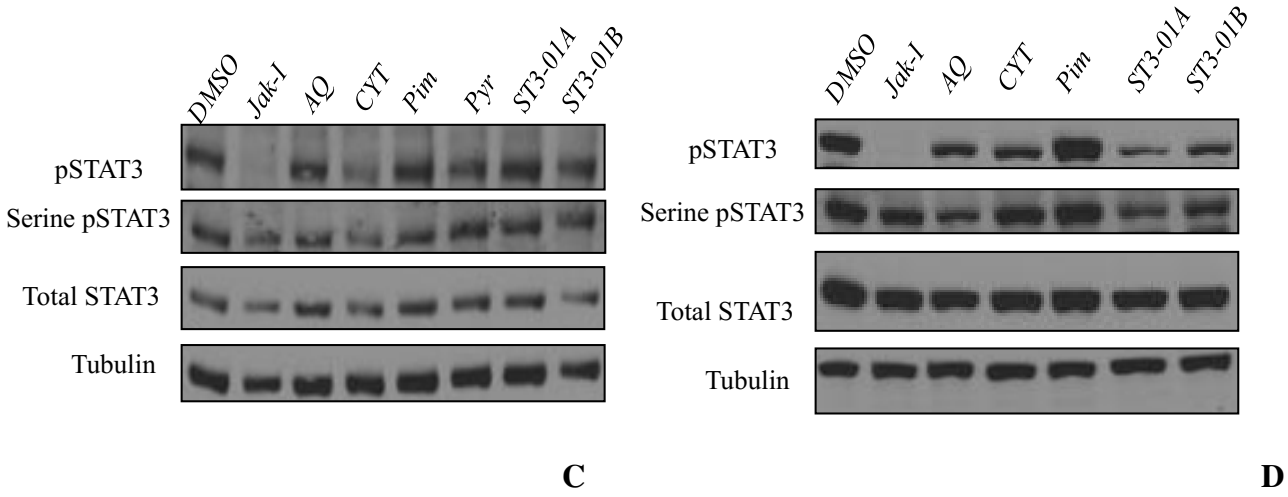

FIGURE 3C: SKOV3 cells were treated with a panel of STAT3 inhibitors for 24 hours. Only JAK-I and CYT seemed to reduce the phosphorylation of STAT3 in SKOV3 cells. Other inhibitors of STAT3 may affect STAT3 activity via different mechanisms of action such as preventing STAT3 nuclear translocation, blocking STAT3 cofactor recruitment, or activating alternative pathways.

FIGURE 3D: Similarly, HeLa cells were treated with the same panel of STAT3 inhibitors for 24 hours. It was observed that all STAT3 inhibitors except for pimozide reduced phosphorylation of STAT3. This suggests that not only do STAT3 inhibitors have different mechanisms of action, but also cancer cells are a heterogeneous group with distinct set of mutations.

FIGURE 4

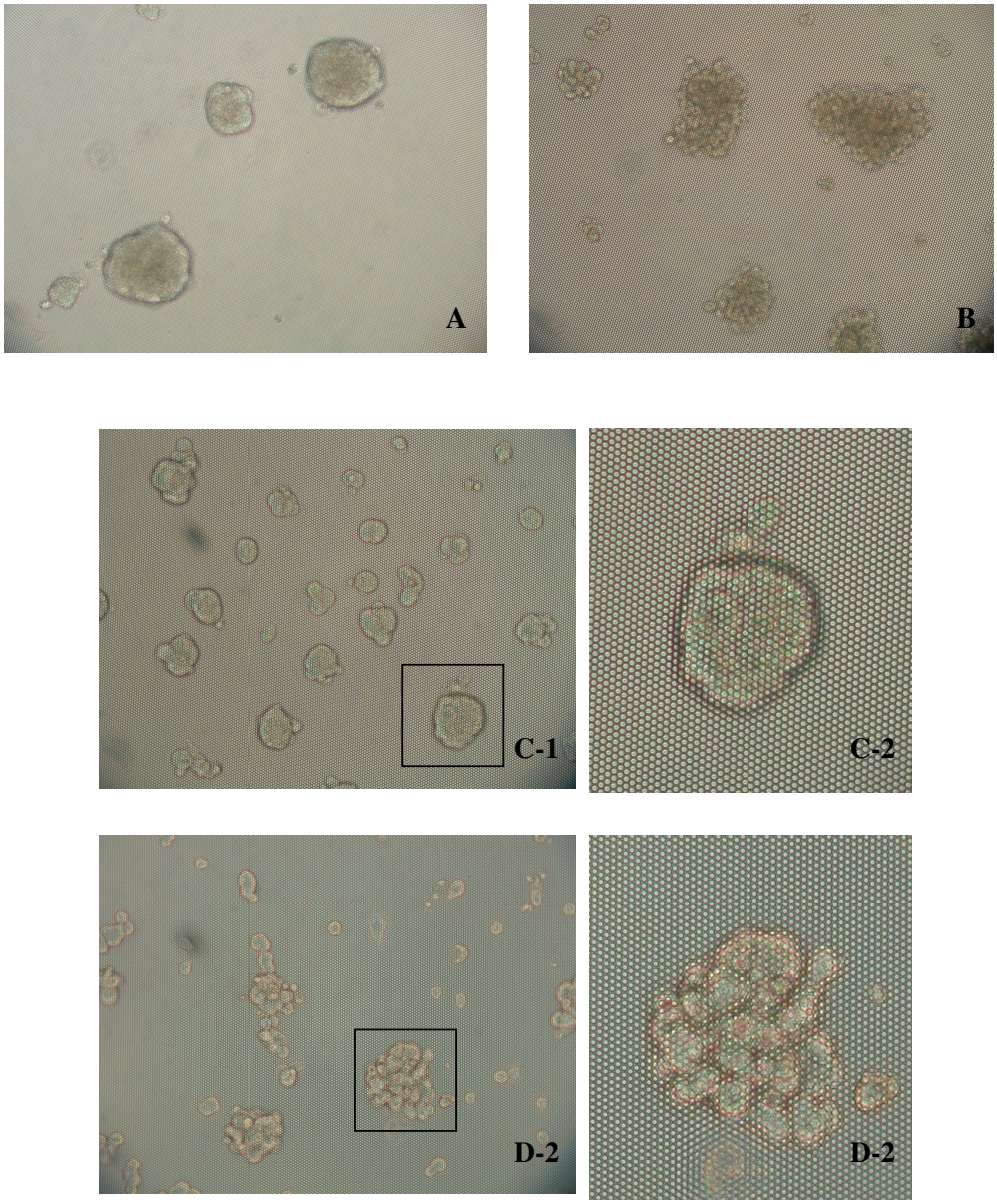

FIGURE 4A: OVCAR8 cells reversely transfected with control siRNA formed spheroids.

FIGURE 4B: On the contrary, STAT3 RNAi obliterated the spheroids, instead, OVCAR8 cells formed irregular clusters. This suggests that STAT3 plays an important role in the overall structure of the ovarian cancer by affecting physical interactions between cells.

FIGURE 4C: OVCAR8 cells treated with vehicle formed spheroids (**C-1**). The spheroids were also shown in the magnified microphotograph (**C-2**).

FIGURE 4D: However, ST3-01 treatment disrupted the spheroid formation **(D-1**) of OVCAR8, which formed clusters similar to STAT3 RNAi treated cells (**D-2**).

FIGURE 5

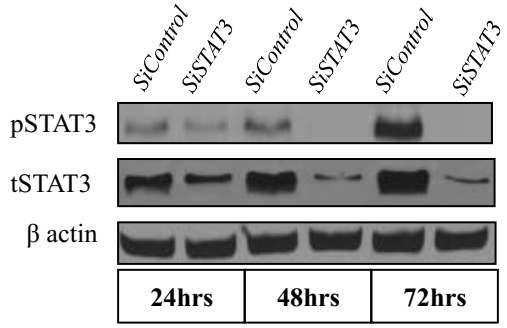

A-1

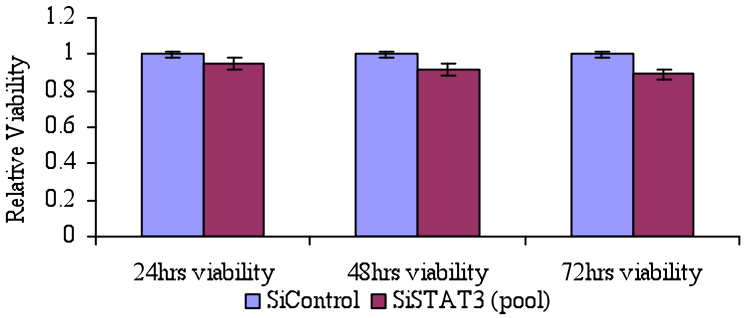

A-2

FIGURE 5A: In OVCAR8 cells, STAT3 RNAi effectively reduced the levels of STAT3, including both phospho-STAT3 and total STAT3 (**A-1**). However, the viability of the ovarian cancer cells only reduced by less than 15% over 72 hours period of time (**A-2**). This suggests that alternative pathways may be activated to compensate for the loss of STAT3 signals in OVCAR8 cells.

FIGURE 5

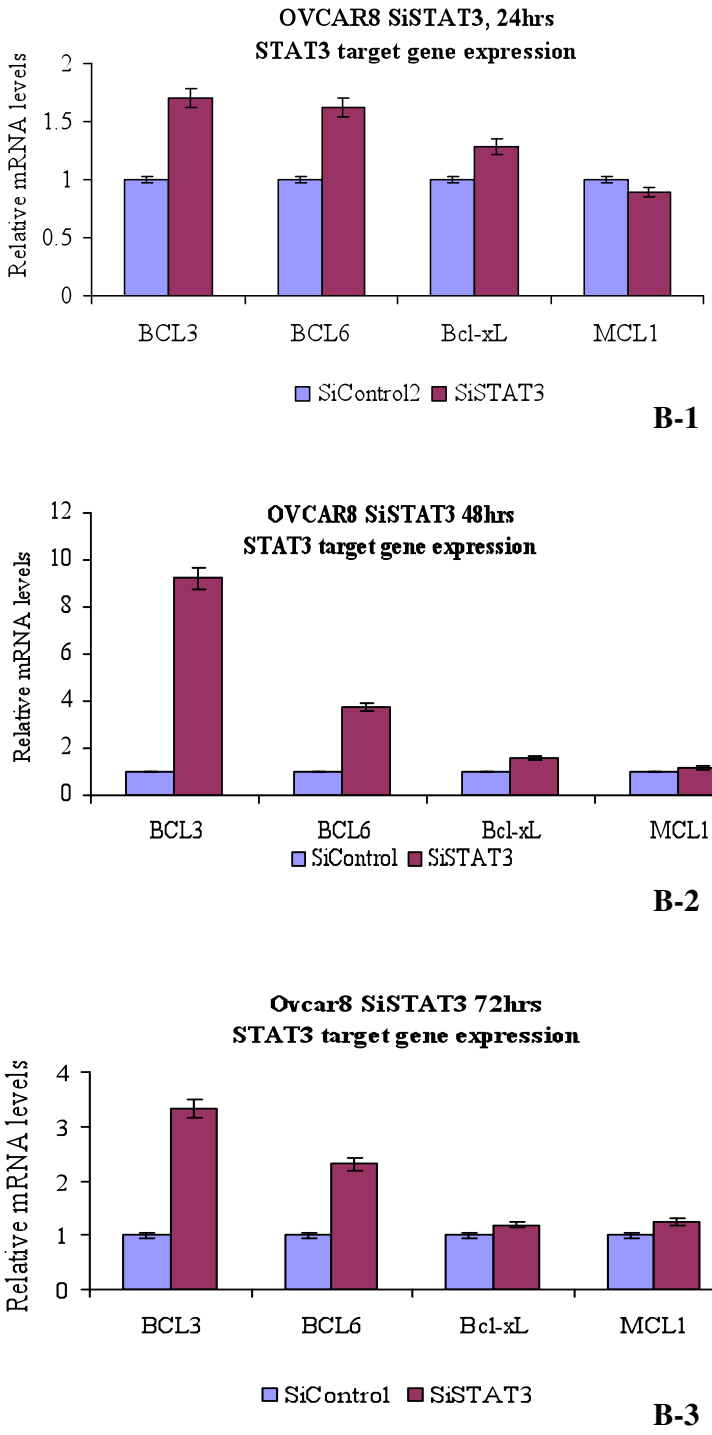

FIGURE 5B: STAT3 RNAi resulted in unexpected upregulation of STAT3 target genes including BCL3, BCL6, Bcl-xL, and MCL1 over 24 hours (**B-1**), 48 hours **(B-2**), and 72 hours **(B-3**). This suggests that one or multiple alternative pathways may be activated when STAT3 is inhibited.

FIGURE 5

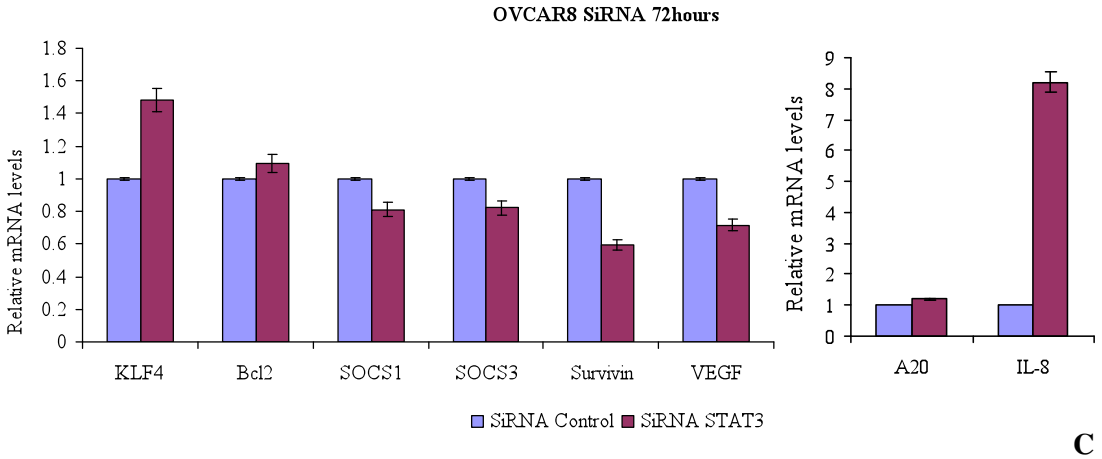

C

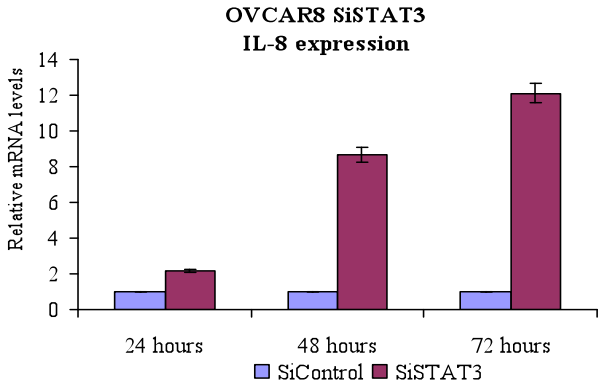

D

FIGURE 5C: The levels of a panel of STAT3 target genes were analyzed by qPCR. The results showed that KLF-4 and Bcl-2 were upregulated, whereas SOCS1, SOCS3, survivin, and VEGF were downregulated, suggesting that not all but a subset of STAT3 target genes were induced when STAT3 was inhibited. In addition, IL-8 was upregulated by more than 8-fold, suggesting that either STAT3 is a negative regulator of IL-8, or that alternative pathways are activated when STAT3 is inhibited.

FIGURE 5D: To confirm the IL-8 upregulation, IL-8 expression levels were analyzed at three different time points. Consistent induction was observed for IL-8 at 1, 2 or 3 days post STAT3 RNAi transfection.

FIGURE 6

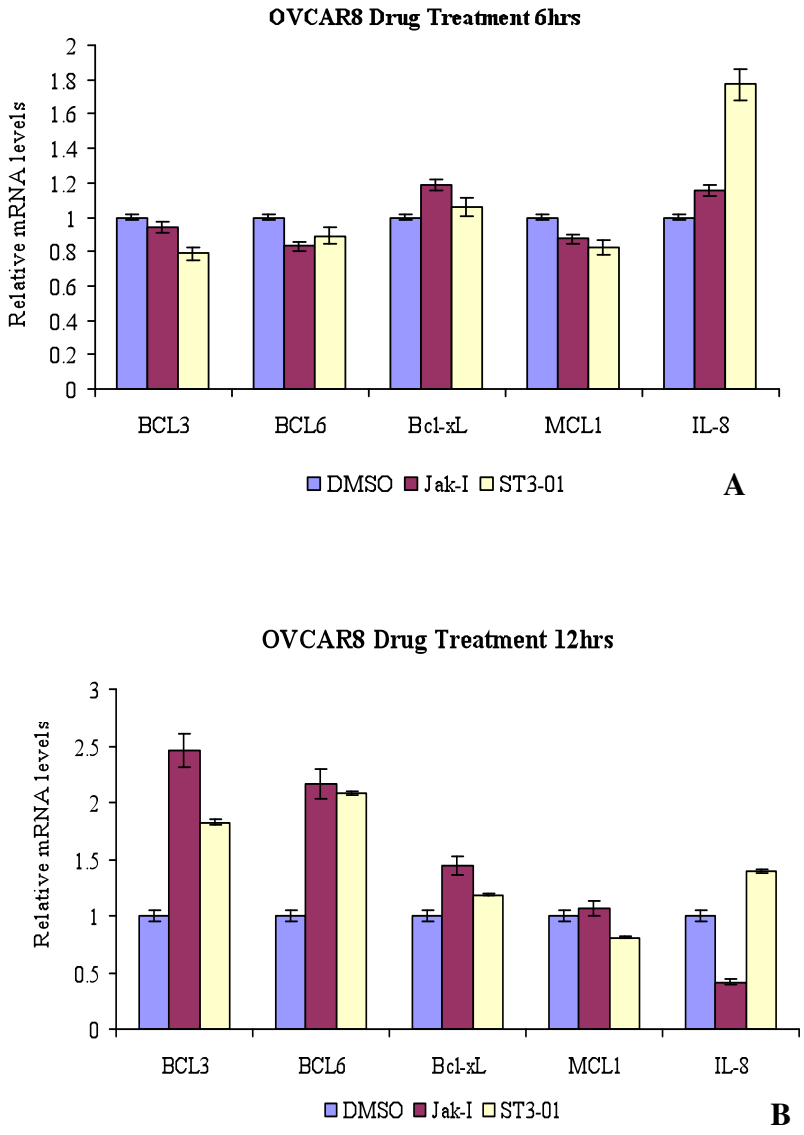

FIGURE 6A: IL-8 upregulation was also seen when STAT3 is inhibited with pharmacological agents as early as 6 hours.

FIGURE 6B: 12 hours post STAT3 inhibitor treatments, STAT3 target genes were upregulated. IL-8 was also seen upregulated.

FIGURE 6

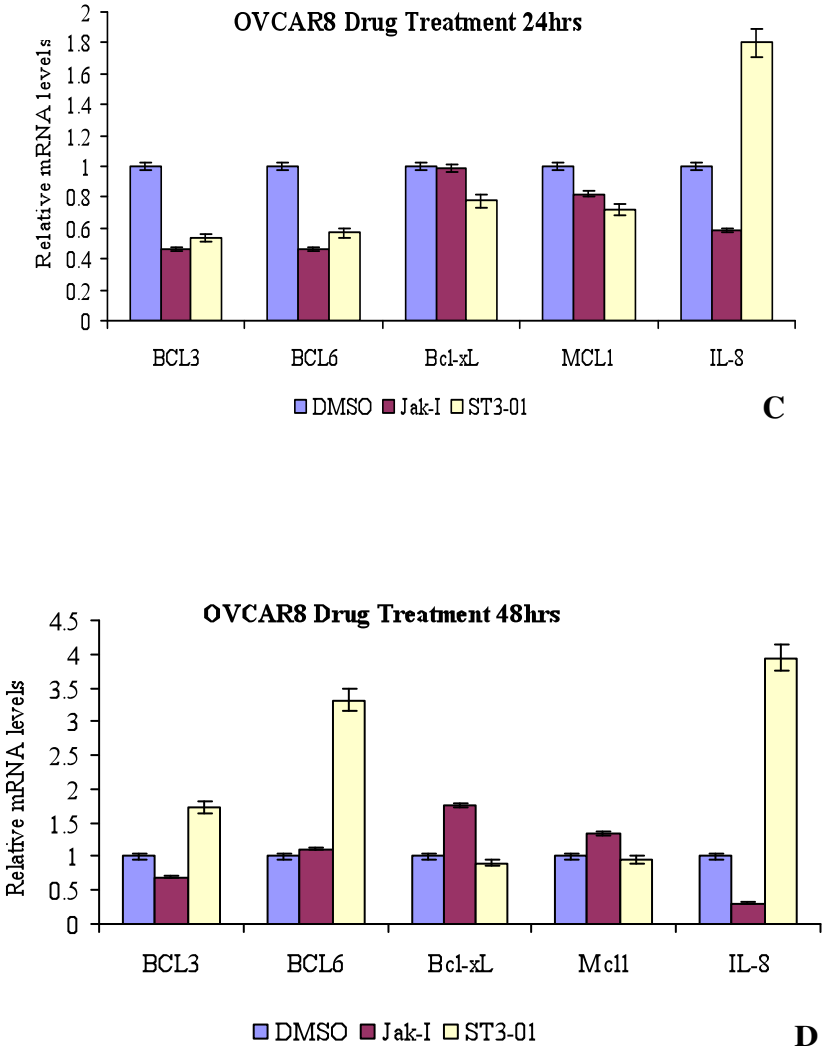

FIGURE 6C: After 24 hours of drug treatment, IL-8 was upregulated, whereas most of the STAT3 target genes were downregulated. This shows the dynamics of gene expression as their levels continue to change when various signaling pathways are activated or inhibited at different times.

FIGURE 6D: IL-8 was induced by more than 4-fold after 2 days of ST3-01 treatment. STAT3 target genes showed different expression patterns, indicating that alternative pathways may also regulate their expression. Overall, IL-8 was seen upregulated consistently when STAT3 was inhibited with siRNA or pharmacological inhibitors.

FIGURE 7

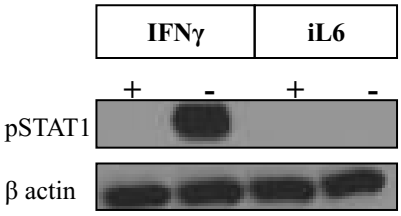

A

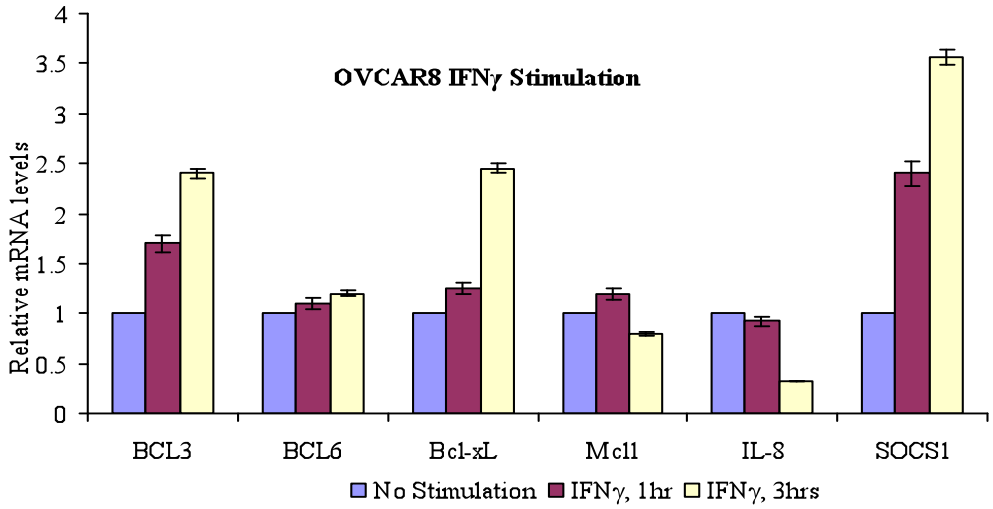

B

FIGURE 7A: To ensure that IL-8 upregulation was not due to non-specific effects of siRNA via activation of the anti-viral STAT1 pathway, OVCAR8 cells were stimulated with interferon gamma (IFNγ) and interleukin 6 (IL-6) for 15 minutes. pSTAT1 levels were increased with IFNγ stimulation, indicating the activation of the STAT1 pathway.

FIGURE 7B: SOCS1, a STAT1 target gene, was upregulated correspondingly. IL-8 expression was reduced for both 1 hour and 3 hours IFNγ stimulations. This suggests that IL-8 upregulation seen with STAT3 inhibition was not due to off-target effects of siRNA.

FIGURE 7

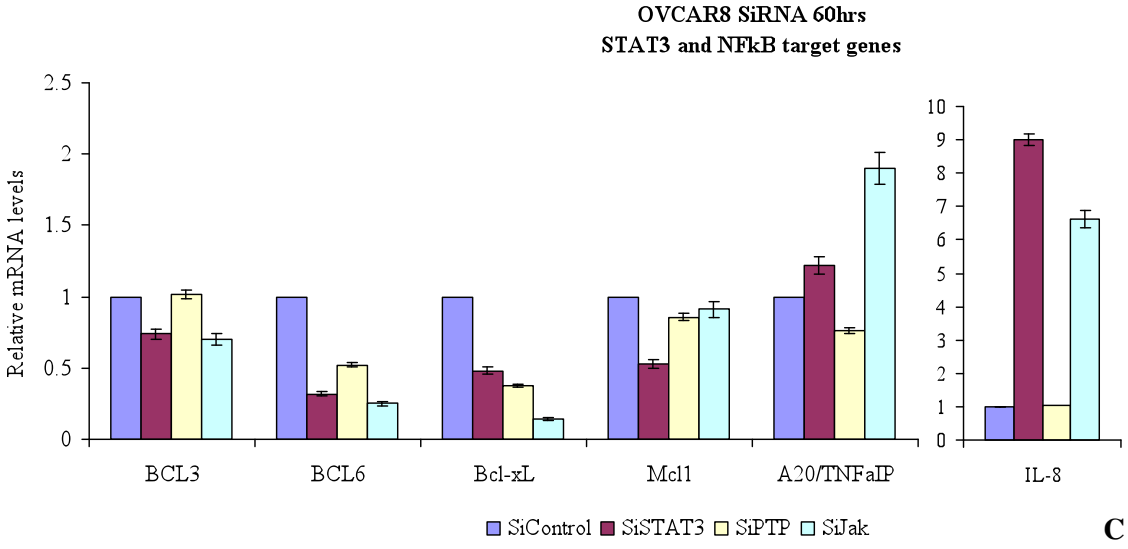

C

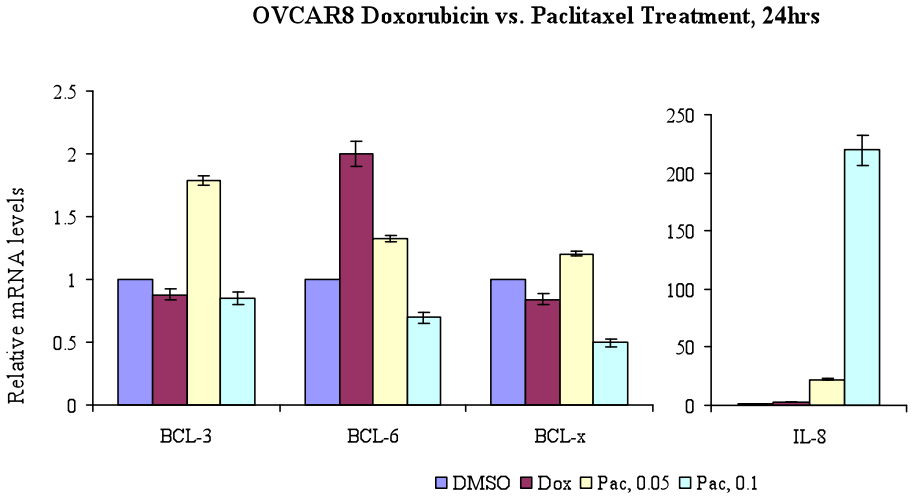

D

FIGURE 7C: To confirm the specificity of IL-8 upregulation to STAT3 inhibition, OVCAR8 cells were treated with STAT3 RNAi, phosphatase N6 (PTP) RNAi, and JAK RNAi. Only siSTAT3 and siJAK led to upregulation of IL-8, whereas siPTP did not. Similar to the expression pattern of IL-8, A20 was upregulated only with siSTAT3 and siJAK, but not siPTP. This suggests that IL-8 upregulation is specific to STAT3 inhibition.

FIGURE 7D: Doxorubicin, a nonspecific chemotherapeutic agent, resulted in no significant upregulation of IL-8 in OVCAR8. However, IL-8 was induced in a dose-dependent manner with paclitaxel treatment. Since paclitaxel was known to inhibit STAT3 activities in cancer cells, IL-8 upregulation seems specifically related to STAT3 inhibition.

FIGURE 8

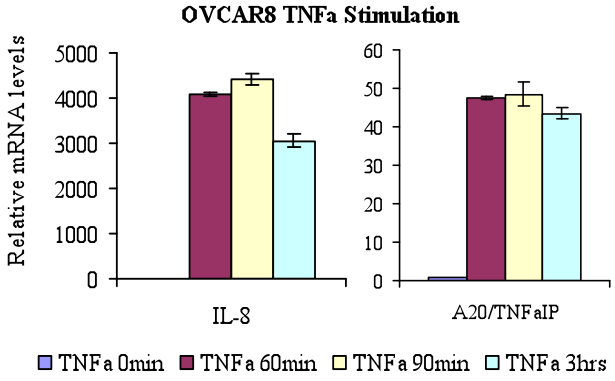

A-1

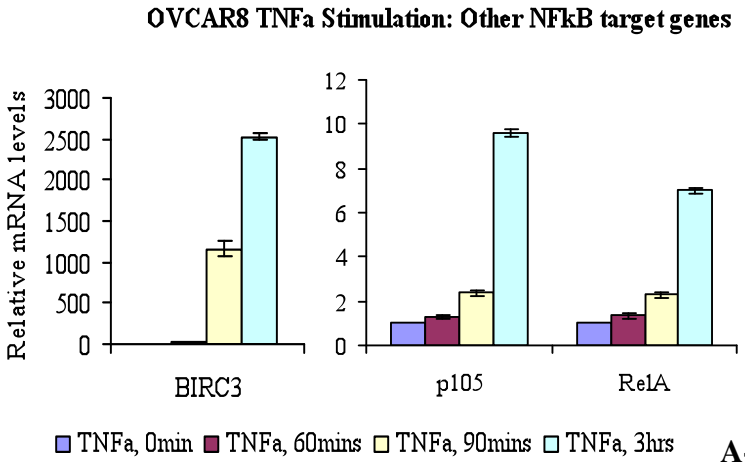

A-2

FIGURE 8A: Based on previous findings, we hypothesized that when STAT3 is inhibited, NF-κB may be activated, which leads to upregulation of IL-8. To validate that IL-8 is a NF-κB target gene in OVCAR8 cells, we stimulated cells with TNFα, which was known to activated the NF-κB pathway. qPCR data indicated that IL-8 was upregulated (**A-1**), as well as other NF-κB target genes including A20, BIRC3, p105, and RelA (**A-2**). This suggests that IL-8 is a NF-κB target gene in OVCAR8 cells.

FIGURE 8

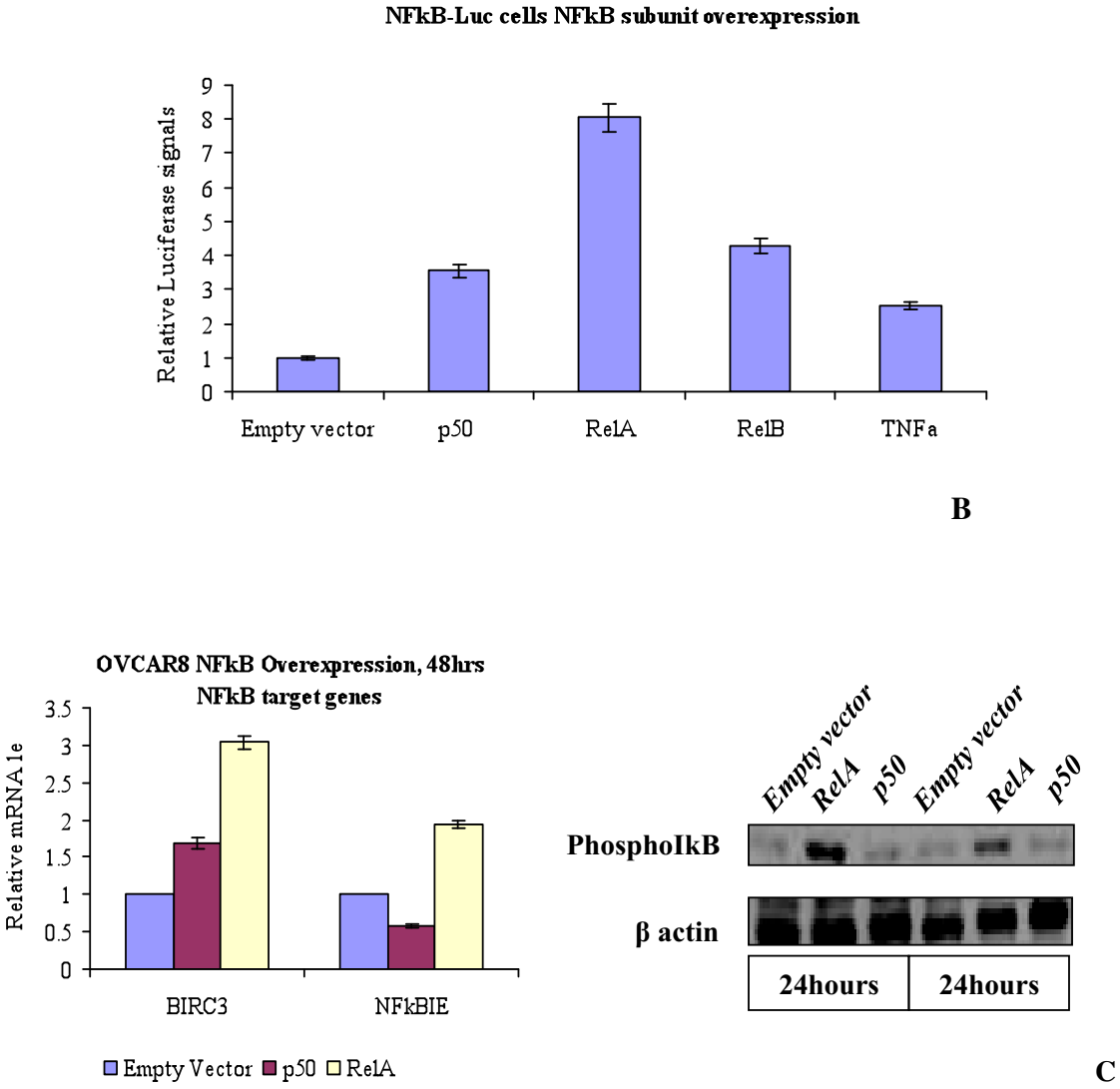

FIGURE 8B: NF-κB activity was studied in NF-κB-Luc cells, when different NF-κB subunits were overexpressed. Compared to empty vector, RelA/p65 overexpression resulted in the highest luciferase signal, indicating 8-fold induction of NF-κB activity, or 4 times the activation induced by TNFα stimulation. Other subunits also induced NF-κB activity when they were overexpressed but not as effective as RelA.

FIGURE 8C: I-κB levels were used to correlate with NF-κB activity. Consistent with the luciferase data, RelA seemed to be most effective in activating NF-κB in OVCAR8 cells. Furthermore, after 48 hours of overexpression, NF-κB target genes (BIRC3 and NFκBIE) were upregulated, indicating the activation of NF-κB.

FIGURE 8

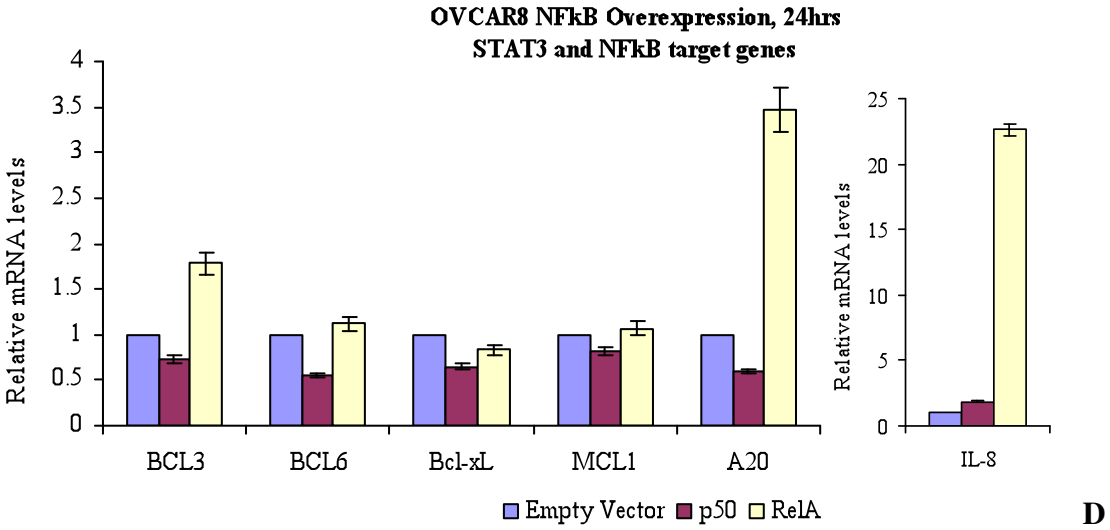

D

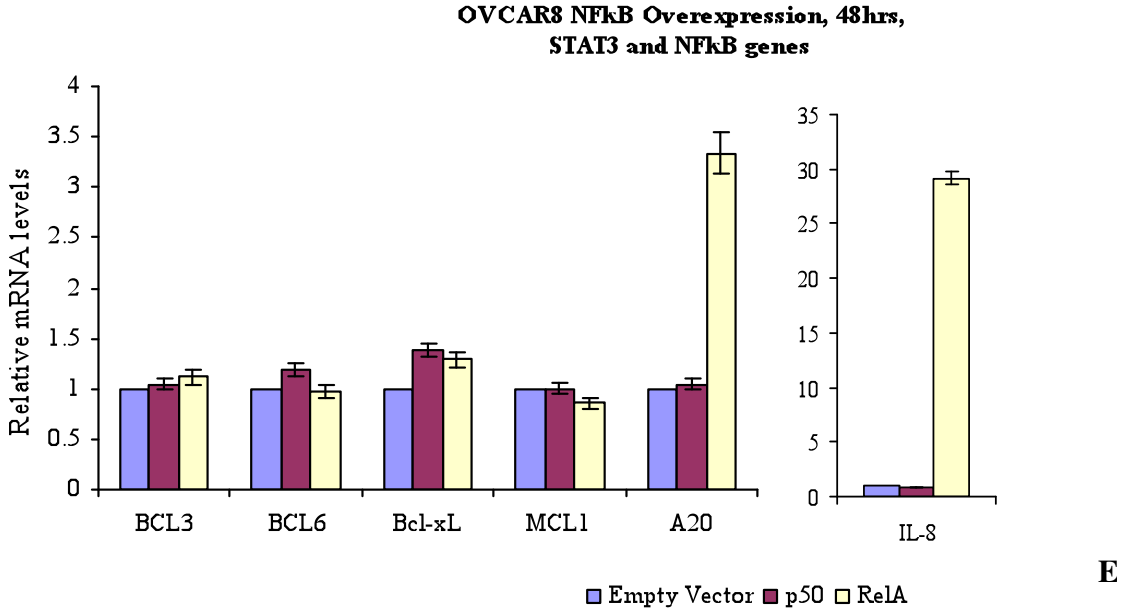

E

FIGURE 8D: After 24 hours of overexpression of RelA, A20 and IL-8 levels were both upregulated compared to p50 overexpression. This is consistent with previous findings that RelA overexpression activated NF-κB, which led to upregulation of IL-8.

FIGURE 8E: Similarly, IL-8 and A20 upregulations were observed with RelA overexpression for 48 hours in OVCAR8 cells.

FIGURE 9

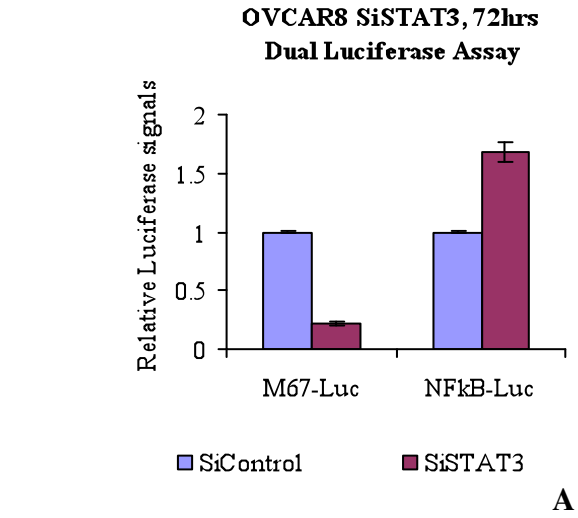

A

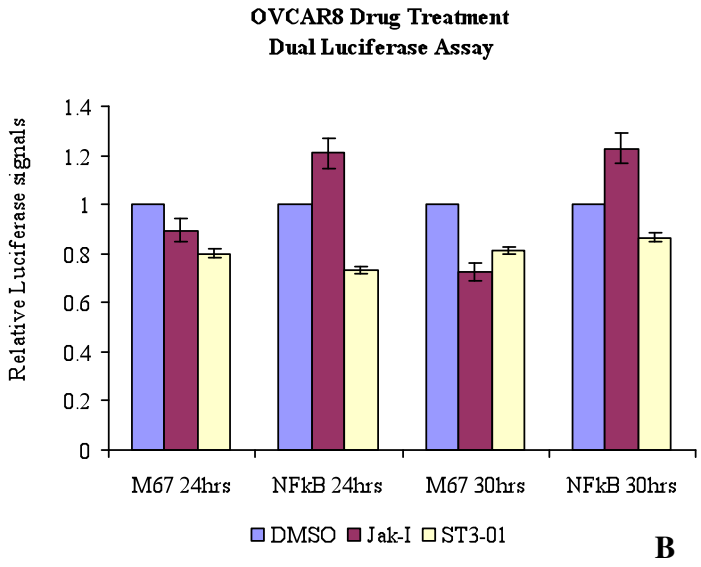

B

FIGURE 9A: STAT3 RNAi reduced the STAT3 promoter activity (M67-Luc) in OVCAR8 cells, as expected. On the contrary, NF-κB dependent reporter activity increased, suggesting that NF-κB activation may be reciprocally related to STAT3 inhibition in OVCAR8 cells.

FIGURE 9B: Similarly, when OVCAR8 cells were treated with STAT3 inhibitors, we observed that STAT3 dependent reporter activity decreased, whereas NF-κB dependent reporter activity increased with JAK-I.

FIGURE 9

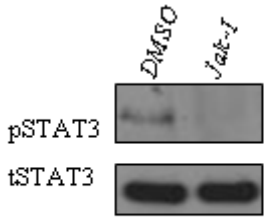

C-1

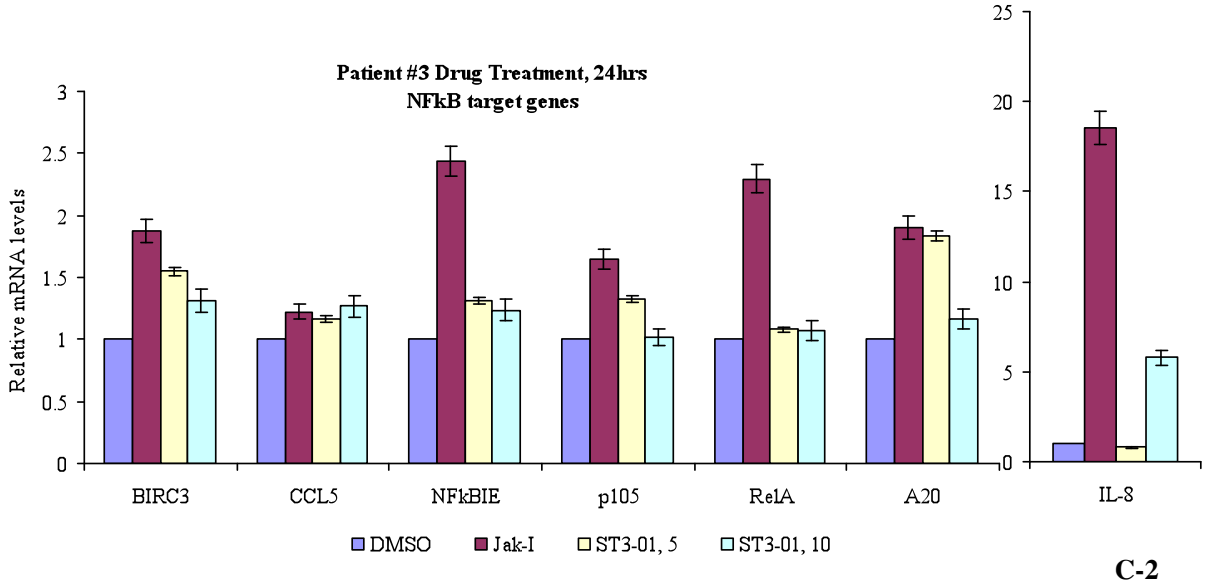

C-2

FIGURE 9C: Cells from ovarian cancer Patient #3 were shown to have constitutively activated STAT3, the phosphorylation of which was inhibited with 1-hour JAK-I treatment (**C-1**). Similarly, we noticed that most of the NF-κB target genes were upregulated when these primary cancer cells were treated with STAT3 inhibitors for 24 hours (**C-2**). This further supports the hypothesis that NF-κB activation is reciprocally related to STAT3 inhibition in ovarian cancers.

FIGURE 9

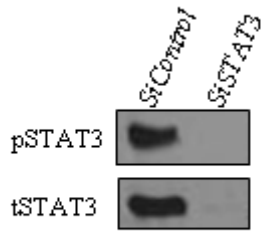

D-1

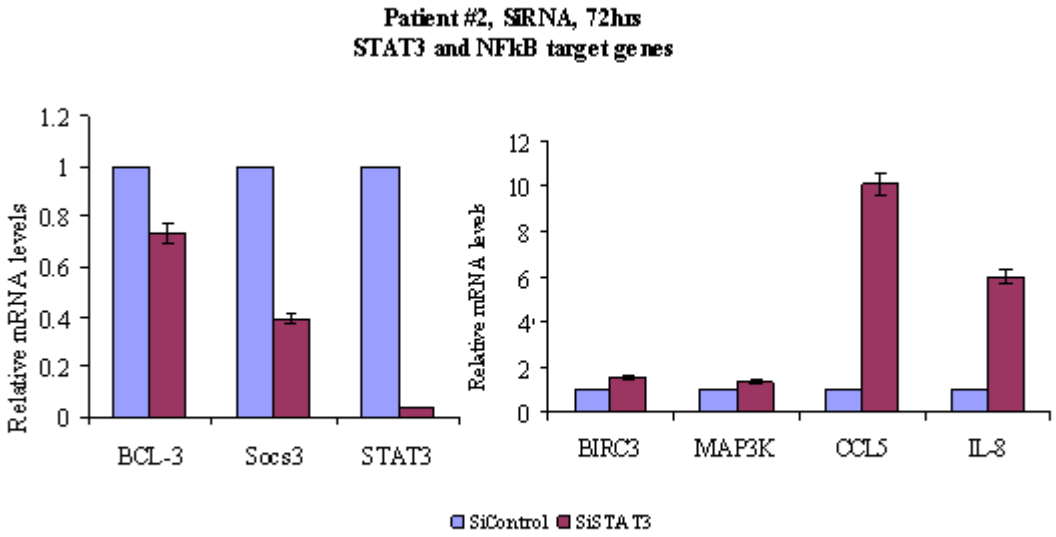

D-2

FIGURE 9D: Primary cancer cells from Patient #2 also had constitutive STAT3 phosphorylation. The levels of STAT3 (both phospho-STAT3 and total STAT3) were reduced by STAT3 RNAi (**D-1**). qPCR analysis showed that when STAT3 was inhibited (BCL-3 and SOCS3 were downregulated), NF-κB was activated (BIRC3, MAP3K, CCL5, and IL-8). This implies that the NF-κB pathway may be reciprocally associated with the STAT3 pathway (**D-2**).

FIGURE 10

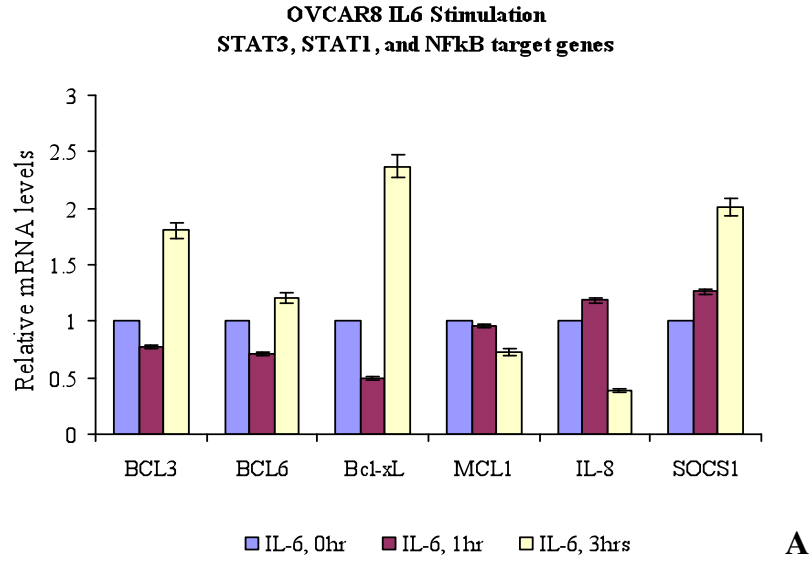

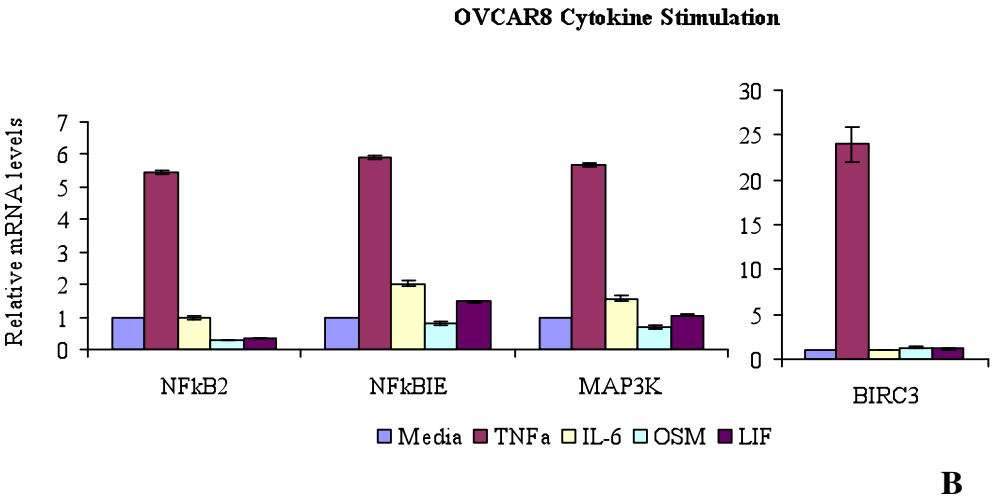

FIGURE 10A: We stimulated OVCAR8 cells with IL-6 to activate the STAT3 pathway. IL-8 was downregulated with 3 hours IL-6 stimulation, suggesting that activating STAT3 downregulates IL-8. This also suggests that either STAT3 negatively regulates IL-8, or that NF-κB activates reciprocally when STAT3 is inhibited.

FIGURE 10B: When OVCAR8 cells were stimulated with OSM and LIF, which could also activate the STAT3 pathway, some of the NF-κB target genes were downregulated. However, this was not consistent for all NF-κB target genes, since some of them were upregulated in response to these cytokine stimulations.

FIGURE 10

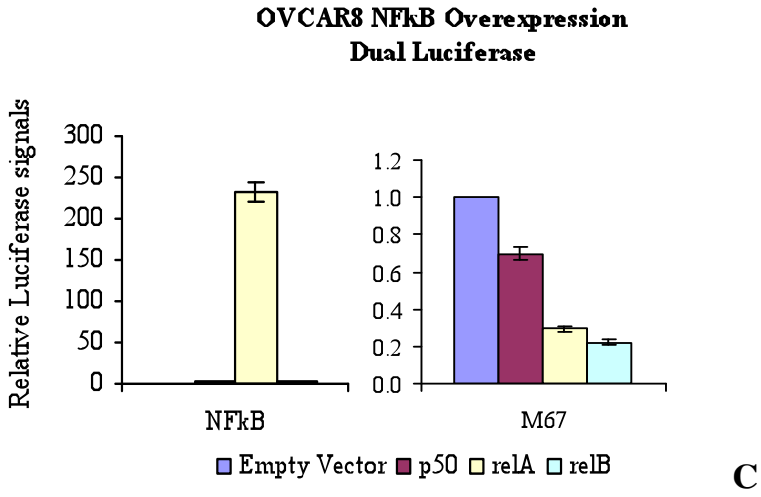

C

FIGURE 10C: When NF-κB subunits were overexpressed in OVCAR8, STAT3 dependent reporter activities were decreased, indicating decreased STAT3 promoter activity. This suggested that STAT3 inhibition may also be reciprocally related to NF-κB activation.

FIGURE 11

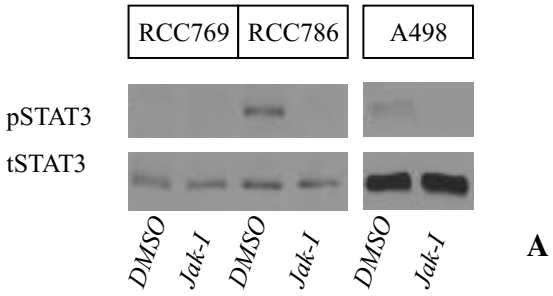

A

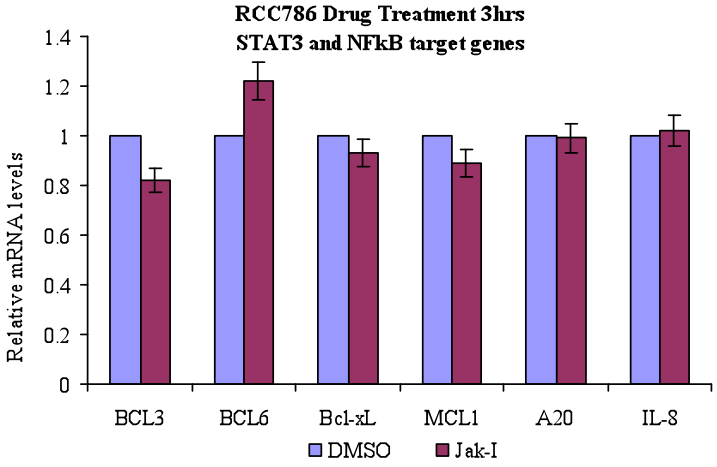

B-1

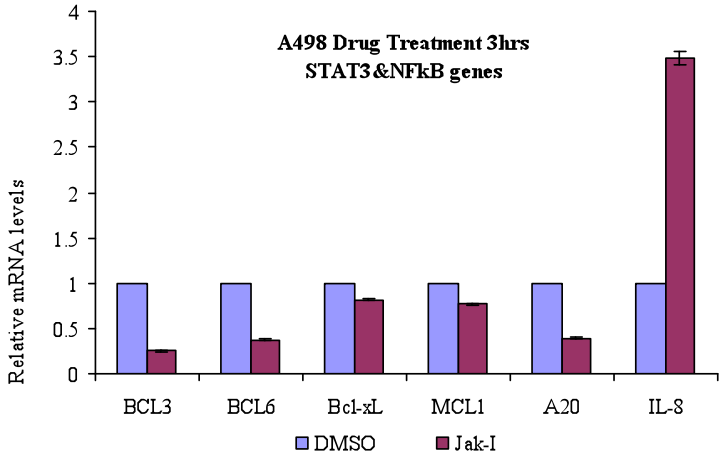

B-2

FIGURE 11A: Immunoblotting analysis of pSTAT3 showed that RCC786 cells and A498 cells contained consistently activated STAT3, whereas RCC769 cells did not.

FIGURE 11B: IL-8 levels did not change after 3 hours of JAK-I treatment in RCC786 cells, whereas it was upregulated by 3.5-fold in A498 cells. This difference suggests that cells with constitutively activated STAT3 may respond to JAK-I differently.

FIGURE 11

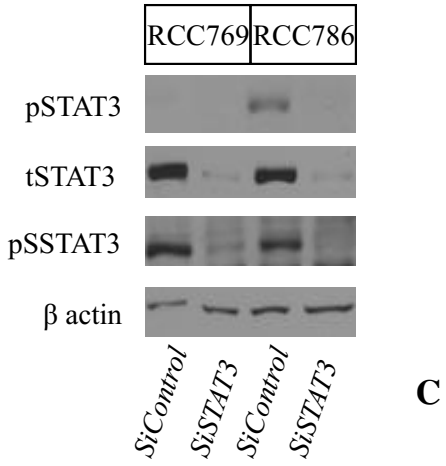

C

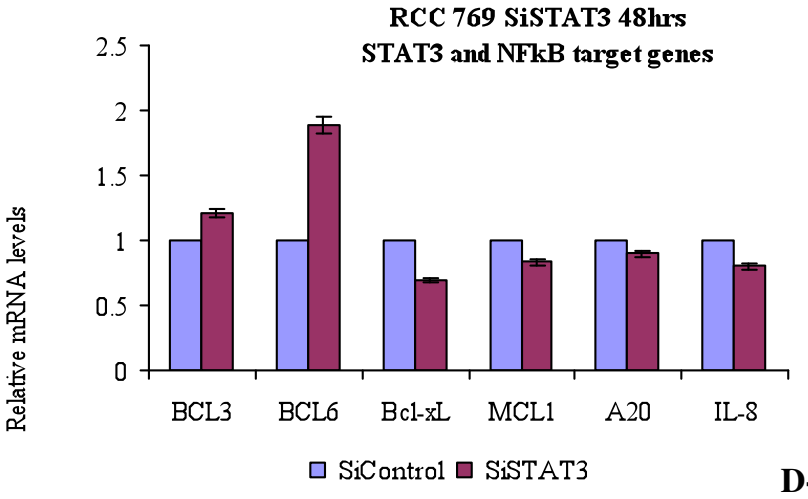

D-1

FIGURE 11C: STAT3 RNAi was performed in renal cell carcinoma cell lines. STAT3 levels were reduced after 48 hours siRNA knock down.

FIGURE 11D: RCC769 cells with no constitutively activated STAT3 showed no upregulation of IL-8. This suggests that IL-8 upregulation is specific to STAT3 inhibition in cancer cells with constitutively activated STAT3.

FIGURE 11

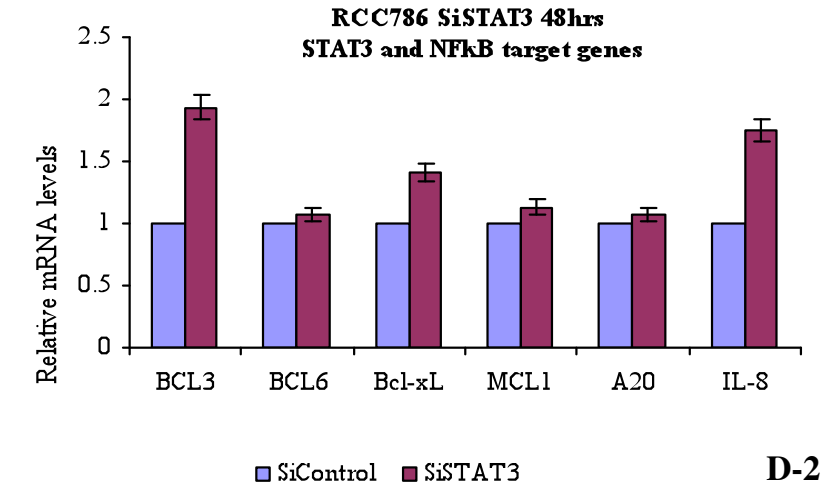

D-2

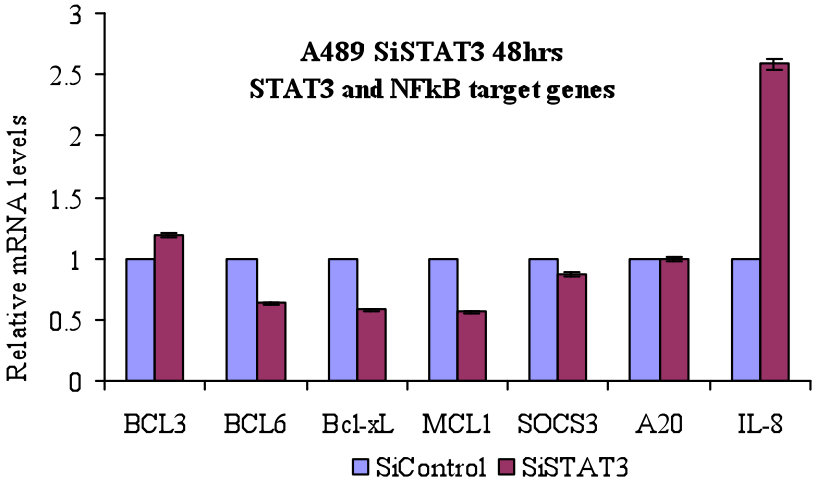

D-3

FIGURE 11D (CONTINUED): On the contrary, renal cancer cell lines with constitutive activated STAT3 showed IL-8 activation. This further suggests that the upregulation of IL-8 related to STAT3 inhibition happens not only in ovarian cancer cells but also in kidney cancer cells with constitutively activated STAT3.

FIGURE 12

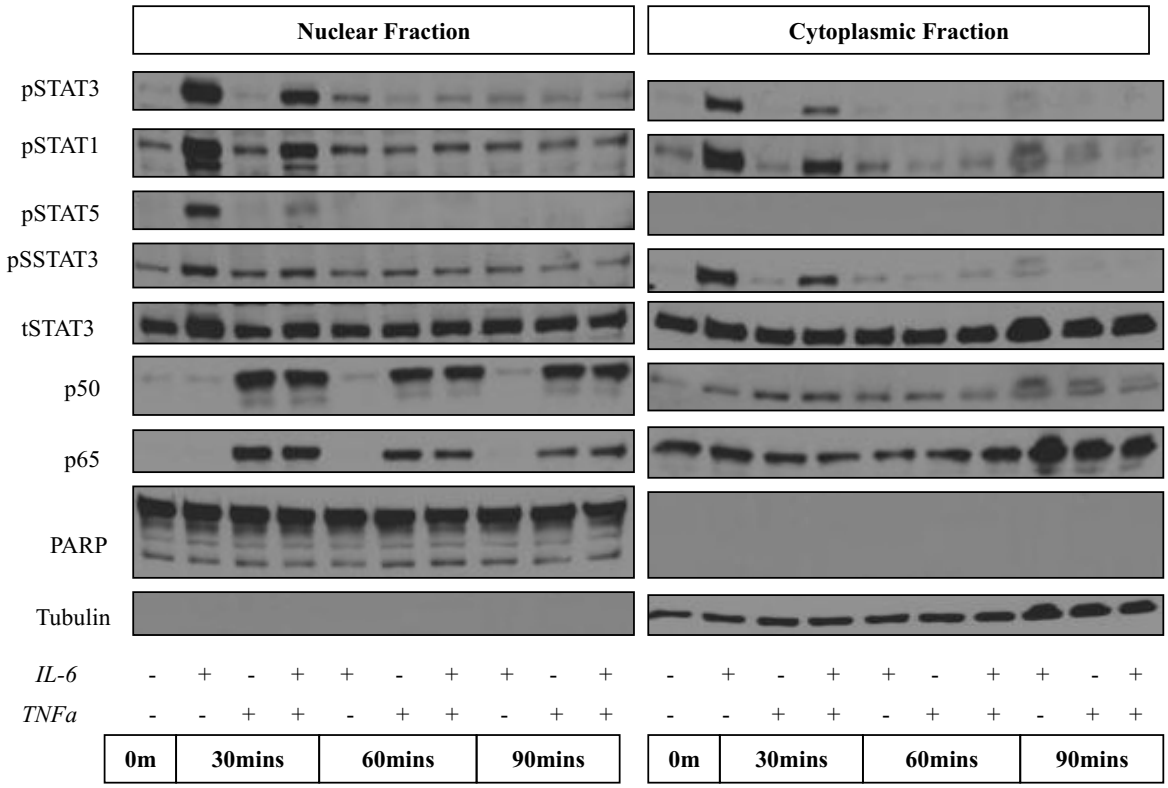

Figure 12A

FIGURE 12A: OVCAR8 cells were stimulated with IL-6, TNFα, or a combination of both for 30, 60, and 90 minutes. Nuclear-cytoplasmic fractionation was performed to study nuclear translocation of STAT3 and more importantly, p65. In OVCAR8 cells, STAT3 and p65 nuclear translocation was observed with IL-6 and TNFα stimulation, respectively. In addition, IL-6 seemed to also activate STAT1 and STAT5, where as TNFα stimulation also caused Nuclear translocation of p50.

FIGURE 12

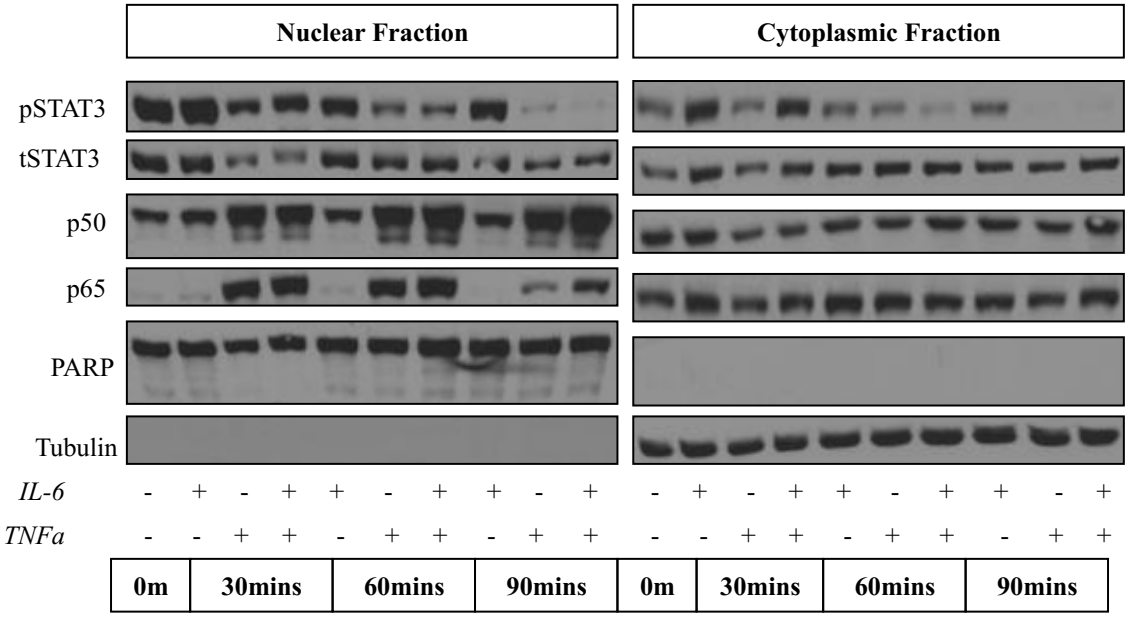

Figure 12B

FIGURE 12B: Similarly, SKOV3 cells were stimulated with IL-6, TNFα, or a combination of both for 30, 60, and 90 minutes. After nuclear-cytoplasmic fractionation was performed, STAT3 and p65 nuclear translocation was observed with IL-6 and TNFα stimulation, respectively.

FIGURE 13

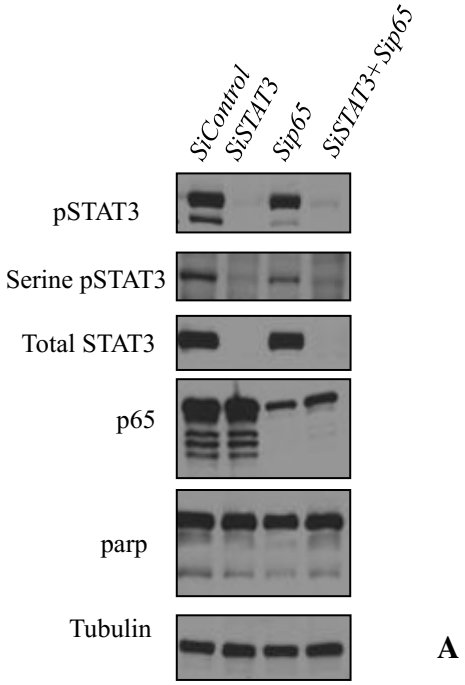

A

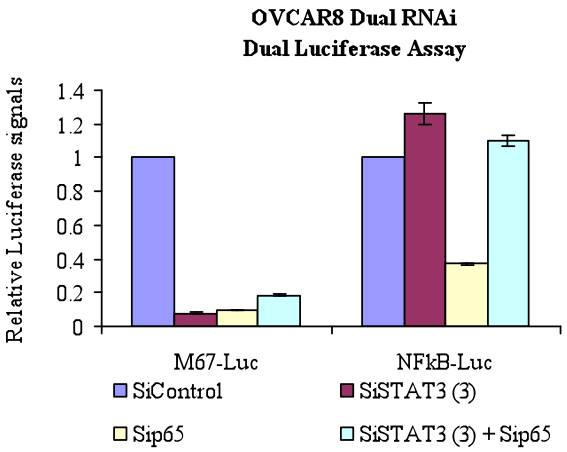

B

FIGURE 13A: OVCAR8 cells were treated with STAT3 siRNA (#3), p65 siRNA, and a combination of STAT3 and p65 siRNAs. STAT3 and p65 protein levels were significantly reduced after 72 hours of knock down.

FIGURE 13B: After reverse transfection of STAT3 siRNA (#3), p65 siRNA, and a combination of STAT3 and p65 siRNAs, dual luciferase was performed. OVCAR8 cells treated with p65 siRNA did not show induced NF-κB dependent reporter activity, indicating that p65 knock down reduces the NF-κB activation reciprocally related to STAT3 inhibition.

FIGURE 13

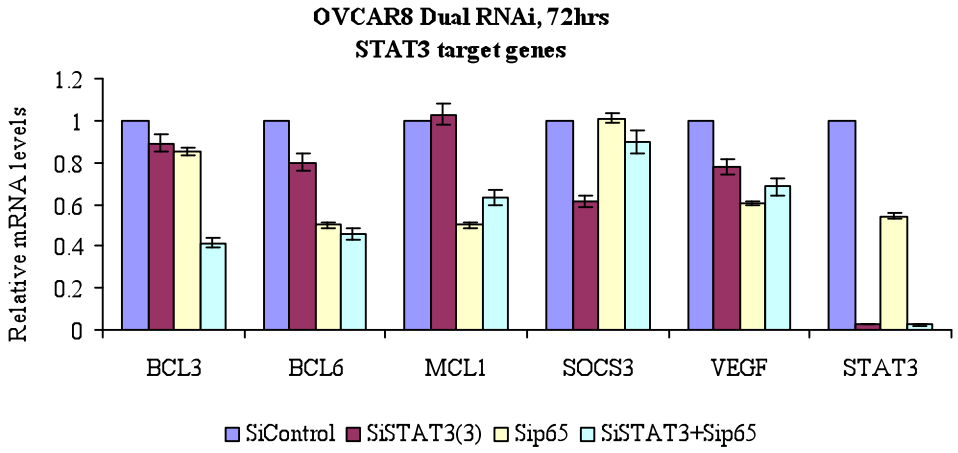

C-1

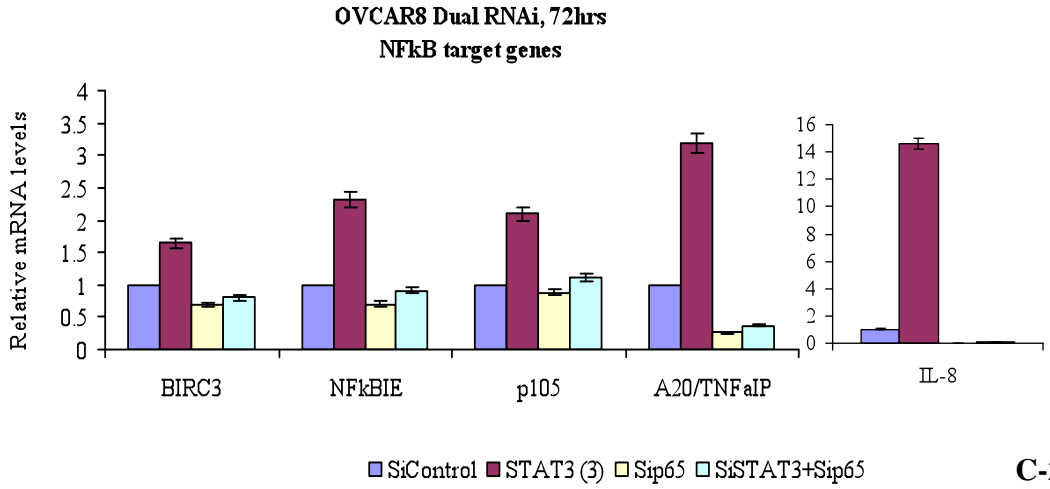

C-2

FIGURE 13C: Some of the STAT3 target genes were downregulated with p65 siRNA (**C-1**). This may be due to p65 regulating the expression of IL-6 gene. More importantly, p65 siRNA abrogated the upregulation of NF-κB target genes in response to STAT3 siRNA (**C-2**). This suggests that p65 plays an important role in the NF-κB activation induced by STAT3 inhibition.

FIGURE 13

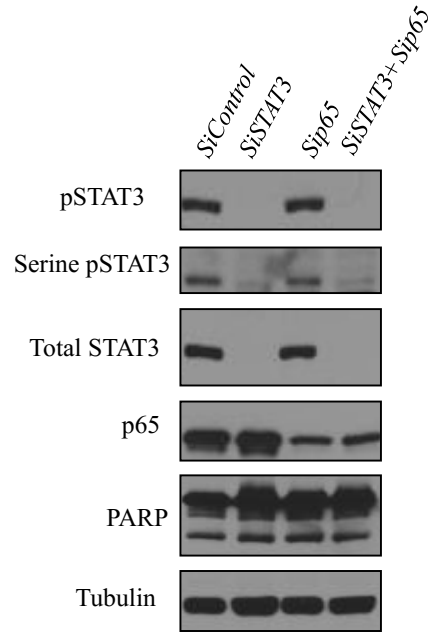

D

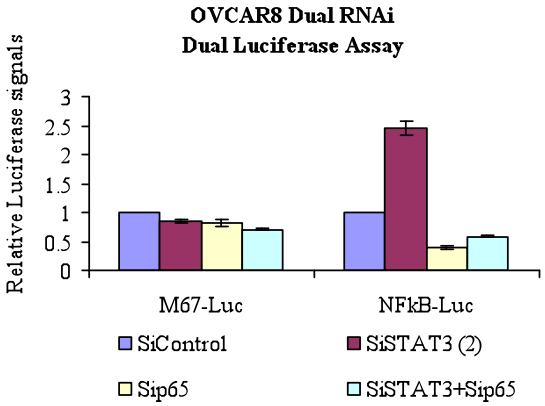

E

FIGURE 13D: To ensure that the previous results were not restricted to a specific sequence of STAT3 siRNA, OVCAR8 cells were treated with STAT3 siRNA (#2), p65 siRNA, and a combination of STAT3 and p65 siRNAs. STAT3 and p65 protein levels were significantly reduced after 72 hours of knock down.

FIGURE 13E: Similarly, reverse transfection of STAT3 siRNA (#3), p65 siRNA, and a combination of STAT3 and p65 siRNAs was followed by dual luciferase assay. p65 knock down reduced the reciprocal NF-κB activation associated with STAT3 inhibition.

FIGURE 13

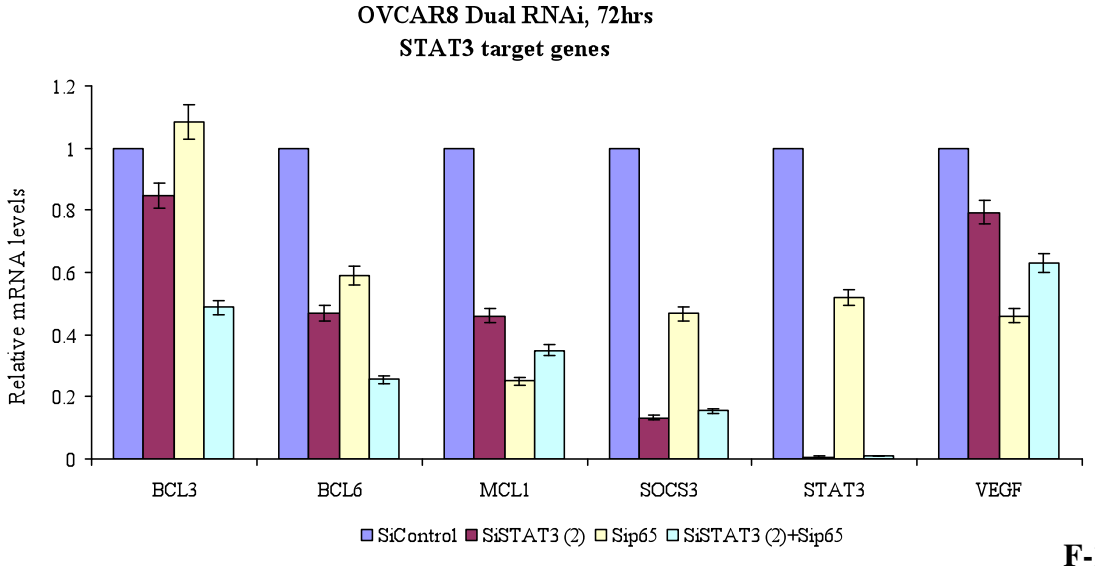

F-1

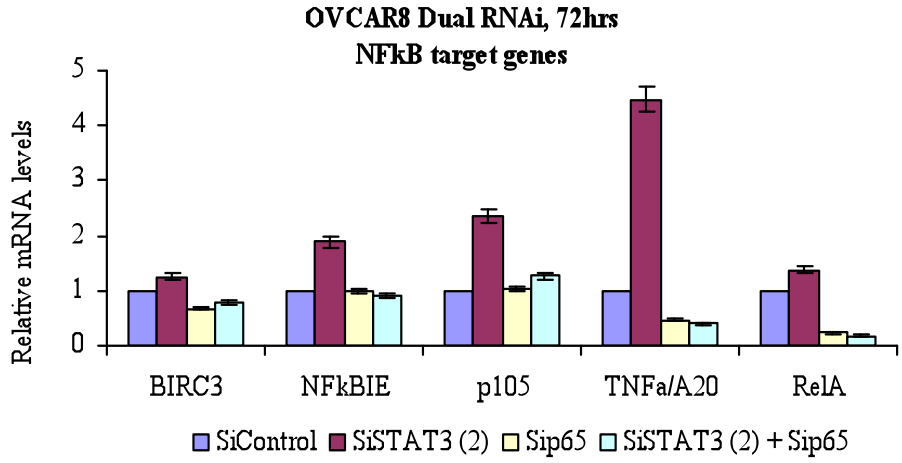

F-2

FIGURE 13F: Similar results showed that STAT3 target genes were downregulated with p65 siRNA due to p65 regulating the expression of IL-6 gene (**F-1**). Furthermore, p65 siRNA diminished the activation of NF-κB when STAT3 was inhibited (**F-2**).

FIGURE 14

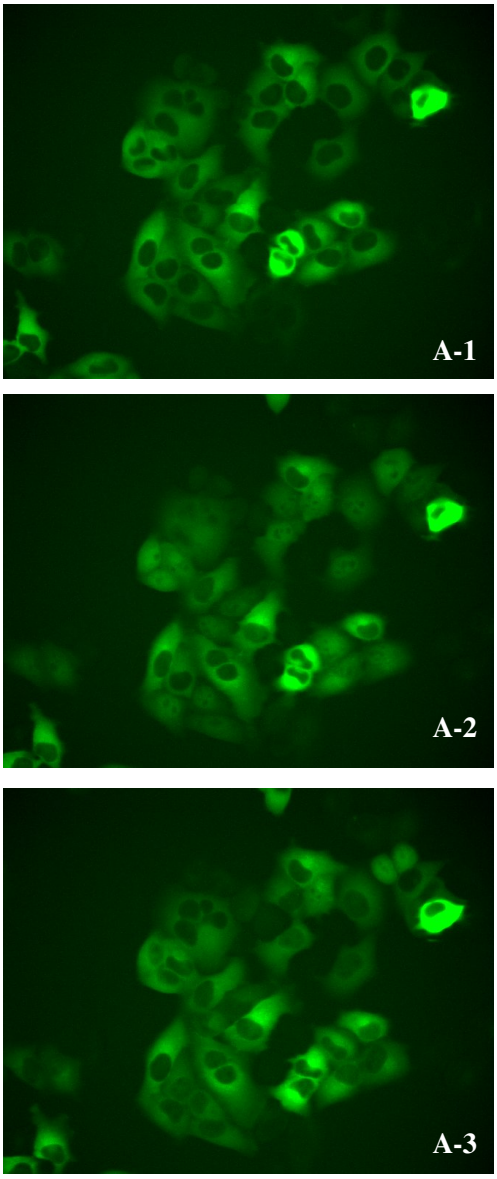

FIGURE 14A: HeLa p65GFP cells with GFP tagged p65 was used to visualize p65 nuclear translocation at the single cell level. Before TNFα stimulation, p65 remained in the cytoplasm (**A-1**). Fifteen minutes after TNFα stimulation, p65 nuclear translocation was visualized (**A-2**). p65 continued to translocate into the nucleus even 2 hours after TNFα stimulation, suggesting that p65 nuclear translocation is important for NF-κB activation.

FIGURE 14

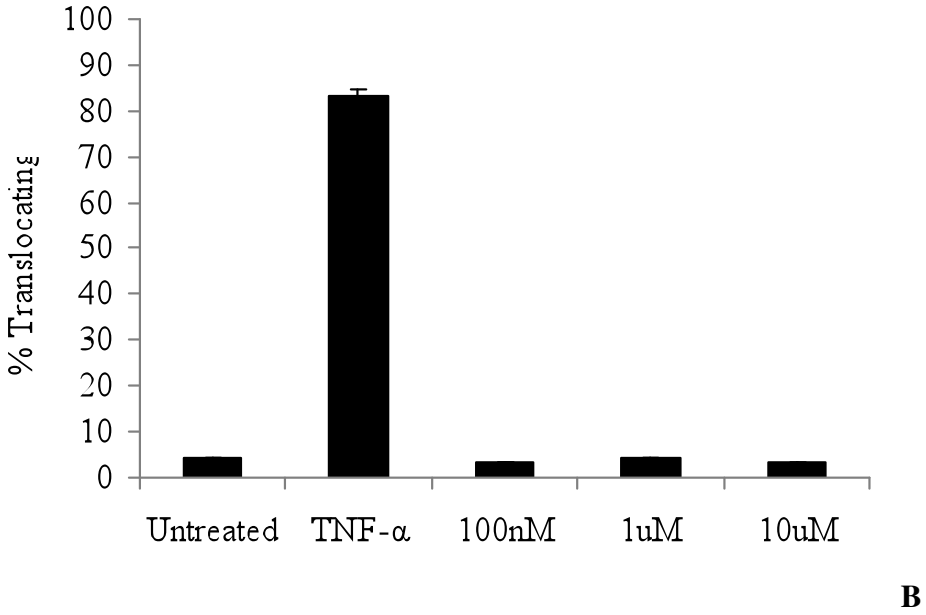

B

FIGURE 14B: However, when HeLa p65GFP cells were treated with ST3-01 to induce NF-κB activation that associated with STAT3 inhibition, no significant p65 nuclear translocation was observed up to 22 hours post treatment. This suggests that in HeLa cells, p65 nuclear translocation may not be the mechanism through which NF-κB is activated when STAT3 is inhibited.

FIGURE 14

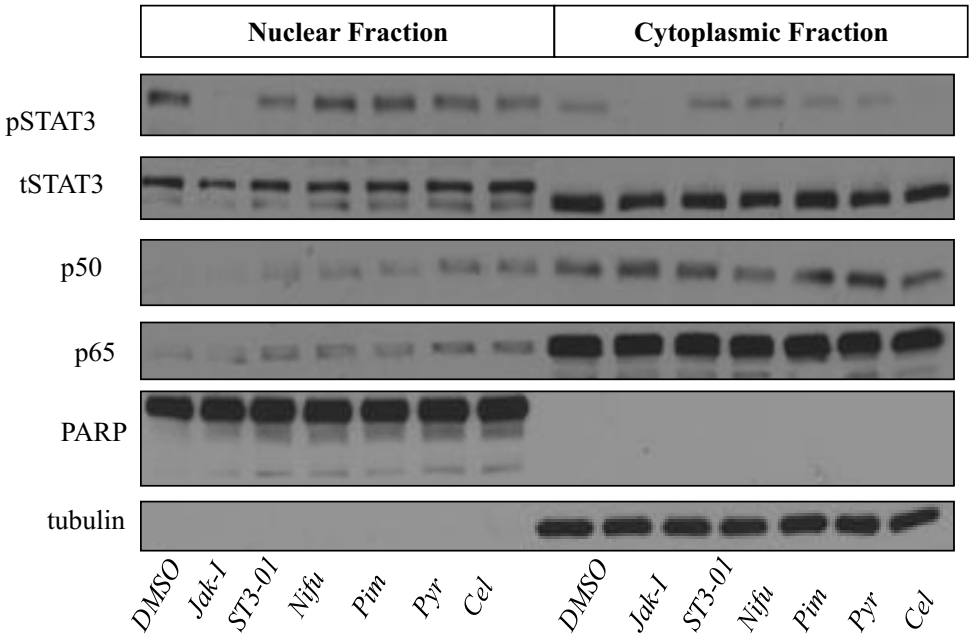

Figure 14C

FIGURE 14C: OVCAR8 cells were treated with a panel of STAT3 inhibitors, as well as celastrol, an NF-κB inhibitor for 6 hours. Nuclear-cytoplasmic fractionation was performed to detect nuclear translocation of singling molecules. Some p65 nuclear translocation was observed with ST3-01, nifuroxazide, pimozide, and pyrimethamine. However, p65 nuclear translocation was also observed with celastrol.

FIGURE 14

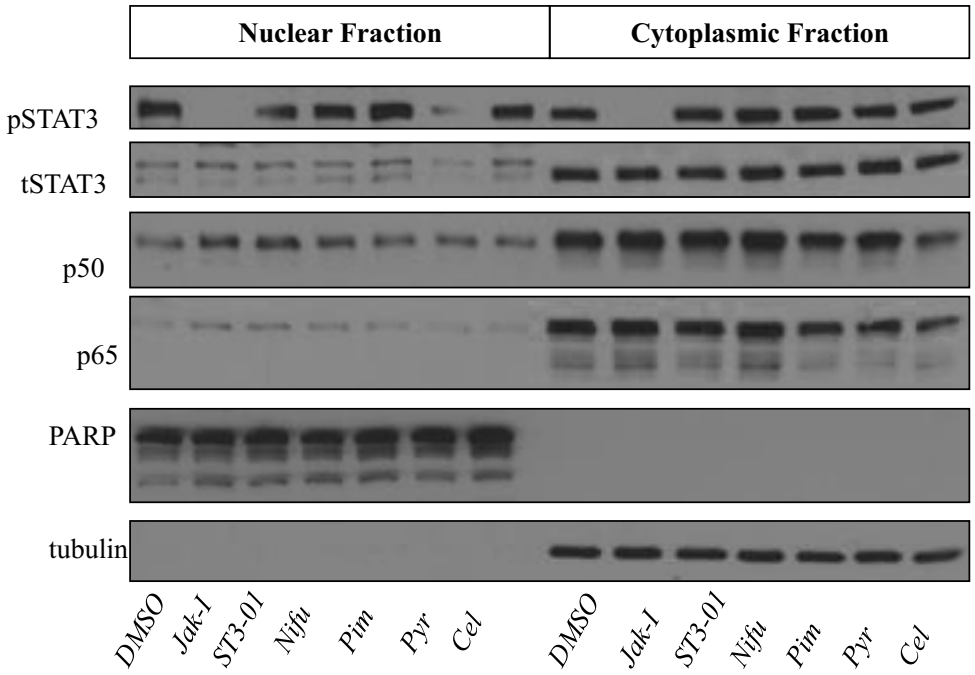

Figure 14D

FIGURE 14D: OVCAR8 cells were treated with a panel of STAT3 inhibitors and celastrol for 24 hours. After nuclear-cytoplasmic fractionation was performed, we observed a slight increase in p65 nuclear translocation with JAK-I, ST3-01, nifuroxazide, and pimozide. This suggests that p65 nuclear translocation may contribute to the NF-κB activation in response to STAT3 inhibition, but only minimally.

FIGURE 14

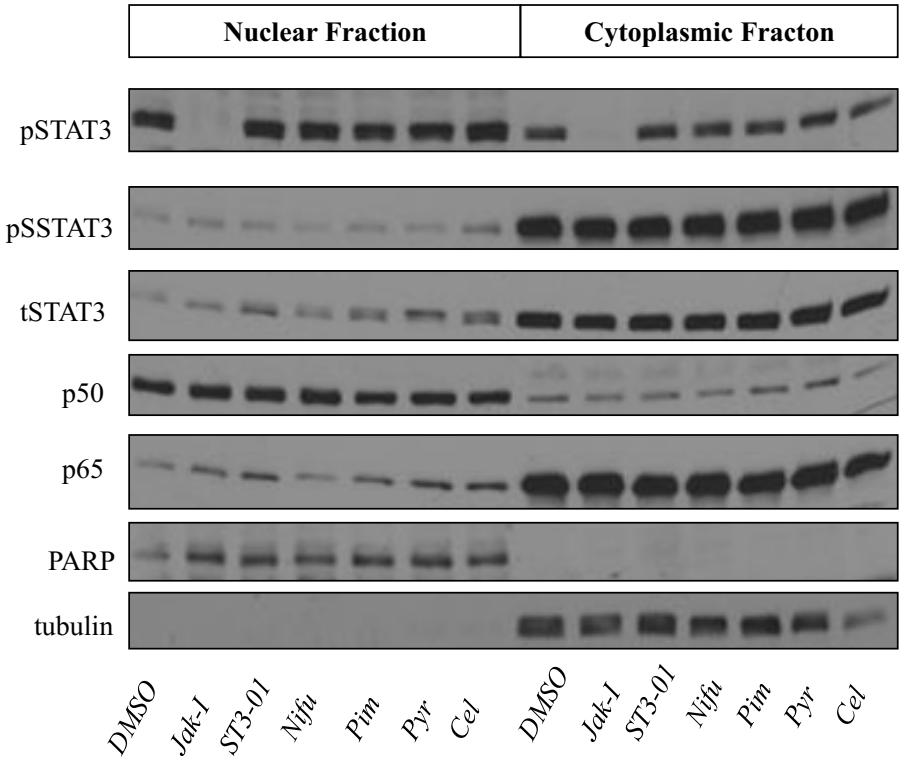

Figure 14E

FIGURE 14E: Similarly, in SKOV3 cells, after 16 hours treatment with the same panel of STAT3 inhibitors, p65 nuclear translocation was increased slightly for JAK-I, ST3-01, pimozide, pyrimethamine, but also for celastrol. This result is inclusive, thus suggesting that p65 nuclear translocation may be contributing minimally to the reciprocal activation of NF-κB with STAT3 inhibition.

FIGURE 14

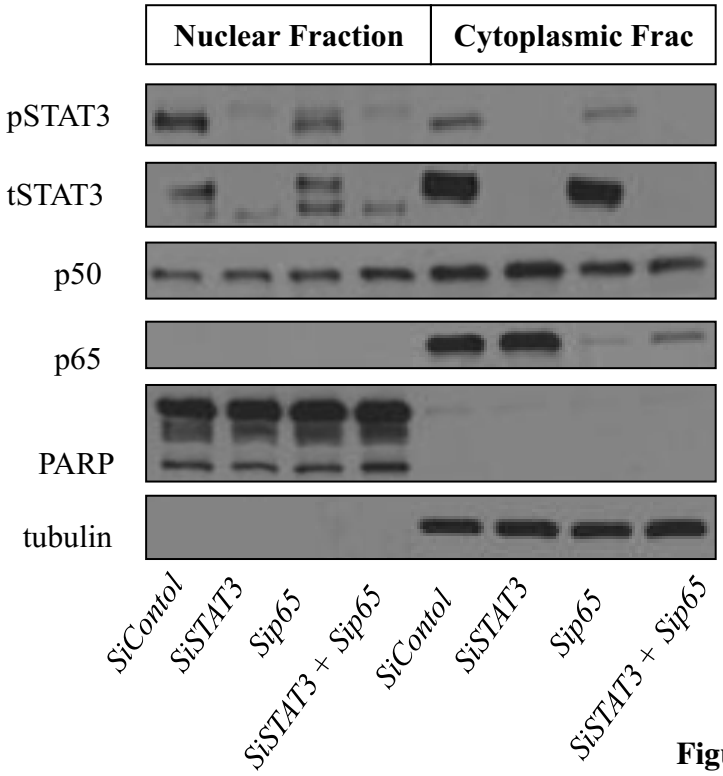

Figure 14F

FIGURE 14F: Furthermore, we reversely transfected STAT3 siRNA, p65 siRNA, and a combination of STAT3 and p65 siRNAs in the OVCAR8 cells for 72 hours. Nuclear-cytoplasmic fractionation detected no p65 nuclear translocation with STAT3 knock down. This further suggests that p65 nuclear translocation plays a minor role in the reciprocal relationship between NF-κB activation and STAT3 inhibition. Alternative mechanisms and hypotheses were proposed in DISCUSSION.

SUPPLEMENTARY FIGURE 1

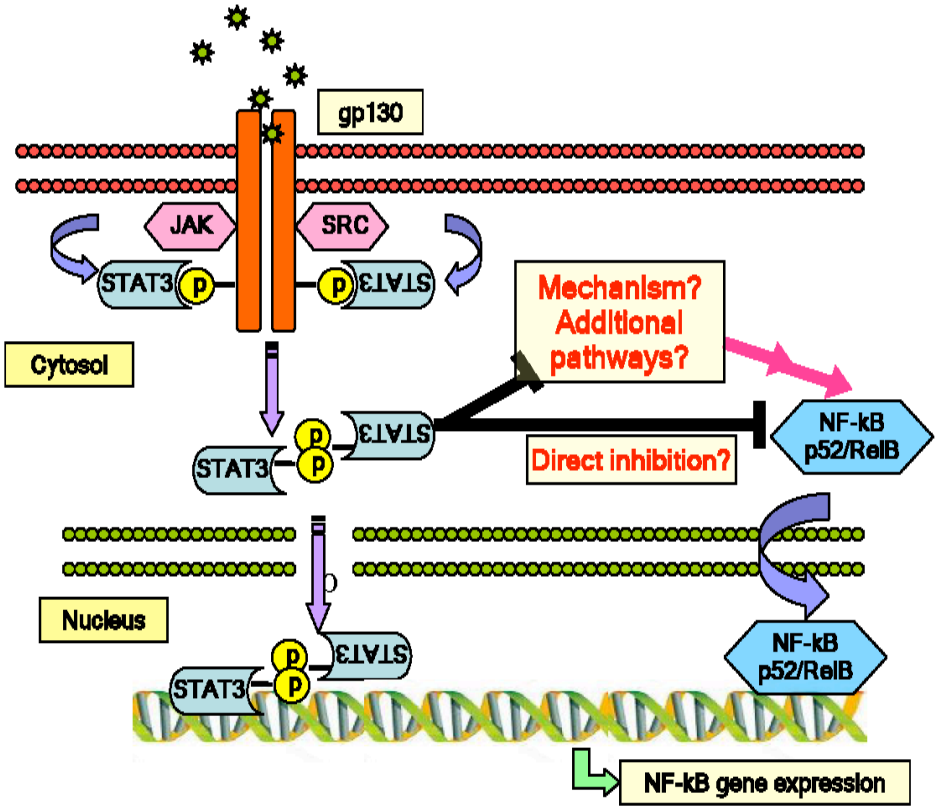

MODEL 1: Inhibition of STAT3 activates the non-canonical NF-κB pathway, resulting in nuclear translocation of p52/RelB and the upregulation of NF-κB target genes.

.

SUPPLEMENTARY FIGURE 2

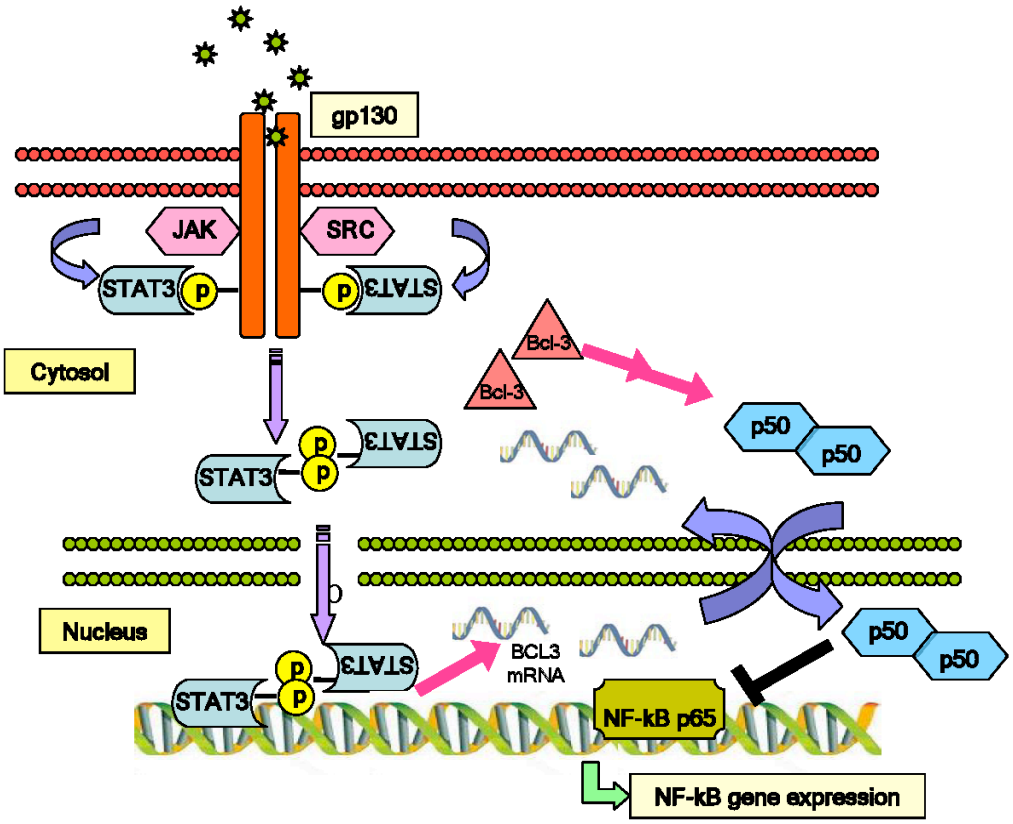

MODEL 2: STAT3 inhibition results initially in downregulation of the endogenous STAT3 target genes, one of them being BCL3. Normally, Bcl3 protein interacts and stablizes the p50 homodimer in the cytoplasm. In the nucleus, the p50 homodimer can prevent the NF-κB p65 from binding DNA and regulating gene expression. When BCL3 is downregulated due to inhibition of the STAT3 pathway, p50 homodimer is destablized, preventing it from blocking the activation of the NF-κB.

SUPPLEMENTARY FIGURE 3

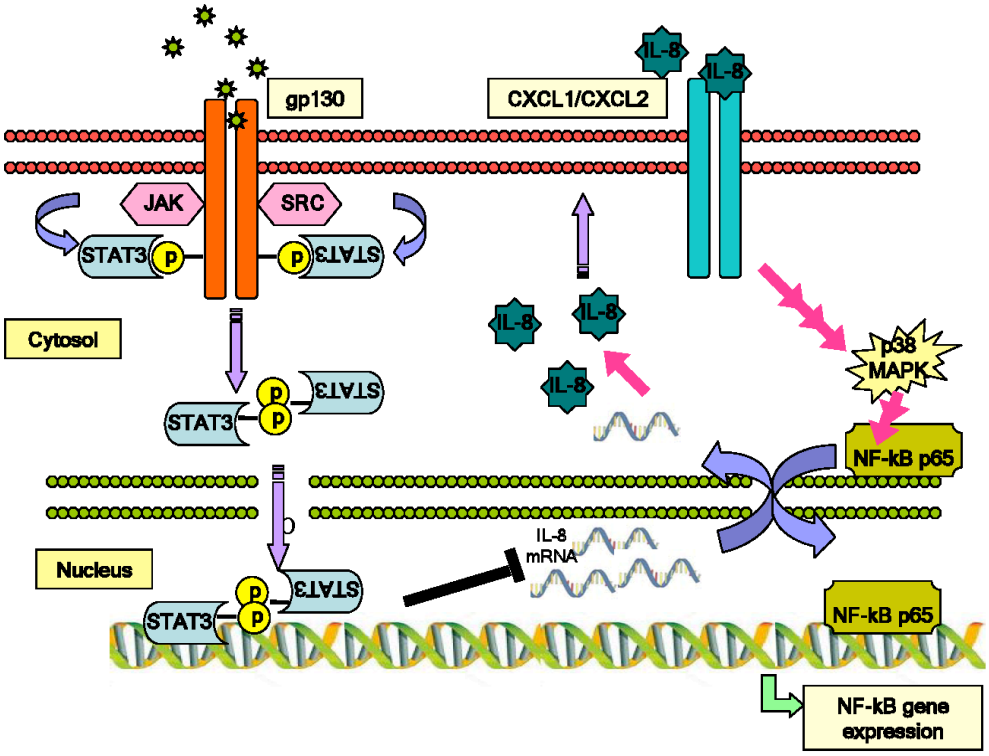

Model 3: STAT3 acts as a negative regulator of IL-8, which has been shown to activate the p38 MAPK pathway. When STAT3 is inhibited, IL-8 is upregulated, leading to the activation of p38 MAPK, which can indirectly activate the NF-κB pathway.

REFERENCES

1. Slamon DJ, Godolphin W, Jones LA, Holt JA, Wong SG, Keith DE, Levin WJ, Stuart SG, Udove J, Ullrich A (1989) Studies of the HER-2/neu proto-oncogene in human breast and ovarian cancer. *Science* (New York, NY) 244(4905):707
2. Yu H, Kortylewski M, Pardoll D. Crosstalk between cancer and immune cells: role of STAT3 in the tumour microenvironment. *Nat Rev Immunology*. 2007;7:41–51.
3. Piek JM, van Diest PJ, Verheijen RH (2008). "Ovarian carcinogenesis: an alternative hypothesis". *Adv. Exp. Med. Biol.* 622: 79–87.
4. Bowman T, Garcia R, Turkson J, Jove R.STATs in oncogenesis. *Oncogene*. 2000 May 15;19(21):2474-88.
5. Stark G, Kerr I, Williams B, Silverman R and Schreiber R. (1998). How cells respond to interferons. *Annu. Rev. Biochem.* 67, 227-264.
6. Frank, D. A., STAT signaling in the pathogenesis and treatment of cancer. *Mol Med* 1999, 5, (7), 432-56.
7. Frank, D. A., STAT3 as a central mediator of neoplastic cellular transformation. *Cancer Lett* 2007, 251, (2), 199-210.
8. Akira S. (2000). Roles of STAT3 defined by tissue-specific gene targeting. *Oncogene* 19, 2607-2611.
9. Turkson J. et al. STAT proteins: novel molecular targets for cancer drug discovery. *Oncogene*. 2000 Dec 27;19(56):6613-26.
10. Bhardwaj, A.; Sethi, G.; Vadhan-Raj, S.; Bueso-Ramos, C.; Takada, Y.; Gaur, U.; Nair, A. S.; Shishodia, S.; Aggarwal, B. B., Resveratrol inhibits proliferation, induces apoptosis, and overcomes chemoresistance through down-regulation of STAT3 and nuclear factor-kappaB-regulated antiapoptotic and cell survival gene products in human multiple myeloma cells. *Blood* 2007, 109, (6), 2293-302.
11. Frank DA. STAT inhibition in the treatment of cancer: Transcription factors as targets for molecular therapy. *Curr Cancer Ther Rev* 2006; 2:57-65.
12. Frank, D. A., STAT signaling in cancer: insights into pathogenesis and treatment strategies. *Cancer Treat Res* 2003, 115, 267-91.

13. Nelson EA, Walker SR, Kepich A, Gashin LB, Hideshima T, Ikeda H, Chauhan D, Anderson KC, Frank DA. Nifuroxazide inhibits survival of multiple myeloma cells by directly inhibiting STAT3. *Blood*. 2008 Dec 15;112(13):5095-102.
14. Tian B, Brasier AR. Identification of a nuclear factor κB-dependent gene network. *Recent Prog. Horm. Res*. 2003, 58: 95-130.
15. Romaine I Fernando, et al. "IL-8 signaling plays a critical role in the epithelial-mesenchymal transition of human carcinoma cells." *Cancer Research*. 71(15) August 1, 2011.
16. Escarcega RO, et al. The transcription factor nuclear factor-κB and cancer. *Clinical Oncology* 19 (2): 154-61.
17. S. Vallabhapurap, M. Karin. Regulation and function of NF-kappaB transcription factors in the immune system. *Annu. Rev. Immunol*., 27 (2009), pp. 693–733.
18. A. Hoffmann, G. Natoli, G. Ghosh. Transcriptional regulation via the NF-kappaB signaling module. *Oncogene*, 25 (2006), pp. 6706–6716.
19. S.G. Pereira, F. Oakley. Nuclear factor-kappaB1: regulation and function. *Int. J. Biochem. Cell Biol*., 40 (8) (2008), pp. 1425–1430.
20. K.J. Min, J.T. Lee, E.H. Joe, T.K. Kwon. An IκBα phosphorylation inhibitor induces heme oxygenase-1(HO-1) expression through the activation of reactive oxygen species (ROS)-Nrf2-ARE signaling and ROS–PI3K/Akt signaling in an NF-κB-independent mechanism. *Cell Signal.,* 3 (9) (2011), pp. 1505–1513
21. M.J. Morgan, Z.G. Liu. Crosstalk of reactive oxygen species and NF-κB signaling. *Cell Res.,* 21 (1) (2011), pp. 103–115
22. Jarboe et al. Evidence of a Latent Precursor (p53 Signature) that May Precede Serous Endometrial Intraepithelial Carcinoma. *Mod Pathol*. 2009. March; 22(3): 345-350.
23. Karst AM, Levanon K, Drapkin R. Proc Natl Acad Sci U S A. Modeling high-grade serous ovarian carcinogenesis from the fallopian tube. 2011 May 3;108(18):7547-52. *Epub* 2011 Apr 18.
24. Lynch HT, et al. Hereditary ovarian carcinoma: Heterogeneity, molecular genetics, pathology, and management. *Mol Oncol*. 2009;3:97–137.
25. Nelson et al. The STAT5 inhibitor pimozide decreases survival of chronic myelogenous leukemia cells resistant to kinase inhibitors. *Blood*. 2011 March 24; 117(12): 3421–3429

26. Sirichaiwat C. et al. (2004). Target guided synthesis of 5-benzyl-2,4-diamonopyrimidines: their antimalarial activities and binding affinities to wild type and mutant dihydrofolate reductases from Plasmodium falciparum. *J Med Chem* 47 (2): 345–54.
27. Alvarez JV, Greulich H, Sellers WR, Meyerson M, Frank DA. (2006) Signal transducer and activator of transcription 3 is required for the oncogenic effects of non-small-cell lung cancer-associated mutations of the epidermal growth factor receptor. *Cancer Res.* 66:3162–3168.
28. Núria de la Iglesia et al. Deregulation of a STAT3–Interleukin 8 Signaling Pathway Promotes Human Glioblastoma Cell Proliferation and Invasiveness. The *Journal of Neuroscience*. June 4, 2008. 28(23):5870 –5878.
29. Tian et al. A TNF-induced gene expression program under oscillatory NF-*κ*B control. *BMC Genomics* 2005, 6:137
30. Whitehead, K. A.; Dahlman, J. E.; Langer, R. S.; Anderson, D. G. Silencing or Stimulation? SiRNA Delivery and the Immune System. *Annual Review of Chemical and Biomolecular Engineering* 2: 2011. 77–96.
31. Schoenborn JR, Wilson CB. Regulation of interferon-gamma during innate and adaptive immune responses. *Adv. Immunol.* 2007. 96: 41–101.
32. Fornari FA, Randolph JK, Yalowich JC, Ritke MK, Gewirtz DA. Interference by doxorubicin with DNA unwinding in MCF-7 breast tumor cells. *Mol Pharmacol* (April 1994). 45 (4): 649–56.
33. Bouwmeester T et al. A physical and functional map of the human TNF-alpha/NF-kappa B signal transduction pathway. *Nat. Cell Biol.* 2004. 6 (2): 97–105.
34. D. Leyfer et al. *cis*-Element clustering correlates with dose-dependent pro- and antisignaling effects of IL18, *Genes and Immunity* (2004) 5, 354–362.
35. Auguste P, Guillet C, Fourcin M, Olivier C, Veziers J, Pouplard-Barthelaix A, Gascan H. Signaling of type II oncostatin M receptor. *J. Biol. Chem.* (June 1997). 272 (25): 15760–4.
36. Brasier AR.The nuclear factor-kappaB-interleukin-6 signalling pathway mediating vascular inflammation. *Cardiovasc Res.* 2010 May 1;86(2):211-8.
37. Lee JH, Choi KJ, Seo WD, Jang SY, Kim M, Lee BW, Kim JY, Kang S, Park KH, Lee YS, Bae S. Enhancement of radiation sensitivity in lung cancer cells by celastrol is mediated by inhibition of Hsp90. *Int J Mol Med.* 2011. **27** (3): 441–446

38. Yu H, Kortylewski M, Pardoll D. Crosstalk between cancer and immune cells: role of STAT3 in the tumour microenvironment. *Nat Rev Immunology*. 2007;7:41–51.
39. Karst AM, Drapkin R. Ovarian cancer pathogenesis: A model in evolution. *J. Oncol* 2010:932371.
40. Frank DA: STAT3 as a central mediator of neoplastic cellular transformation. *Cancer Lett* 2007;251:199-21
41. Przybycin CG, Kurman RJ, Ronnett BM, Shih IeM, Vang R (2010) Are all pelvic (nonuterine) serous carcinomas of tubal origin? *Am J Surg Pathol* 34:1407–1416.
42. Crum CP. Intercepting pelvic cancer in the distal fallopian tube: Theories andrealities. *Mol Oncol* 3:165–170.
43. R. Strauss, Z. Y. Li, Y. Liu et al., "Analysis of epithelial and mesenchymal markers in ovarian cancer reveals phenotypic heterogeneity and plasticity," *PLoS One*, vol. 6, no. 1, Article ID e16186, 2011.
44. Walker SR, Chaudhury M, Nelson EA, Frank DA. Microtubule-targeted chemotherapeutic agents inhibit signal transducer and activator of transcription 3 (STAT3) signaling. *Mol Pharmacol.* 2010 Nov;78(5):903-8.
45. Shahzad M et al. "Stress effects on FosB- and interleukin-8 (IL8)-driven ovarian cancer growth and metastasis.*" J Biol Chem.* 2010 Nov 12;285(46):35462-70.
46. Braden C. McFarland, G. Kenneth Gray, Susan E. Nozell, et al. Activation of the NK-kB pathway by the STAT3 inhibitor JSI-124 in human glioblastoma cells. *Mol Cancer Res* Published Online First February 5, 2013.
47. Ghosh S, Karin M. Missing pieces in the NF-kB puzzle. Cell 2002; 109(Suppl):S81–96.
48. Haura EB, Turkson J, Jove R. Mechanisms of disease: Insights into the emerging role of signal transducers and activators of transcription in cancer. *Nat Clin Pract Oncol* 2005;2:315–24.
49. Karin M, Cao Y, Greten FR, Li ZW. NF-kB in cancer: from innocent bystander to major culprit. *Nat Rev Cancer* 2002;2:301–10.
50. Vallabhapurapu S, Karin M. Regulation and function of NF-kappaB transcription factors in the immune system. *Annu Rev Immunol* 2009;27:693–733.
51. Bezbradica JS, Medzhitov R. Integration of cytokine and heterologous receptor signaling pathways. *Nat Immunol* 2009;10:333–9.

52. Karin M. The IkappaB kinase—a bridge between inflammation and cancer. *Cell Res* 2008;18:334–42.
53. Grivennikov SI, Karin M. Dangerous liaisons: STAT3 and NF-kappaB collaboration and crosstalk in cancer. *Cytokine Growth Factor Rev.* 2010 Feb;21(1):11-9
54. Kato T, Jr., Delhase M, Hoffmann A, Karin M. CK2 is a C-terminal IkappaB kinase responsisve for NFappaB activation during the UV response. *Mol Cell.* 2003; 12:829-39.
55. Alvarez JV, Frank DA. Genome-wide analysis of STAT target genes: elucidating the mechanism of STAT-mediated oncogenesis. *Cancer Biol Ther.* 2004 Nov;3(11):1045-50.
56. Akhtar LN, et al. Suppressor of cytokine signaling 3 inhibits antiviral IFN-beta signaling to enhance HIV-1 replication in macrophages. *J Immunol.* 2010, 185: 2393-404.
57. Pauli EK, Schmolke M, Wolff T, Viemann D. Roth J, Bode JG, et al. Influenz A virus inhibts type I IFN signaling via NF-kappa-dependent induction of SOCS-3 expression. *PLoS Pathog.* 2008: 4:e1000196.
58. Wang YH et al. Regulatory mechanisms of interleukin-8 production induced by tumour necrosis factor-α in human hepatocellular carcinoma cells. *Journal of Cellular and Molecular Medicine*. Volume 16, Issue 3, pages 496–506, March 2012.
59. Wertz IE, O'Rourke KM, Zhou H, Eby M, Aravind L, Seshagiri S, et al. De-ubiquitination and ubiquitin ligase domains of A20 downregulate NF-kappaB signalling. *Nature* 2004;430:694–9.
60. D. Hanahan, R.A. Weinberg, The hallmarks of cancer. Cell, 100 (2000), pp. 57–70.
61. Boone DL, Turer EE, Lee EG, Ahmad RC, Wheeler MT, Tsui C, et al. The ubiquitin-modifying enzyme A20 is required for termination of Toll-like receptor responses. *Nat Immunol* 2004;5:1052–60.
62. D.J. Dauer, B. Ferraro, L. Song et al. Stat3 regulates genes common to both wound healing and cancer. *Oncogene*, 24 (2005), pp. 3397–3408.
63. Thornburg, Natalie J; Pathmanathan Rajadurai, Raab-Traub Nancy. "Activation of nuclear factor-kappaB p50 homodimer/Bcl-3 complexes in nasopharyngeal carcinoma". *Cancer Res.* Dec 2003 63 (23): 8293–301.
64. Bours, V; Franzoso G, Azarenko V, Park S, Kanno T, Brown K, Siebenlist. "The oncoprotein Bcl-3 directly transactivates through kappa B motifs via association with DNA-binding p50B homodimers". *Cell* Mar. 1993 72 (5): 729–39.

65. Puthier D, Bataille R, Amiot M. IL-6 up-regulates mcl-1 in human myeloma cells through JAK/STAT rather than ras/MAP kinase pathway. *Eur J Immunol* 1999; 29: 3945–50.
66. Puthier D, Bataille R, Amiot M. IL-6 up-regulates mcl-1 in human myeloma cells through JAK/STAT rather than ras/MAP kinase pathway. *Eur J Immunol* 1999; 29: 3945–50.
67. Alvarez JV, Febbo PG, Ramaswamy S, Loda M, Richardson A, Frank DA. Identification of a genetic signature of activated signal transducer and activator of transcription 3 in human tumors. *Cancer Res.* 2005 Jun 15;65(12):5054-62.
68. Benjamin Chun Yu Wong, et al. Suppression of RelA/p65 nuclear translocation independent of IB- degradation by cyclooxygenase-2 inhibitor in gastric cancer. (2003) 22, 1189–1197.
69. Brian P. Ashburner,1,† Sandy D. Westerheide,1 andAlbert S. Baldwin. The p65 (RelA) Subunit of NF-κB Interacts with the Histone Deacetylase (HDAC) Corepressors HDAC1 and HDAC2 To Negatively Regulate Gene Expression. *Mol Cell Biol.* 2001 October; 21(20): 7065–7077.
70. Chao Zheng, Qian Yin, and Hao Wu. Structural studies of NF-κB signaling. *Cell Res.* 2011 January; 21(1): 183–195.
71. Bosisio D, Marazzi I, Agresti A, Shimizu N, Bianchi ME, Natoli G. A hyper-dynamic equilibrium between promoter-bound and nucleoplasmic dimers controls NF-kappaB-dependent gene activity. *EMBO J.* 2006 Feb 22; 25(4):798-810.
72. Carson SD, Pirruccello SJHeLa cell heterogeneity and coxsackievirus B3 cytopathic effect: implications for inter-laboratory reproducibility of results. *J Med Virol.* 2013 Apr;85(4):677-83.
73. Sun SC, Ley SC. New insights into NF-kappaB regulation and function. *Trends Immunol.* 2008 Oct; 29(10):469-78.
74. Dejardin E.The alternative NF-kappaB pathway from biochemistry to biology: pitfalls and promises for future drug development. *Biochem Pharmacol.* 2006 Oct 30;72(9):1161-79.
75. Moynagh P. N. (2005) The NFkB pathway. *J Cell Sci.* 118, 4389-4392.
76. Hayden M. S., Ghosh. (2004) Signaling to NFkB. *Genes Dev.* 18, 2195-2224.
77. Li T, Morgan MJ, Choksi S, Zhang Y, Kim YS, Liu ZG. MicroRNAs modulate the noncanonical transcription factor NF-kappaB pathway by regulating expression of the kinase IKKalpha during macrophage differentiation. *Nat Immunol.* 2010 Sep;11(9):799-805.
78. G. P. Nolan et al., The bcl-3 proto-oncogene encodes a nuclear I kappa B-like molecule that

preferentially interacts with NF-kappa B p50 and p52 in a phosphorylation-dependent manner. *Mol. Cell. Biol.* 13, 3557 (1993)

79. Diane L. Bundy. Diverse Effects of BCL3 Phosphorylation on Its Modulation of NF-κB p52 Homodimer Binding to DNA. *Journal of Biological Chemistry*, 272, 33132-33139.
80. Cogswell P. C., Guttridge D. C., Funkhouser W. K., Baldwin A. S., Jr. Selective activation of NF-κB subunits in human breast cancer: potential roles for NF-κB2/p52 and for Bcl-3. *Oncogene*, 19: 1123-1131, 2000.
81. Xiao G, Rabson AB, Young W, Qing G, Qu Z. Alternative pathways of NF-kappaB activation: a double-edged sword in health and disease. *Cytokine Growth Factor Rev.* 2006 Aug;17(4):281-93.
82. Ruaidhrí J. Carmody, et al. Negative Regulation of Toll-Like Receptor Signaling by NF-κB p50 Ubiquitination Blockade. *Science* August 2007: Vol. 317 no. 5838 pp. 675-678.
83. Mélisande Richard, Jamila Louahed, Jean-Baptiste Demoulin and Jean-Christophe Renauld. Interleukin-9 Regulates NF-kB Activity Through BCL3 Gene Induction. *Blood.* 1999 93: 4318-4327
84. Kerr LD, Duckett CS, Wamsley P, Zhang Q, Chiao P, Nabel G, McKeithan TW, Baeuerle PA, Verma IM. The proto-oncogene bcl-3 encodes an IκB protein. *Genes Dev* 1992;6:235
85. Bours V, Franzoso G, Azarenko V, Park S, Kanno T, Brown K, Siebenlist U. The oncoprotein Bcl-3 directly transactivates through κB motifs via association with DNA-binding p50B homodimers. *Cell* 1993;72:729
86. Norikiko Sakai, et al. p38 MAPK phosphorylation and NF-kB activation in human crescentic glomerulonephritis. *Nephrol Dial Transplant* 2002 17: 998-1004

FUNDING

This work was supported by the Paul Calabresi Medical Student Fellowship of the PhRMA foundation (2012-2013), Harvard Medical School Scholar in Medicine (TargetCancer, Summer 2011), and Harvard Medical School & MIT Health Science and Technology (HST) Research Assistantship (Fall 2011).